Supporting Information

Manganese-Catalyzed Transfer Semihydrogenation of Internal Alkynes to *E*-Alkenes with iPrOH as Hydrogen Source

Antonio Torres-Calis and Juventino J. García*

juvent@unam.mx

Facultad de Química, Universidad Nacional Autónoma de México, Mexico City, 04510, Mexico

Index

Index of Figures

Index of Tables

Index of Schemes

I. Characterization of prepared Mn(I) complexes

Characterization of fac-[Mn(OTf)(dippe)(CO)$_3$] (**Mn-1**)

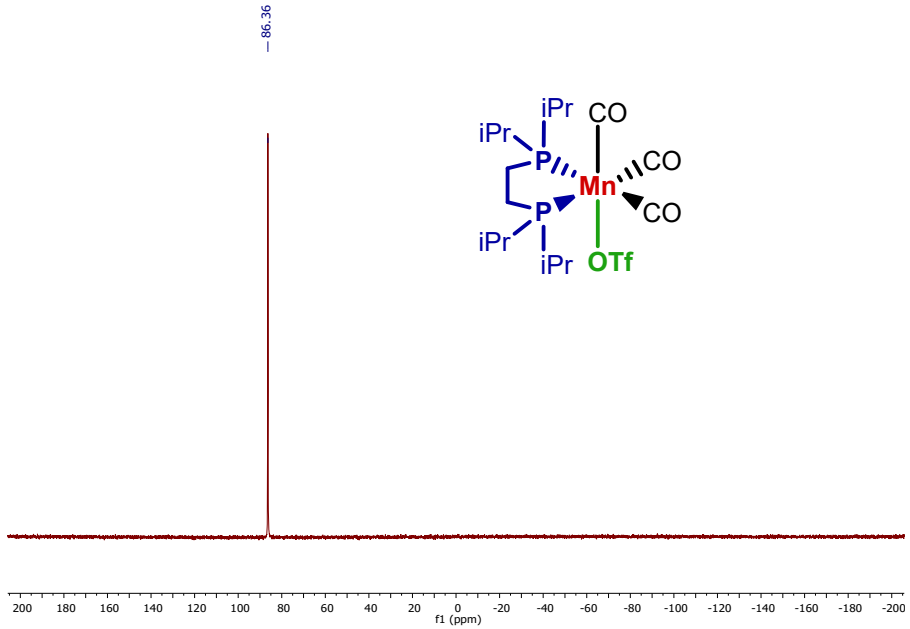

Figure S1. $^{31}P\{^{1}H\}$ NMR (243 MHz, THF-d_8) spectrum for **Mn-1**

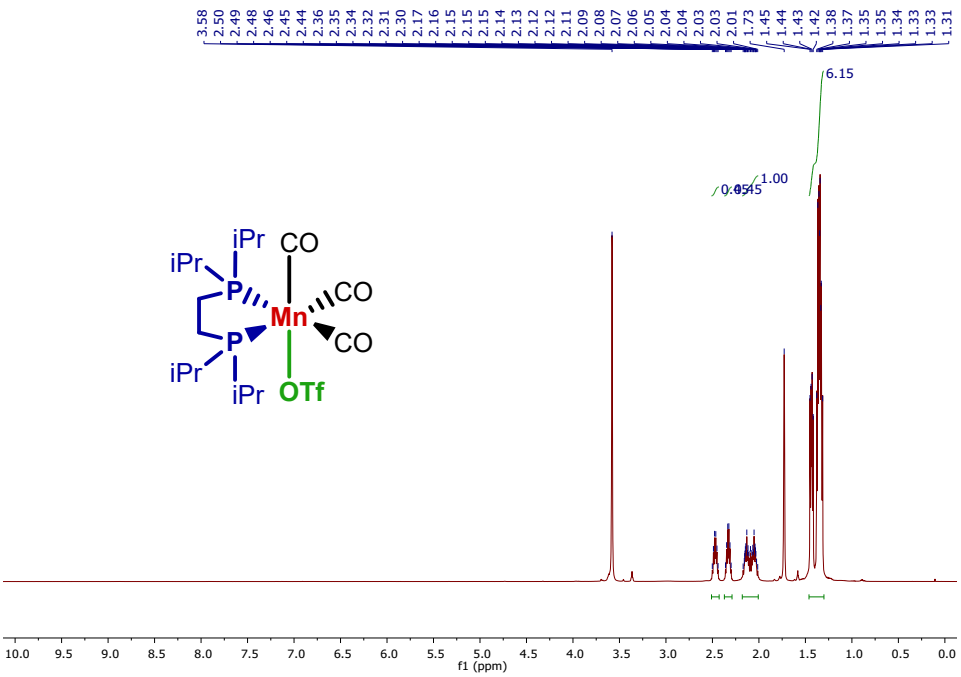

Figure S2. ^{1}H NMR (600 MHz, THF-d_8) spectrum for **Mn-1**

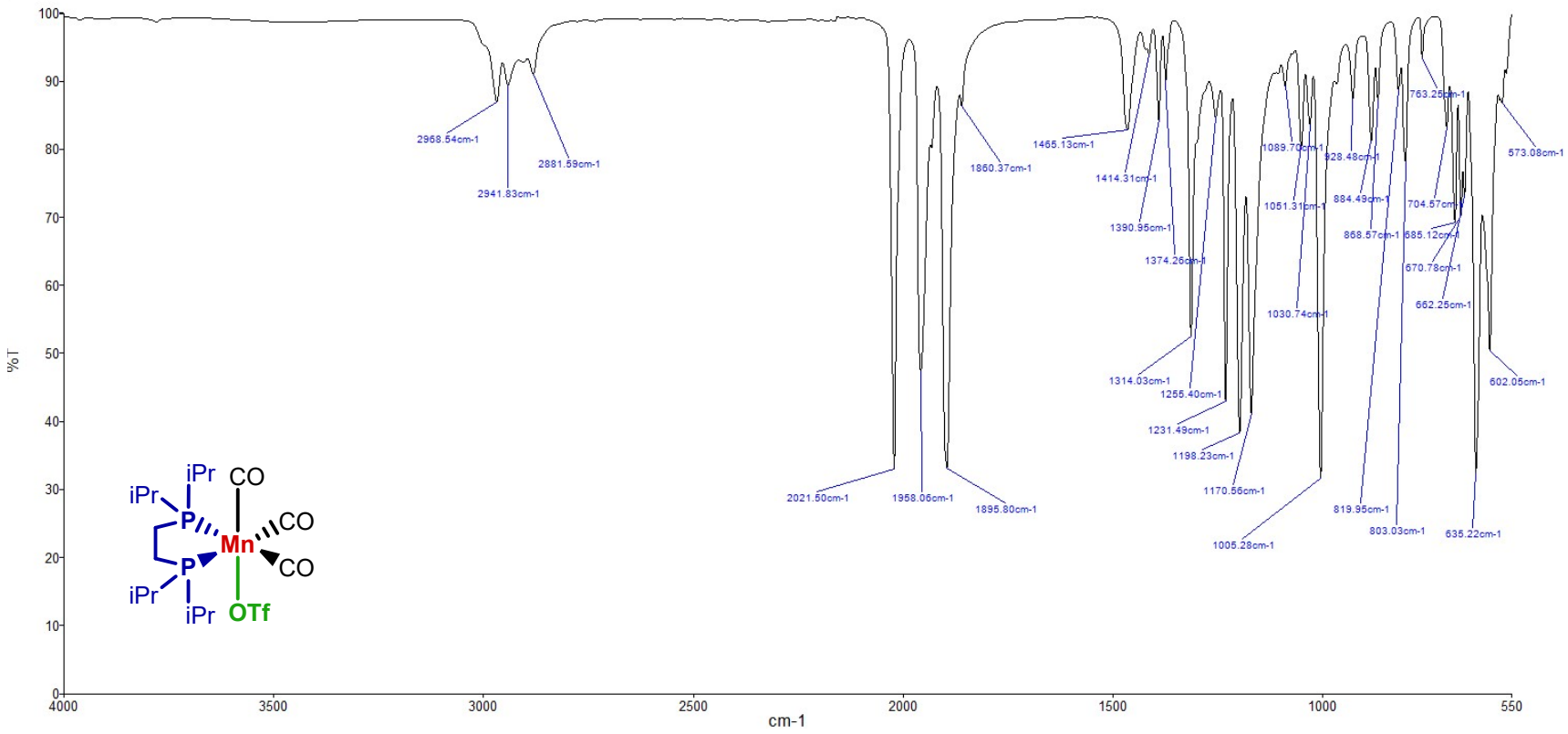

Figure S3. FTIR (ATR) spectrum for **Mn-1**

Characterization of fac-[Mn(Br)(dippe)(CO)$_3$] (**Mn-2**)

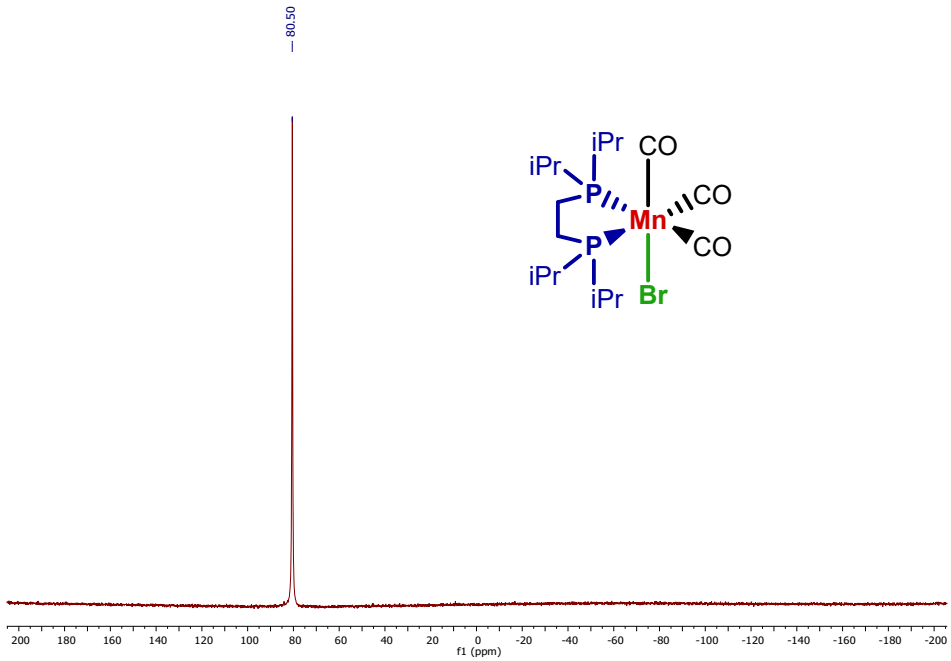

Figure S4. $^{31}P\{^{1}H\}$ NMR (243 MHz, THF-d_8) spectrum for **Mn-2**

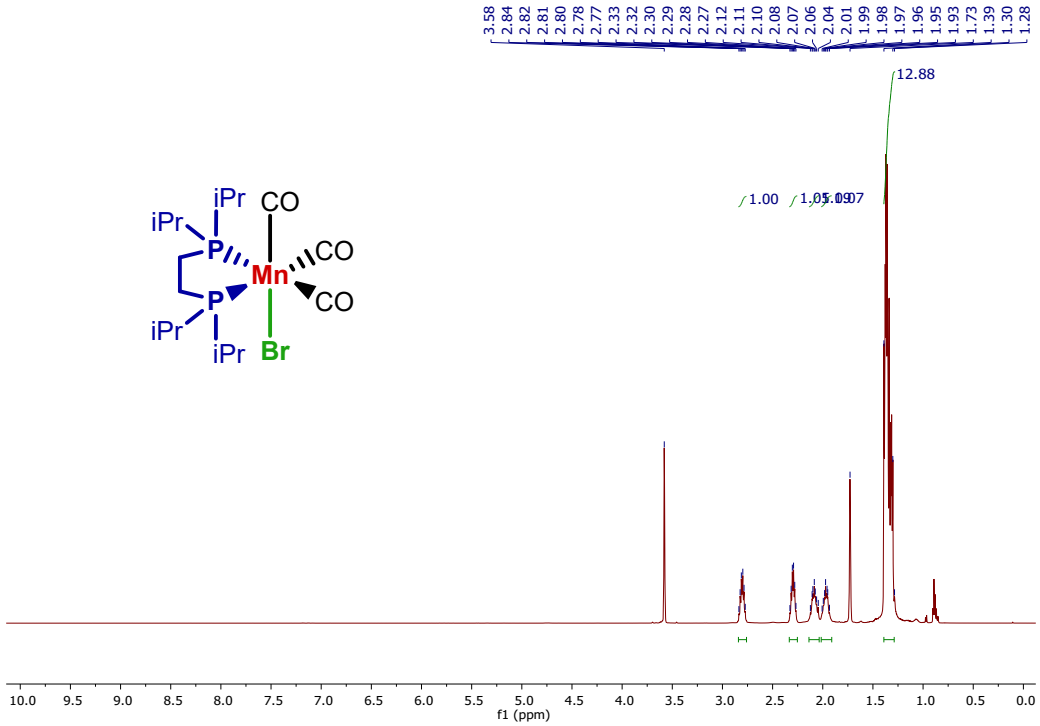

Figure S5. ^{1}H NMR (600 MHz, THF-d_8) spectrum for **Mn-2**

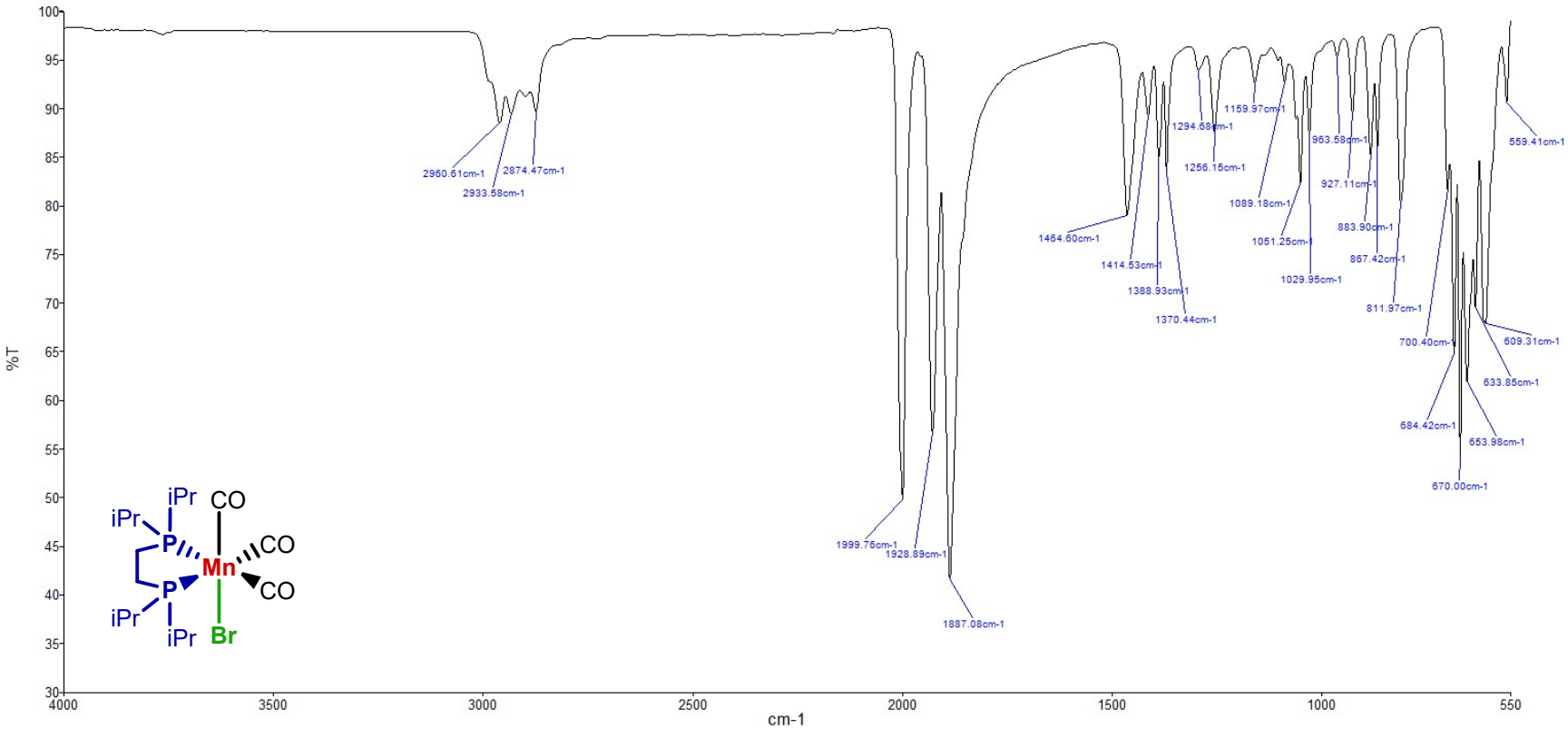

Figure S6. FTIR (ATR) spectrum for **Mn-2**

Characterization of fac-[Mn(Br)(dcype)(CO)$_3$] (**Mn-3**)

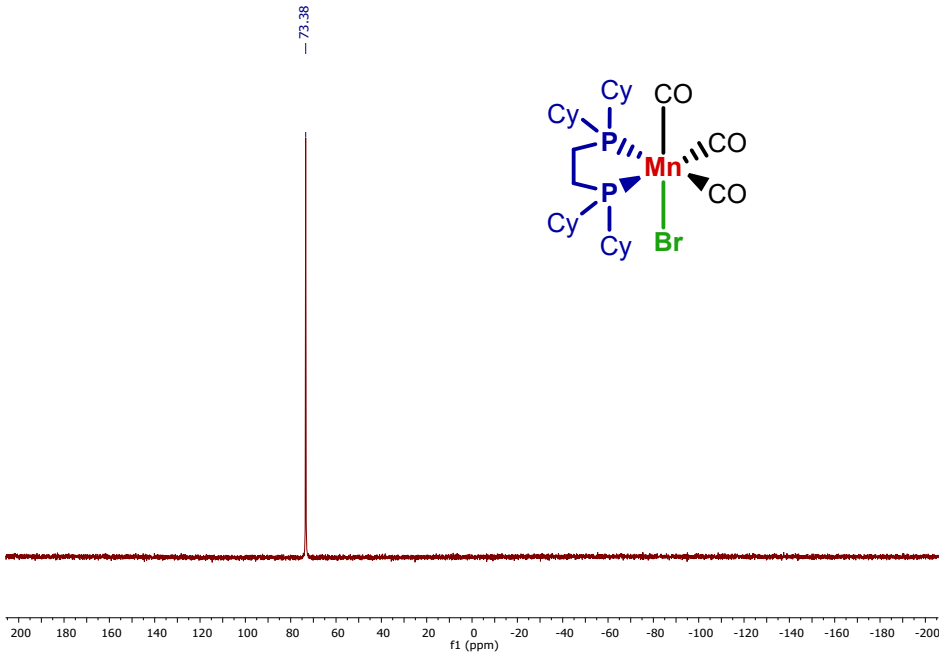

Figure S7. $^{31}P\{^{1}H\}$ NMR (243 MHz, THF-d_8) spectrum for **Mn-3**

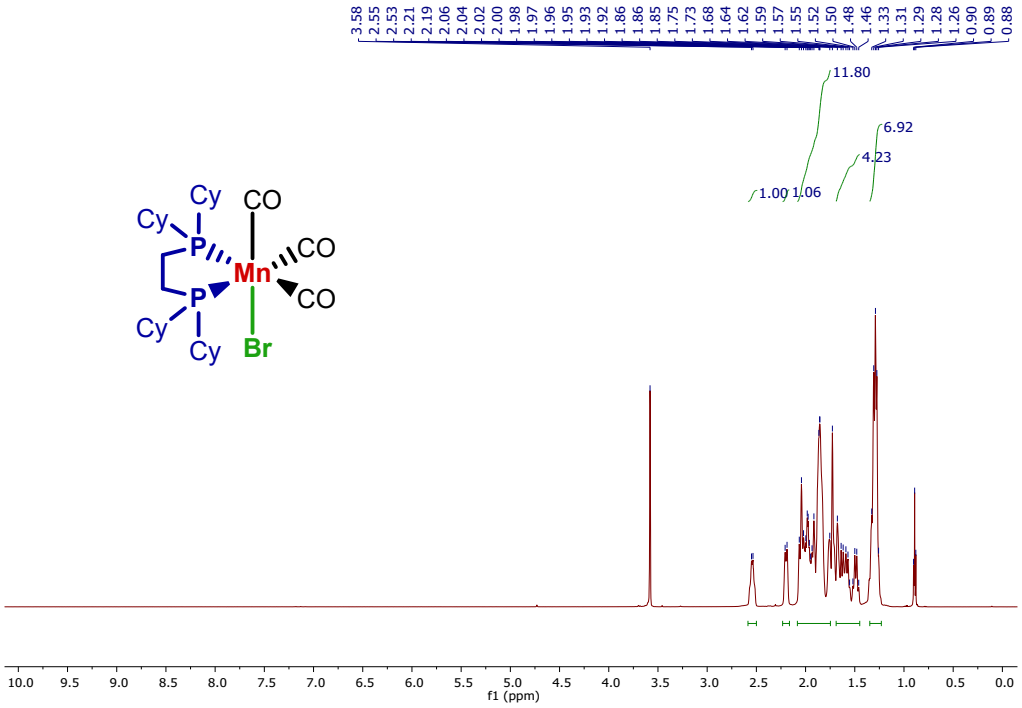

Figure S8. ^{1}H NMR (600 MHz, THF-d_8) spectrum for **Mn-3**

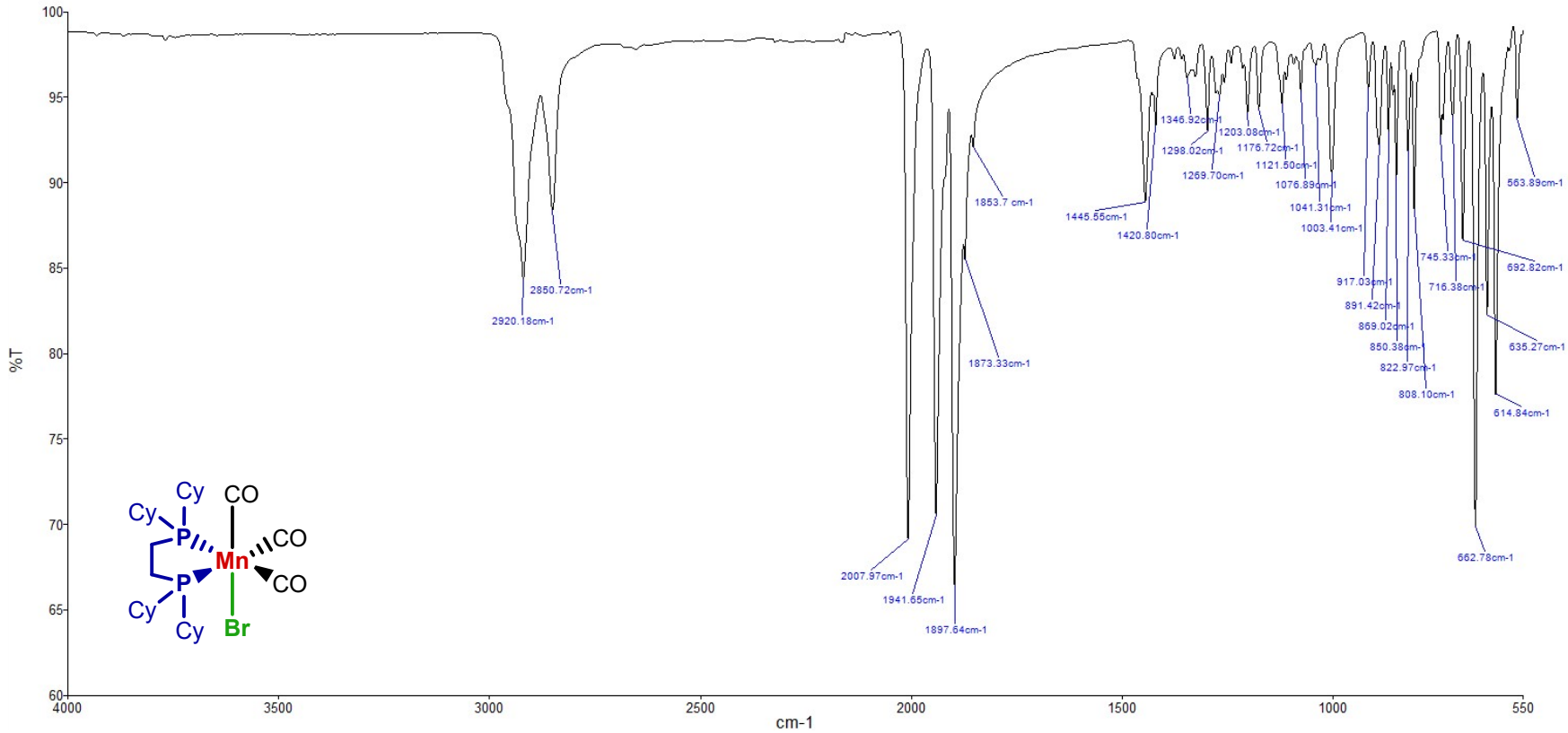

Figure S9. FTIR (ATR) spectrum for **Mn-3**

Characterization of fac-[Mn(Br)(dppe)(CO)$_3$] (**Mn-4**)

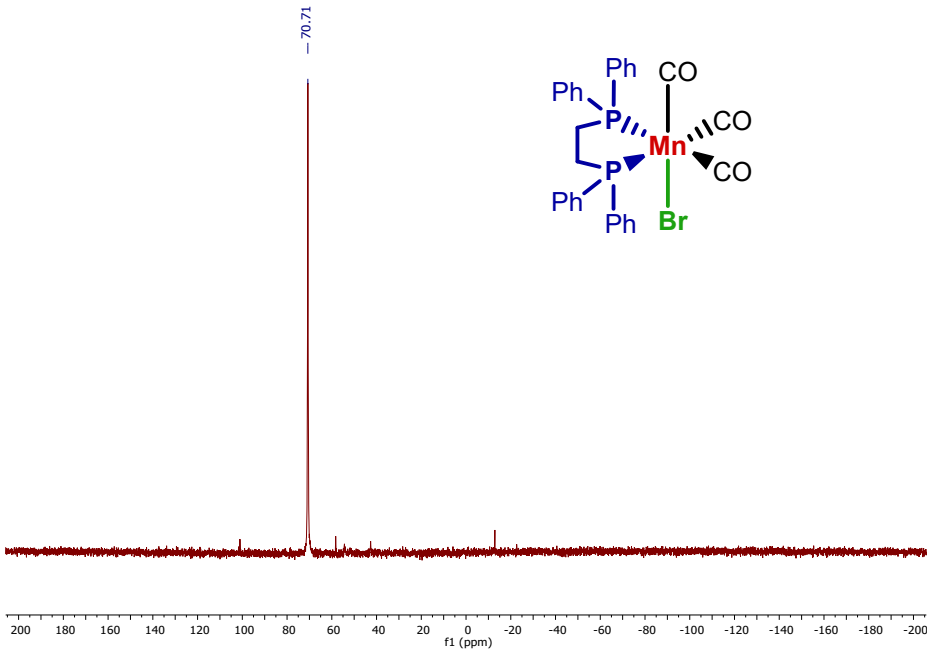

Figure S10. ^{31}P{^{1}H} NMR (243 MHz, THF-d_8) spectrum for **Mn-4**

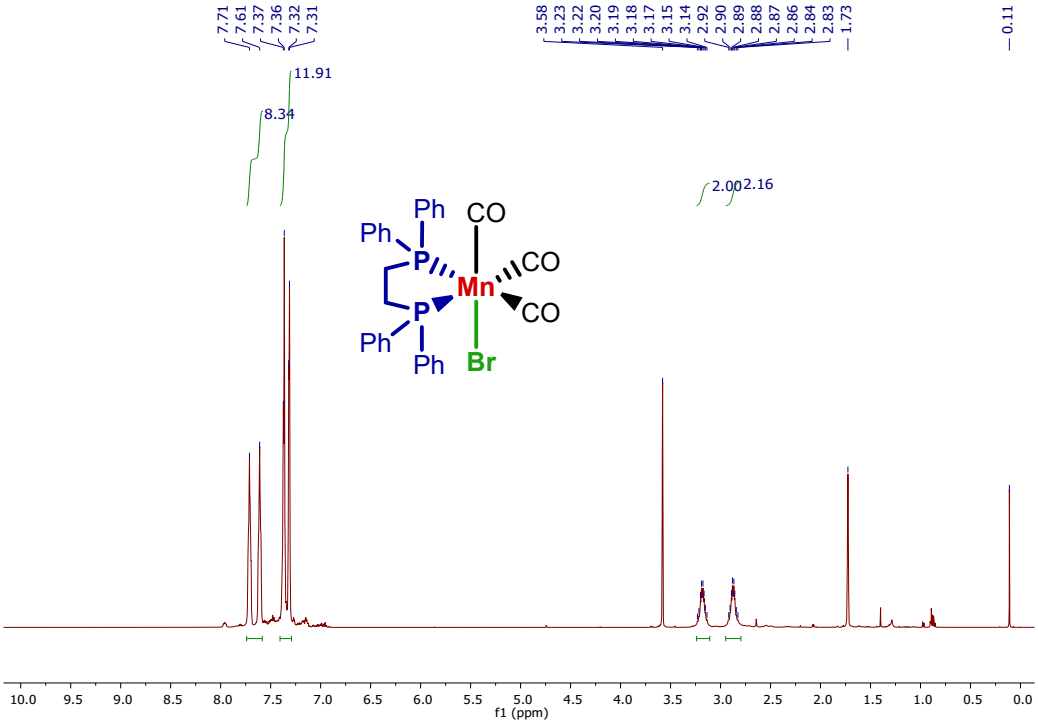

Figure S11. ^{1}H NMR (600 MHz, THF-d_8) spectrum for **Mn-4**

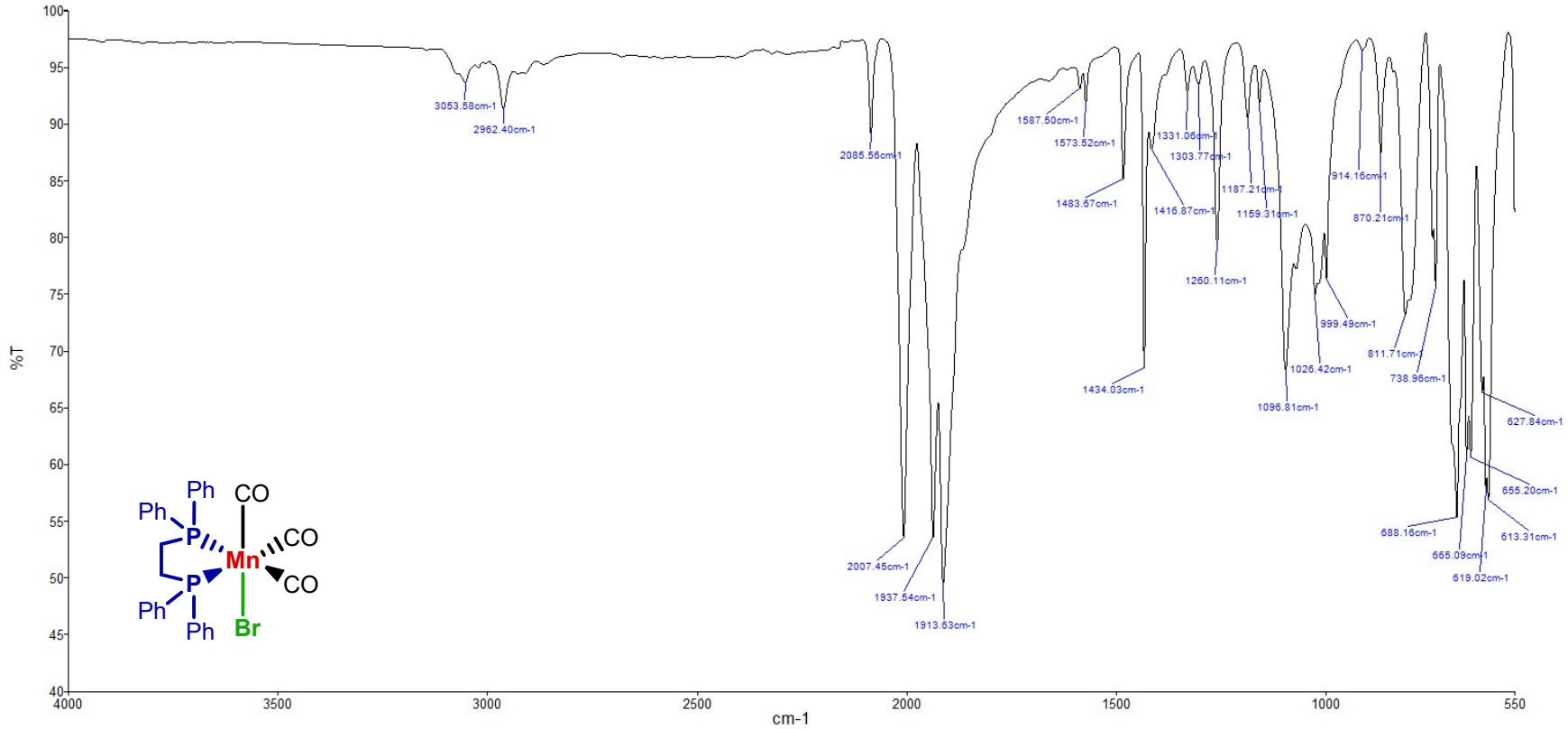
%T
cm-1
3053.58cm-1
2962.40cm-1
2085.56cm-1
2007.45cm-1
1937.54cm-1
1913.63cm-1
1587.50cm-1
1573.52cm-1
1483.67cm-1
1434.03cm-1
1331.06cm-1
1303.77cm-1
1416.87cm-1
1260.11cm-1
1187.21cm-1
1159.31cm-1
1096.81cm-1
1026.42cm-1
999.49cm-1
914.16cm-1
870.21cm-1
811.71cm-1
738.96cm-1
688.16cm-1
665.09cm-1
655.20cm-1
627.84cm-1
619.02cm-1
613.31cm-1
Ph
Ph
P
CO
Mn
CO
CO
P
Ph
Ph
Br

Figure S12. FTIR (ATR) spectrum for **Mn-4**

Characterization of fac-[Mn(H)(dippe)(CO)$_3$] (**Mn-5**)

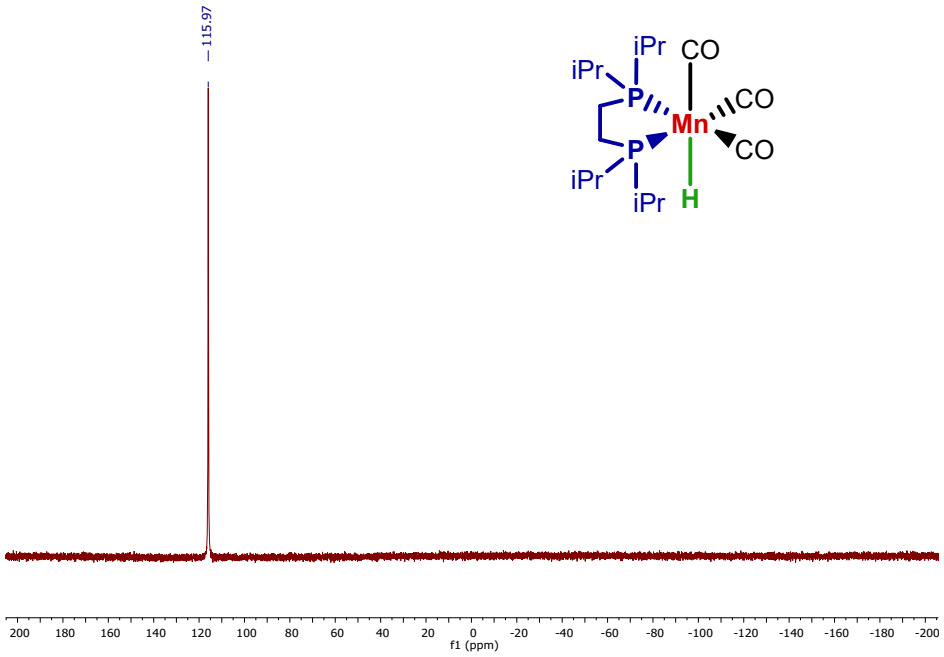

Figure S13. $^{31}P\{^{1}H\}$ NMR (243 MHz, THF-d_8) spectrum for **Mn-5**

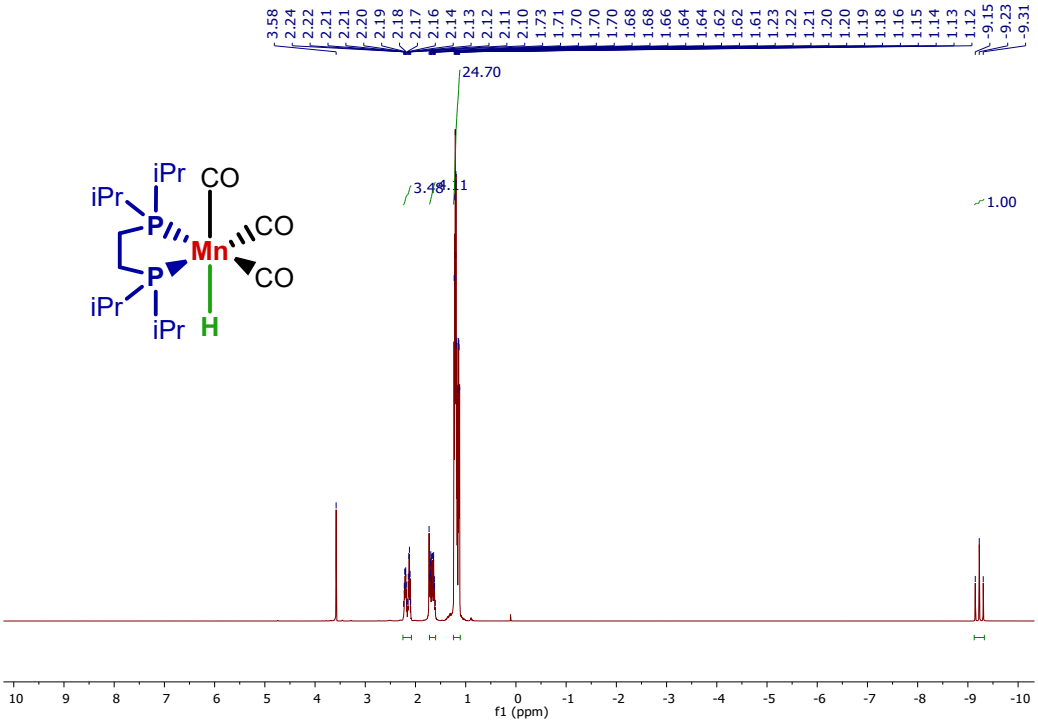

Figure S14. ^{1}H NMR (600 MHz, THF-d_8) spectrum for **Mn-5**

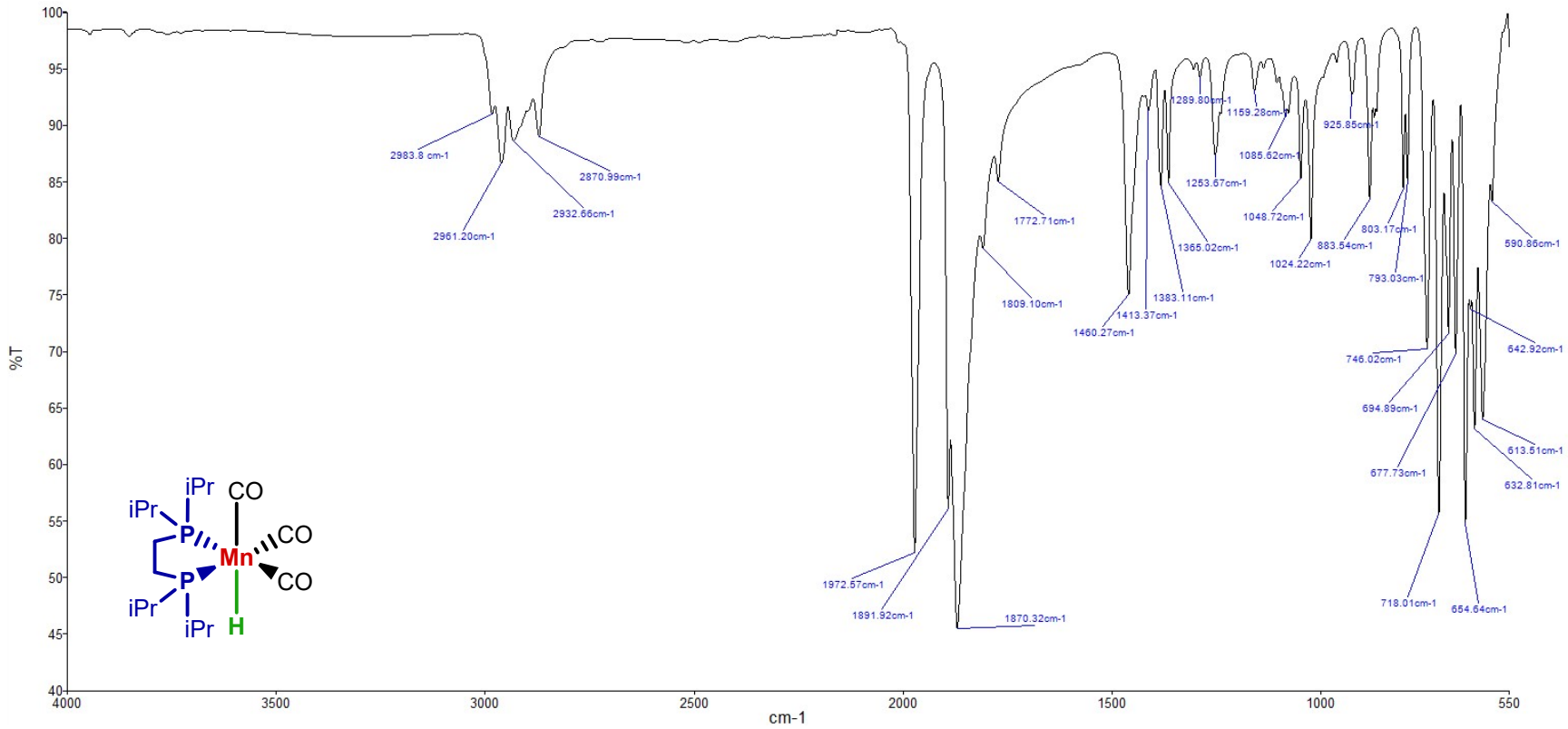
%T
cm-1
2983.8 cm-1
2961.20cm-1
2932.66cm-1
2870.99cm-1
1772.71cm-1
1809.10cm-1
1972.57cm-1
1891.92cm-1
1870.32cm-1
1460.27cm-1
1413.37cm-1
1383.11cm-1
1365.02cm-1
1253.67cm-1
1289.80cm-1
1159.28cm-1
1085.62cm-1
1048.72cm-1
1024.22cm-1
925.85cm-1
883.54cm-1
803.17cm-1
793.03cm-1
746.02cm-1
694.89cm-1
677.73cm-1
718.01cm-1
654.64cm-1
632.81cm-1
613.51cm-1
642.92cm-1
590.86cm-1
iPr
iPr
iPr
iPr
P
P
Mn
CO
CO
CO
H

Figure S15. FTIR (ATR) spectrum for **Mn-5**

II. Optimization of *E*-selective transfer semihydrogenation of diphenylacetylene (1) using Mn(I)-based precursors

Table S1. Full optimization of transfer semihydrogenation of diphenylacetylene (**1**) with Mn-based precursors[a]

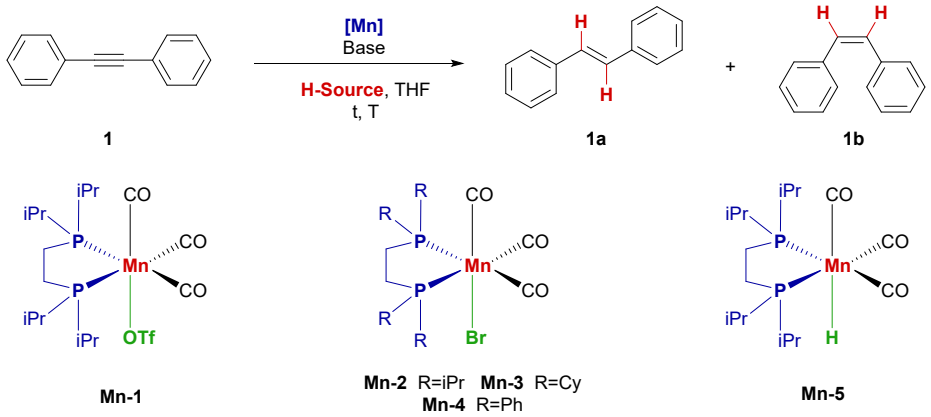

Entry	[Mn] (mol%)	Base (mol%)	H-Source (mL)	T (°C)	t (h)	Conversion (%)[b]
1	Mn-1 (3)	^{t}BuOK (10)	iPrOH (3)	100	18	88, 90:10 *E*/*Z*
2	Mn-1 (3)	^{t}BuOK (10)	iPrOH (3)	120	22	88, 91:9 *E*/*Z*
3	Mn-1 (6)	^{t}BuOK (20)	iPrOH (3)	100	18	98, 99:1 *E*/*Z*
4	Mn-1 (5)	^{t}BuOK (20)	iPrOH (3)	100	18	98, 98:2 *E*/*Z*
5	Mn-1 (5)	^{t}BuOK (15)	iPrOH (3)	100	18	96, 96:4 *E*/*Z*
6	Mn-1 (4)	^{t}BuOK (20)	iPrOH (3)	100	18	93, 96:4 *E*/*Z*
7[c]	Mn-1 (5)	^{t}BuOK (20)	iPrOH (3)	100	18	n.d.
8	Mn-1 (5)	^{t}BuOK (20)	iPrOH (1)	100	18	97, 97:3 *E*/*Z*
9	Mn-1 (5)	NEt_3 (20)	iPrOH (1)	100	18	4, 12:88 *E*/*Z*
10	Mn-1 (5)	K_2CO_3 (20)	iPrOH (1)	100	18	62, 64:36 *E*/*Z*
11	Mn-1 (5)	K_2CO_3 (40)	iPrOH (1)	100	18	77, 77:23 *E*/*Z*
12	Mn-1 (5)	Na_2CO_3 (20)	iPrOH (1)	100	18	68, 84:16 *E*/*Z*
13	Mn-1 (5)	Cs_2CO_3 (20)	iPrOH (1)	100	18	46, 45:55 *E*/*Z*
14	Mn-1 (5)	KOH (20)	iPrOH (1)	100	18	97, 97:3 *E*/*Z*

15	Mn-1 (5)	NaOH (20)	iPrOH (1)	100	18	97, 98:2 *E*/*Z*
16	Mn-1 (5)	MeONa (20)	iPrOH (1)	100	18	98, 98:2 *E*/*Z*
17	Mn-1 (5)	MeONa (10)	iPrOH (1)	100	18	98, 98:2 *E*/*Z*
18	Mn-1 (5)	MeONa (5)	iPrOH (1)	100	18	95, 96:4 *E*/*Z*
19	Mn-1 (5)	/	iPrOH (1)	100	18	7, 36:64 *E*/*Z*
20	Mn-1 (4)	MeONa (10)	iPrOH (1)	100	18	96, 97:3 *E*/*Z*
21	Mn-1 (3)	MeONa (10)	iPrOH (1)	100	18	93, 96:4 *E*/*Z*
22	Mn-1 (4)	MeONa (10)	iPrOH (1)	100	4	95, 97:3 *E*/*Z*
23	Mn-1 (4)	MeONa (10)	iPrOH (1)	100	3	95, 94:6 *E*/*Z*
24	Mn-1 (4)	MeONa (10)	iPrOH (1)	90	4	87, 89:11 *E*/*Z*
25	Mn-2 (4)	MeONa (10)	iPrOH (1)	100	4	98, 97:3 *E*/*Z*
26	Mn-3 (4)	MeONa (10)	iPrOH (1)	100	4	87, 82:18 *E*/*Z*
27	Mn-4 (4)	MeONa (10)	iPrOH (1)	100	4	31, 38:62 *E*/*Z*
28	Mn-5 (4)	MeONa (10)	iPrOH (1)	100	4	13, 2:98 *E*/*Z*
29	$Mn(Br)(CO)_5$ (4)	MeONa (10)	iPrOH (1)	100	4	n.d.
30	/	MeONa (10)	iPrOH (1)	100	4	n.d.
31	Mn-2 (4)	KOH (10)	iPrOH (1)	100	4	93, 93:7 *E*/*Z*
32	Mn-2 (4)	NaOH (10)	iPrOH (1)	100	4	92, 93:7 *E*/*Z*
33	Mn-2 (4)	MeONa (10)	MeOH (1)	100	4	2, 48:52 *E*/*Z*
34	Mn-2 (4)	MeONa (10)	EtOH (1)	100	4	12, 10:90 *E*/*Z*
35	Mn-2 (4)	MeONa (10)	HCO_2H (1)	100	4	8, 31:69 *E*/*Z*
36	Mn-2 (4)	MeONa (10)	*n*-BuOH (1)	100	4	8, 23:77 *E*/*Z*
37	Mn-2 (4)	MeONa (10)	2-BuOH (1)	100	4	88, 89:11 *E*/*Z*
38	Mn-2 (4)	MeONa (10)	Ethylene glycol (1)	100	4	n.d.
39	Mn-2 (4)	MeONa (10)	Glycerol (1)	100	4	2, 39:61 *E*/*Z*
40[d]	Mn-2 (4)	MeONa (10)	iPrOH (1)	100	4	91, 93:7 *E*/*Z*
41[e]	Mn-2 (4)	MeONa (10)	iPrOH (1)	100	4	90, 91:9 *E*/*Z*

[a] Reaction conditions: diphenylacetylene (0.224 mmol), THF (1 mL). [b] Conversions and stereoselectivities were determined by GC-MS. [c] No THF [d] Hg drop test. [e] TEMPO (1.1 eq) was added.

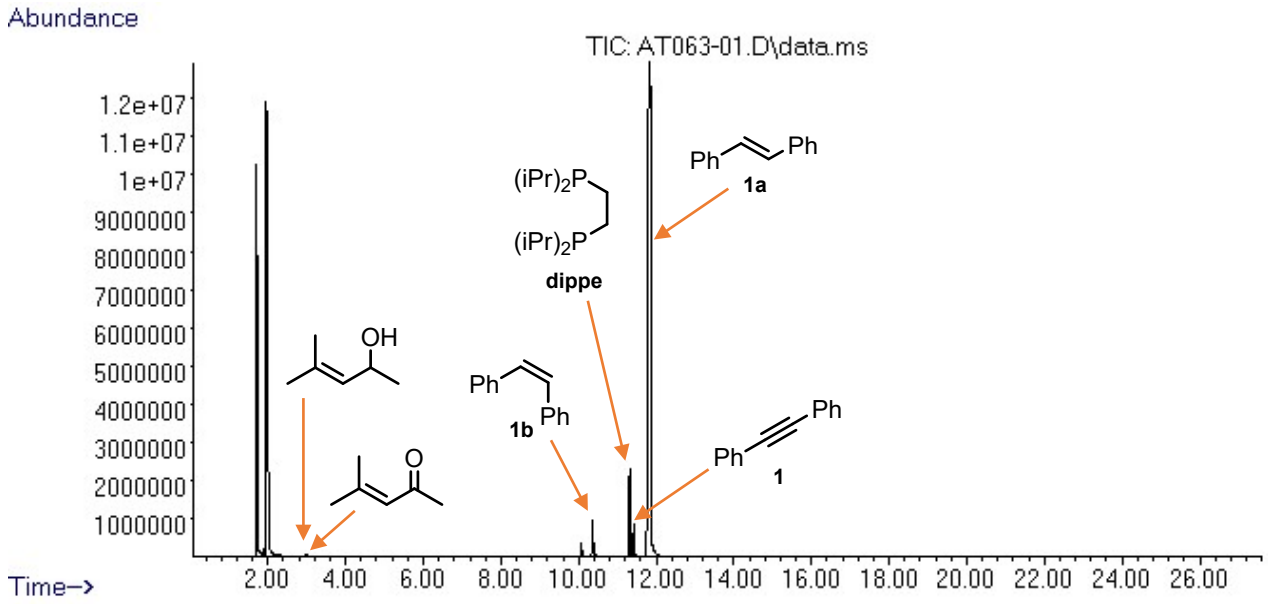

Figure S16. Typical GC of the crude mixture for **1** transfer semihydrogenation with iPrOH catalyzed by **Mn-2**

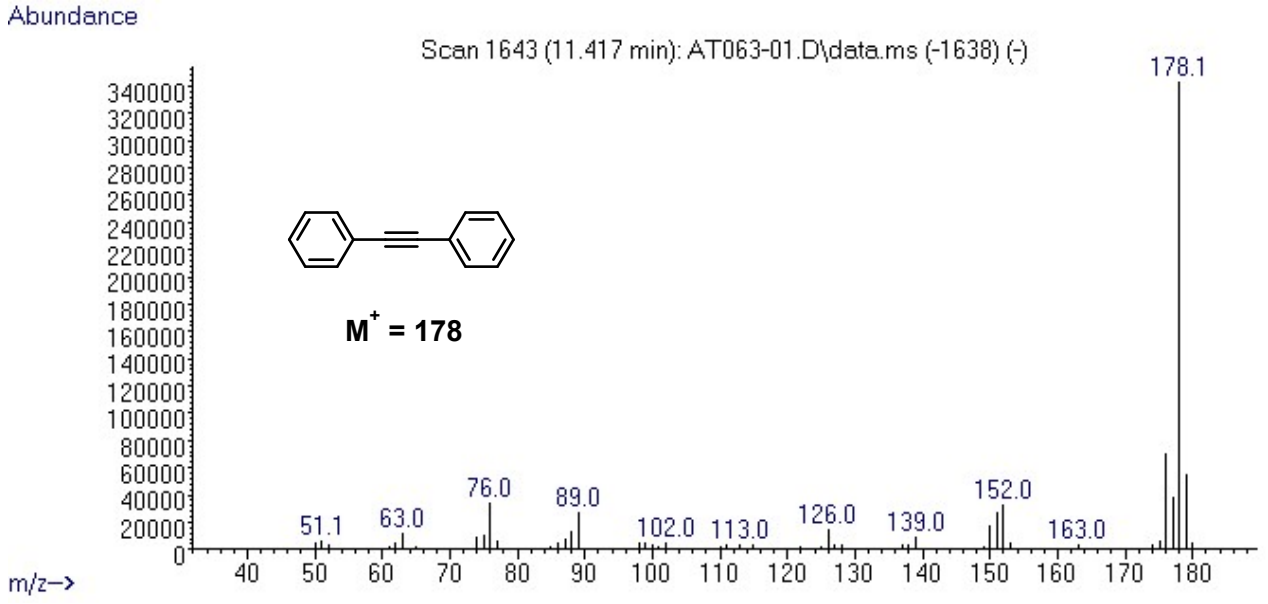

Figure S17. MS for diphenylacetylene (**1**) detected by GC

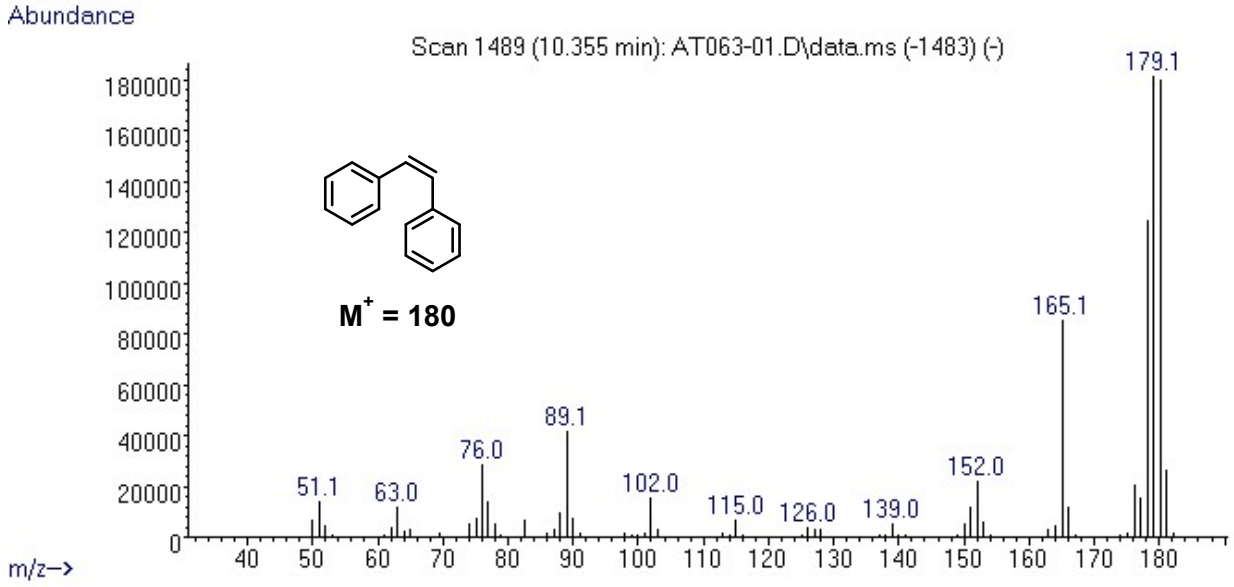

Figure S18. MS for *cis*-stilbene (**1b**) detected by GC

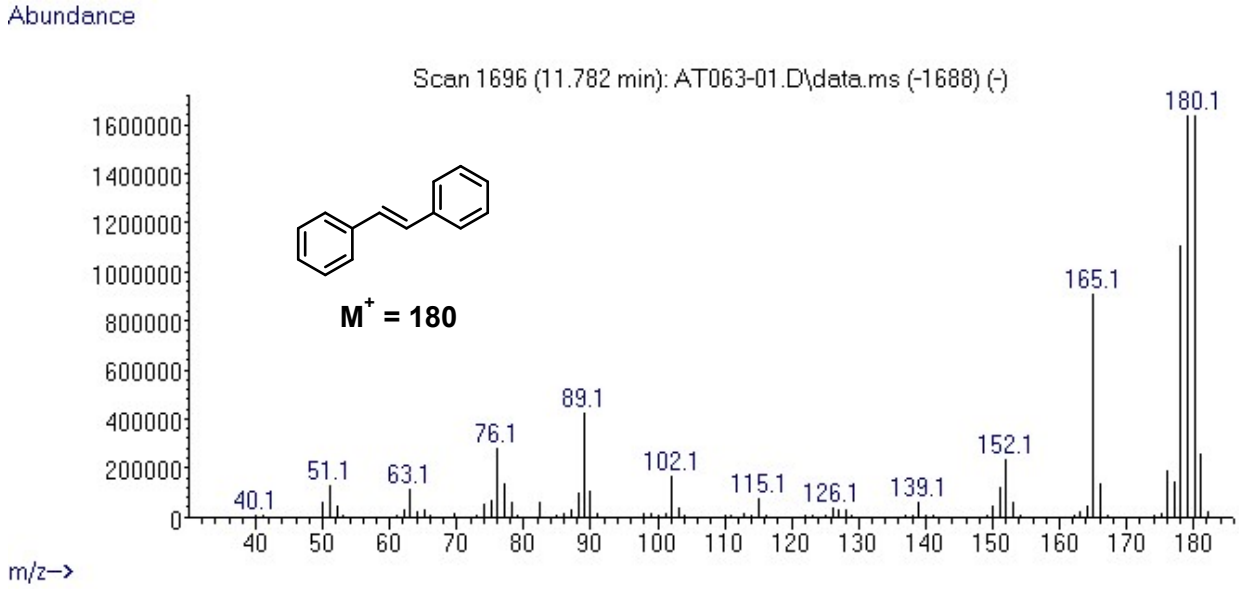

Figure S19. MS for *trans*-stilbene (**1a**) detected by GC

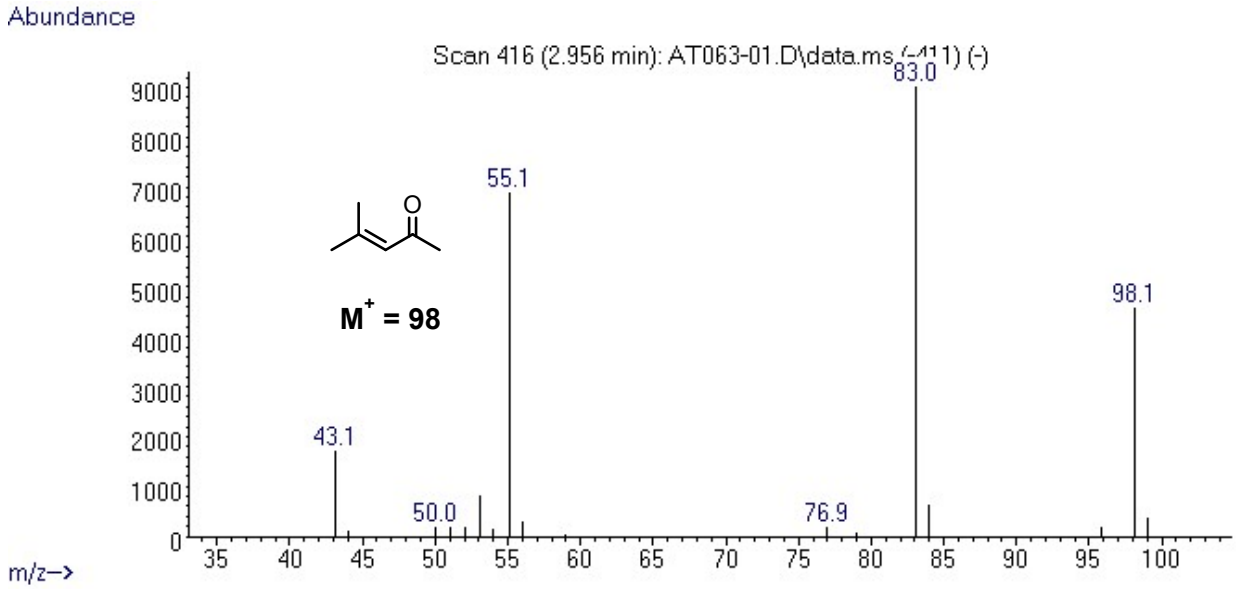

Figure S20. MS for 4-methylpent-3-en-2-one detected by GC

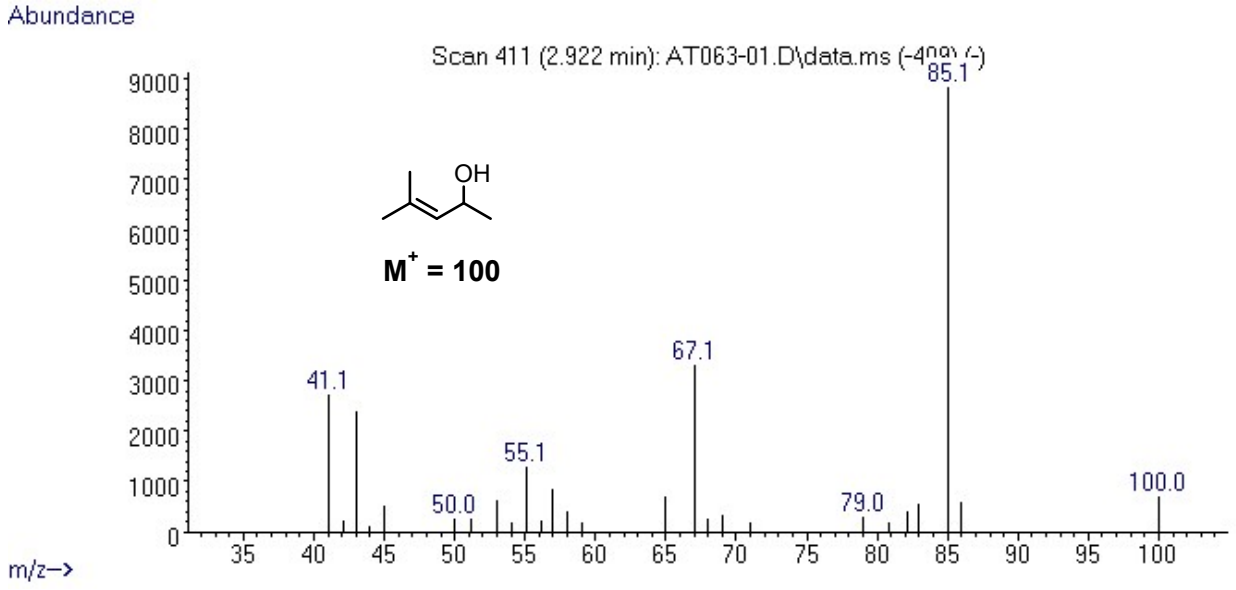

Figure S21. MS for 4-methylpent-3-en-2-ol detected by GC

III. Scope

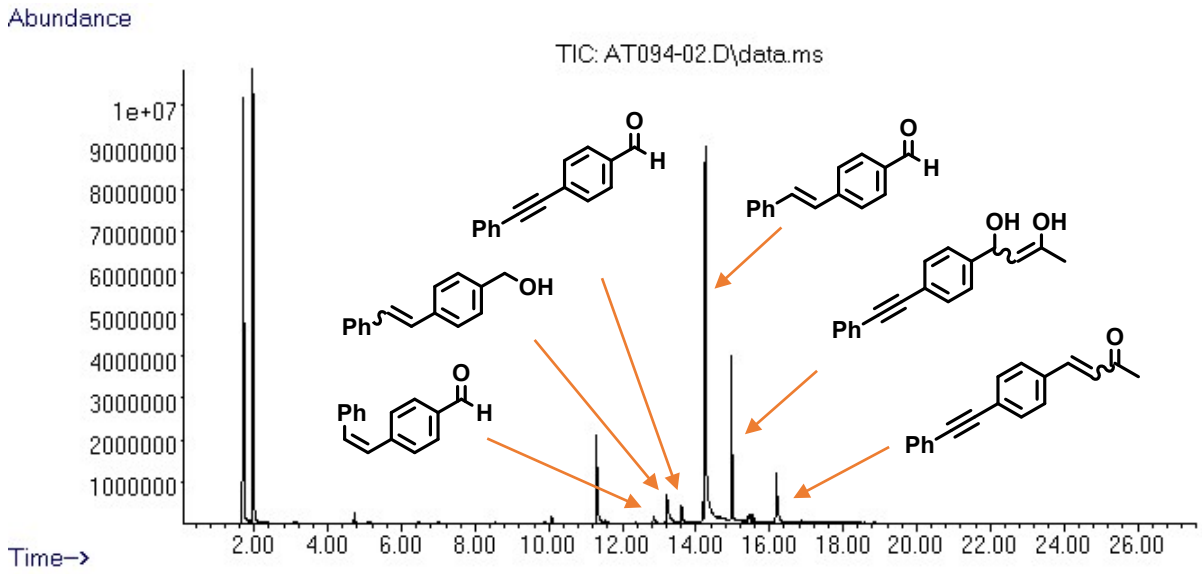

Figure S22. GC of the crude mixture of 4-(phenylethynyl)benzaldehyde (**2**) transfer semihydrogenation with iPrOH catalyzed by **Mn-2**

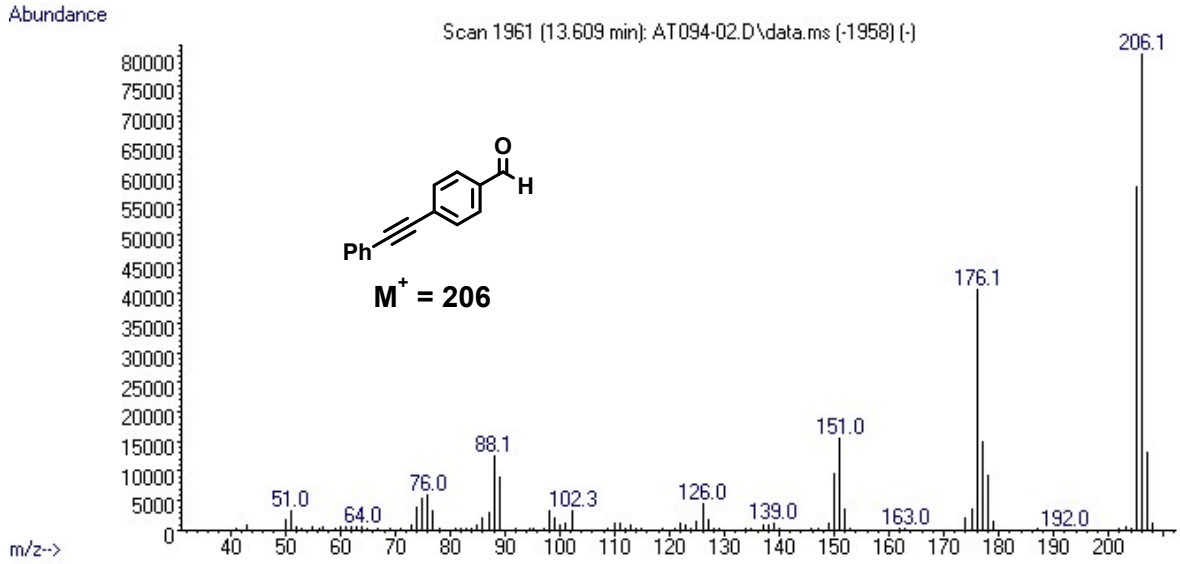

Figure S23. MS for 4-(phenylethynyl)benzaldehyde (**2**) detected by GC

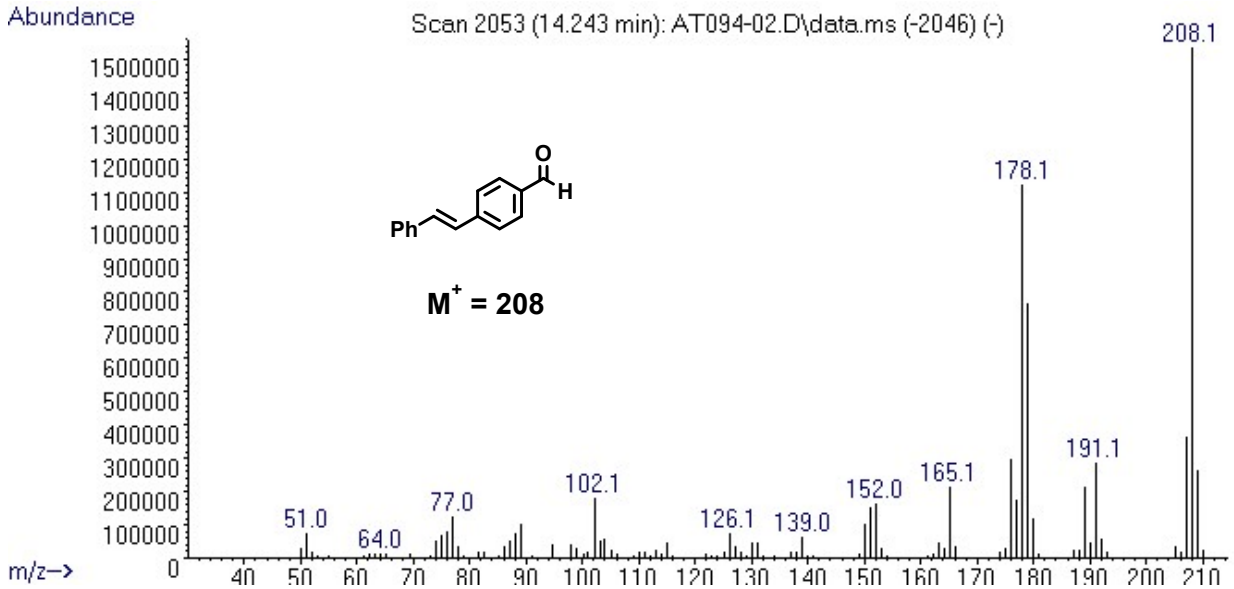

Figure S24. MS for (*E*)-4-styrylbenzaldehyde (**2a**) detected by GC

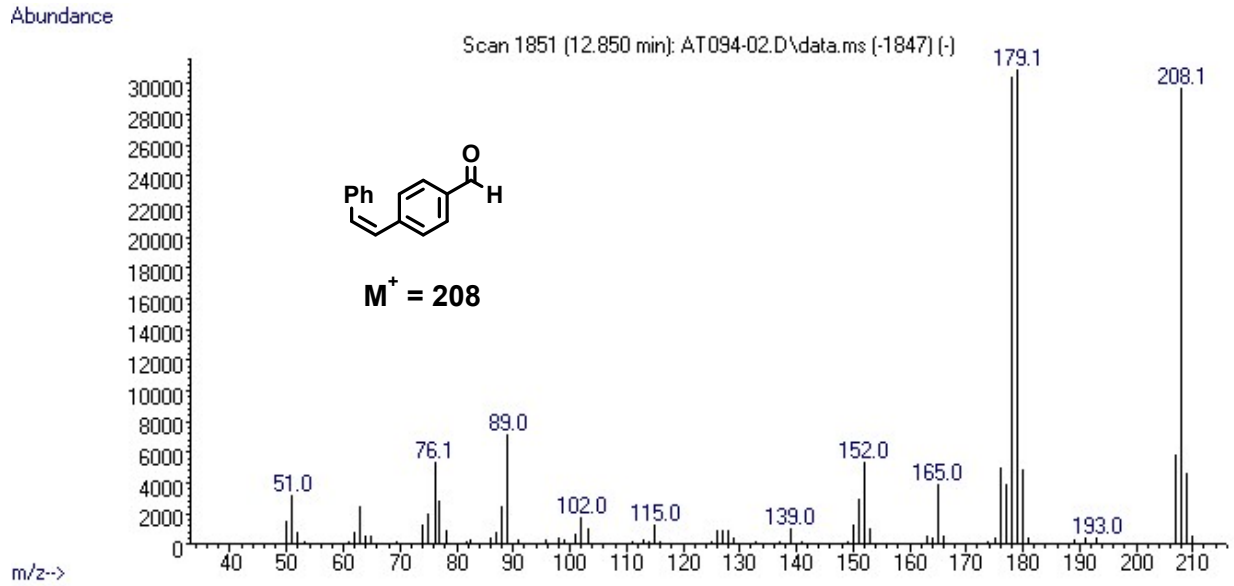

Figure S25. MS for (*Z*)-4-styrylbenzaldehyde (**2b**) detected by GC

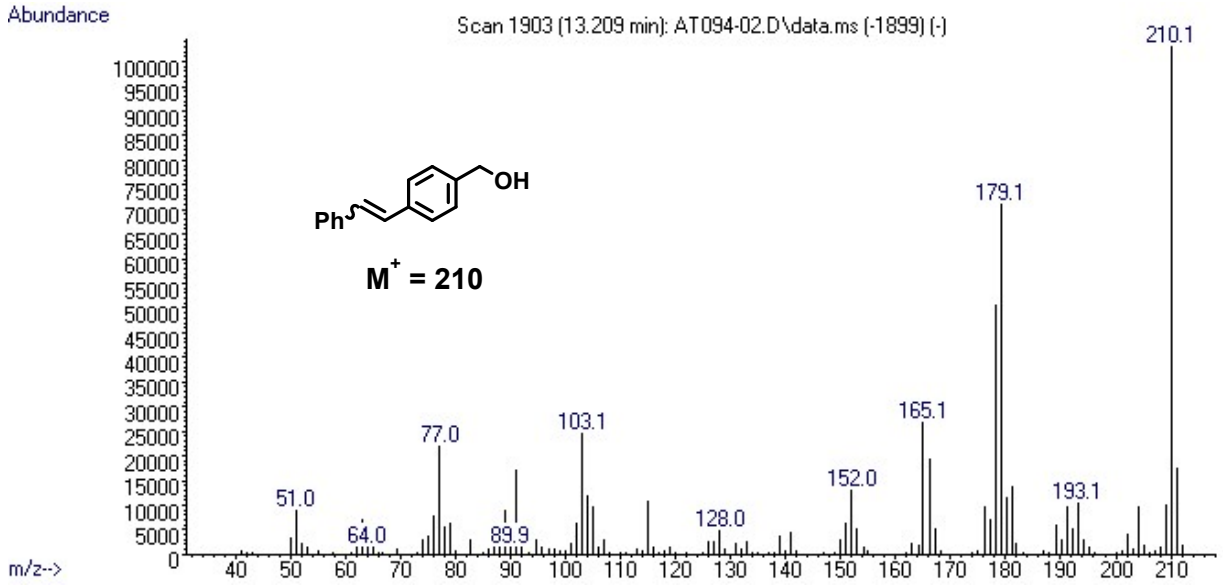

Figure S26. MS for (4-styrylphenyl)methanol detected by GC

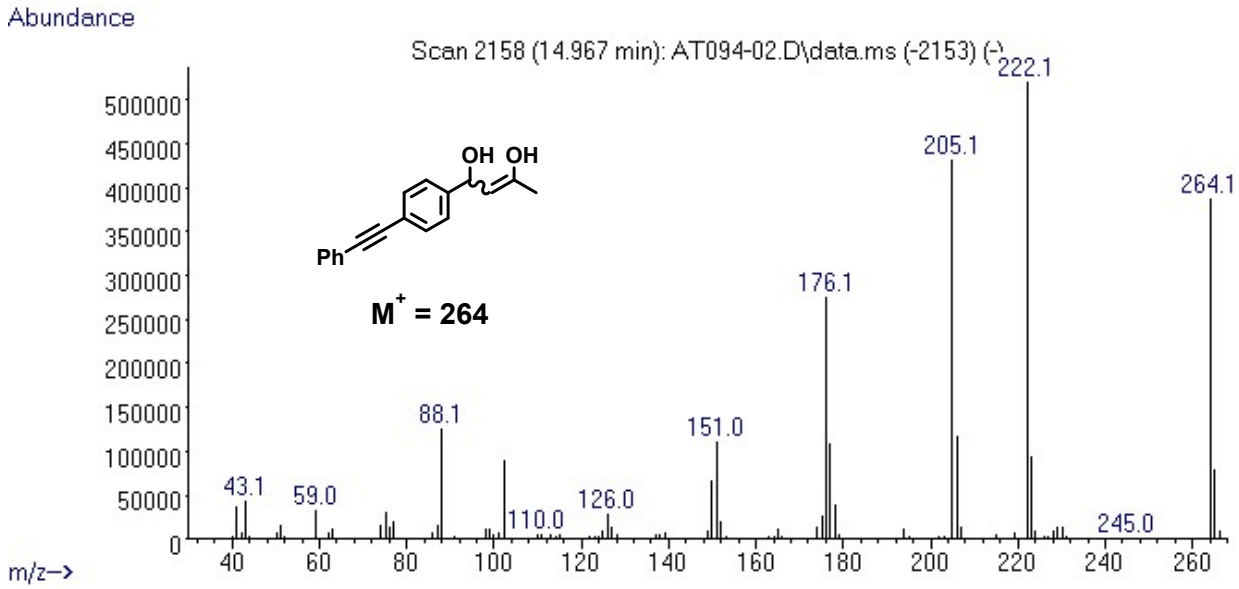

Figure S27. MS for 1-(4-(phenylethynyl)phenyl)but-2-ene-1,3-diol detected by GC

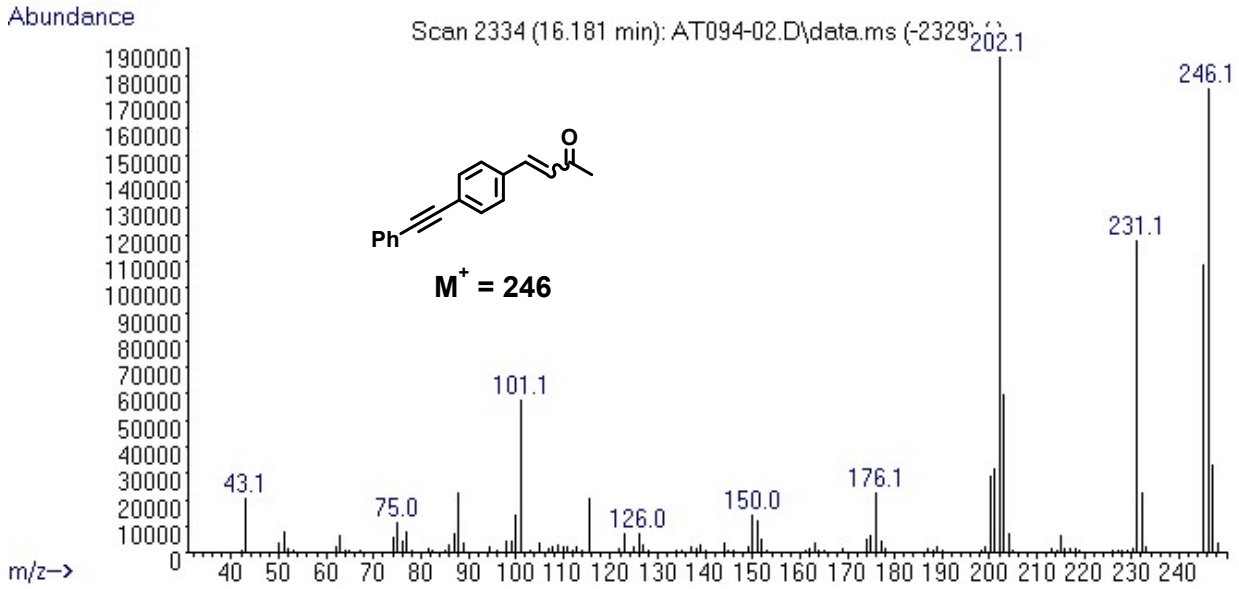

Figure S28. MS for 4-(4-(phenylethynyl)phenyl)but-3-en-2-one detected by GC

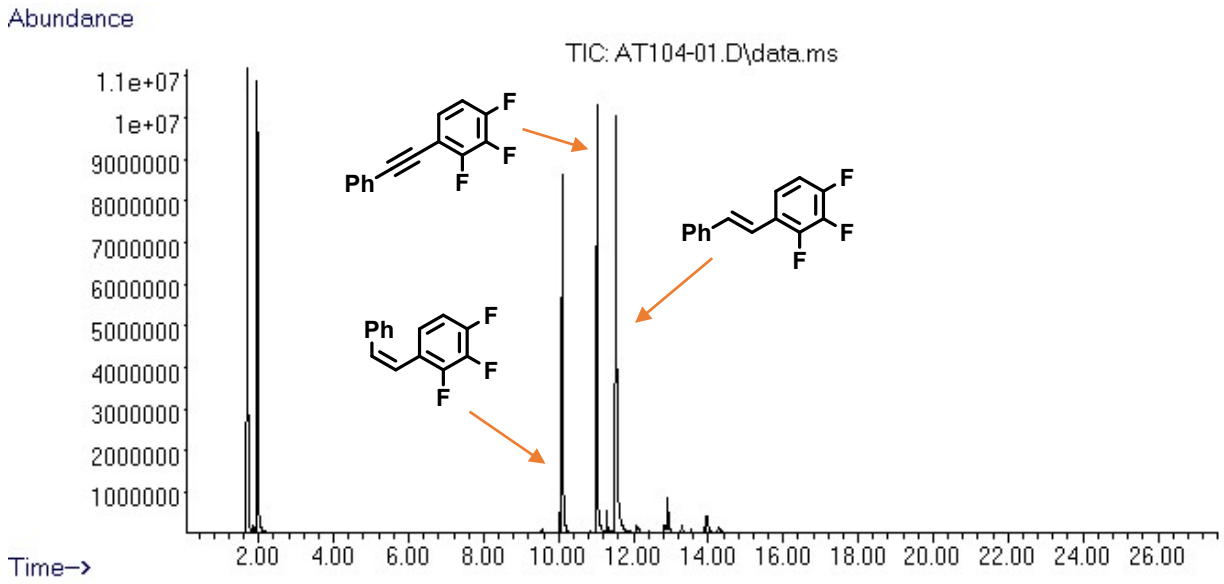

Figure S29. GC of the crude mixture of 1,2,3-trifluoro-4-(phenylethynyl)benzene (**3**) transfer semihydrogenation with iPrOH catalyzed by **Mn-2**

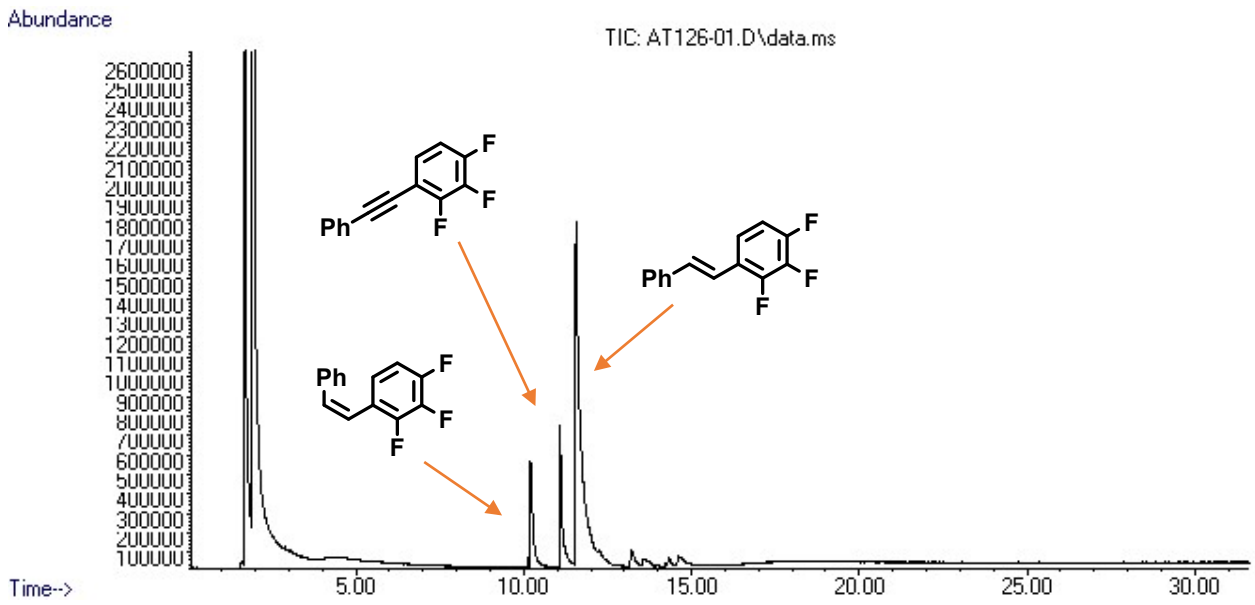

Figure S30. GC of the crude mixture of 1,2,3-trifluoro-4-(phenylethynyl)benzene (**3**) transfer semihydrogenation with iPrOH catalyzed by **Mn-2** after heating at 100 °C for 16 h

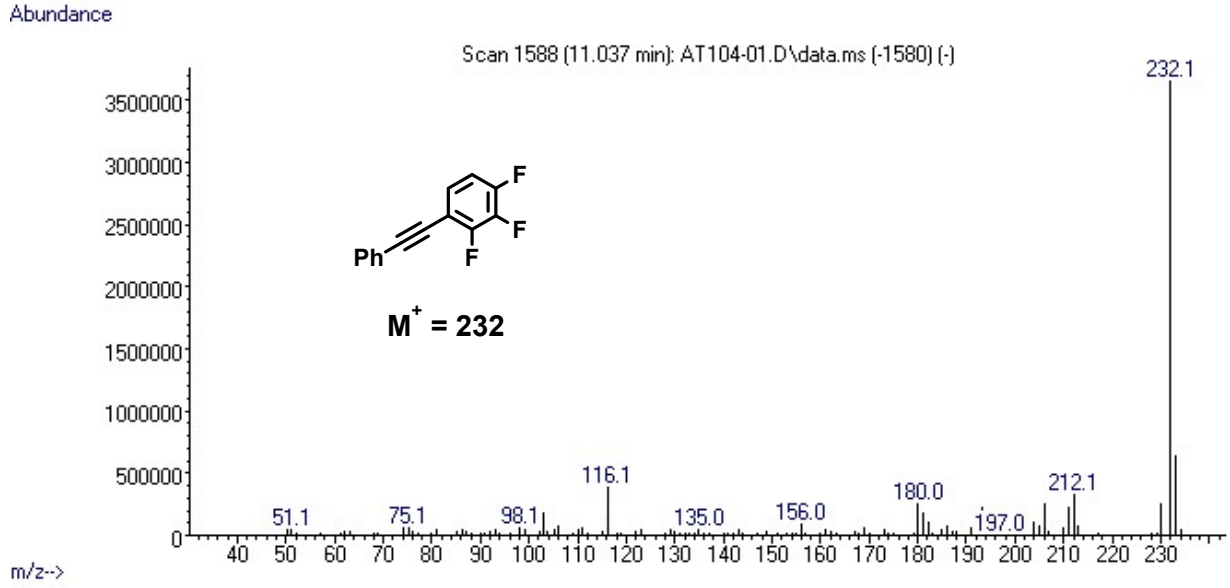

Figure S31. MS for 1,2,3-trifluoro-4-(phenylethynyl)benzene (**3**) detected by GC

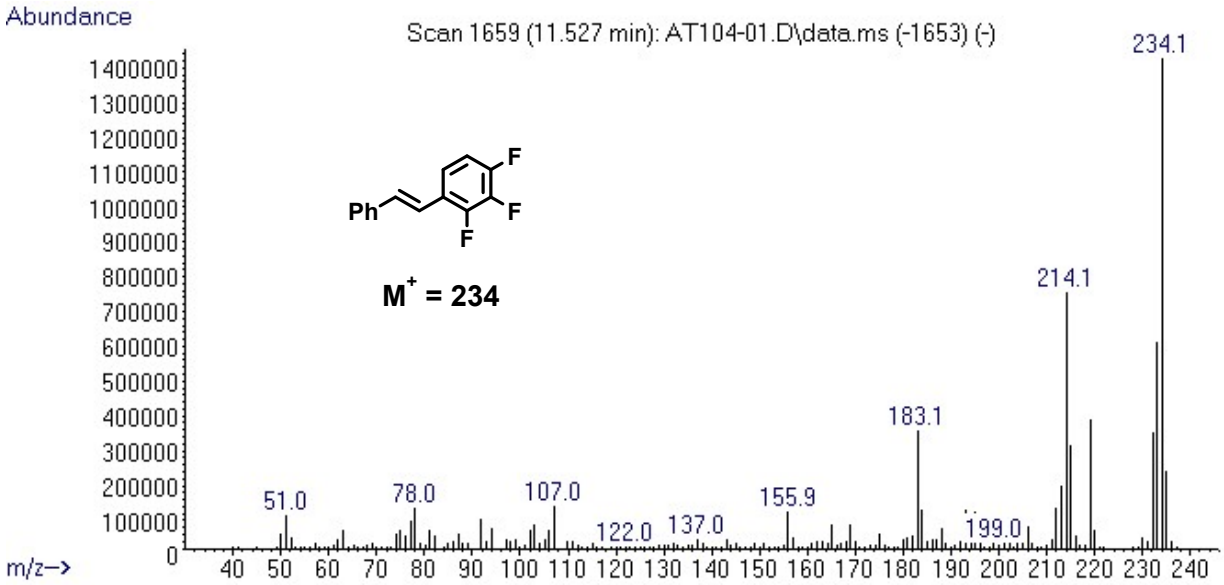

Figure S32. MS for (*E*)-1,2,3-trifluoro-4-styrylbenzene (**3a**) detected by GC

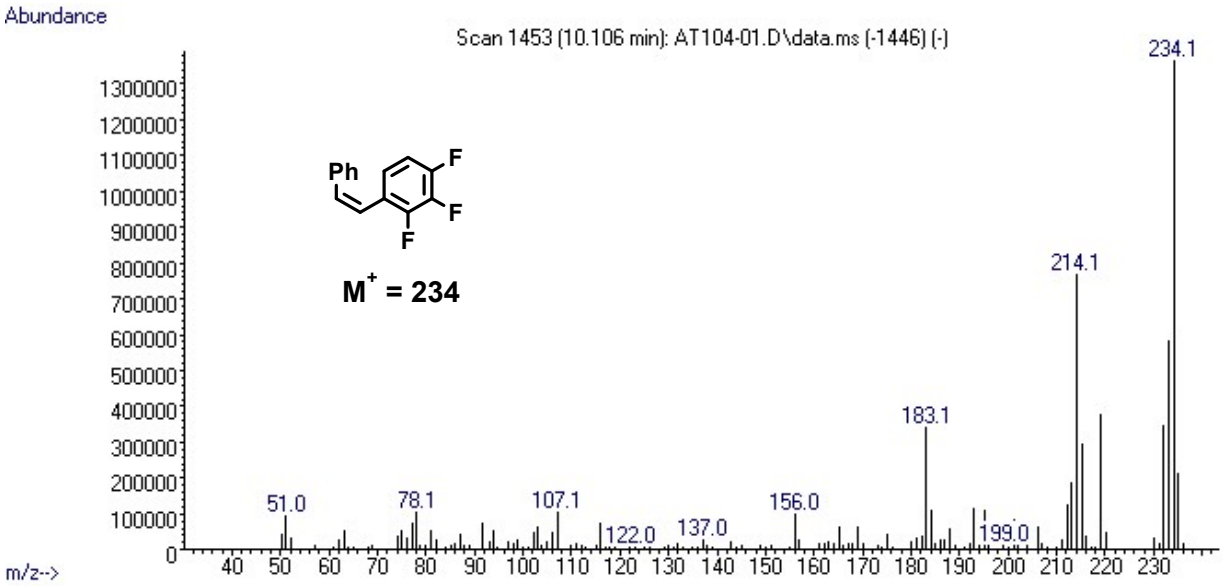

Figure S33. MS for (*Z*)-1,2,3-trifluoro-4-styrylbenzene (**3b**) detected by GC

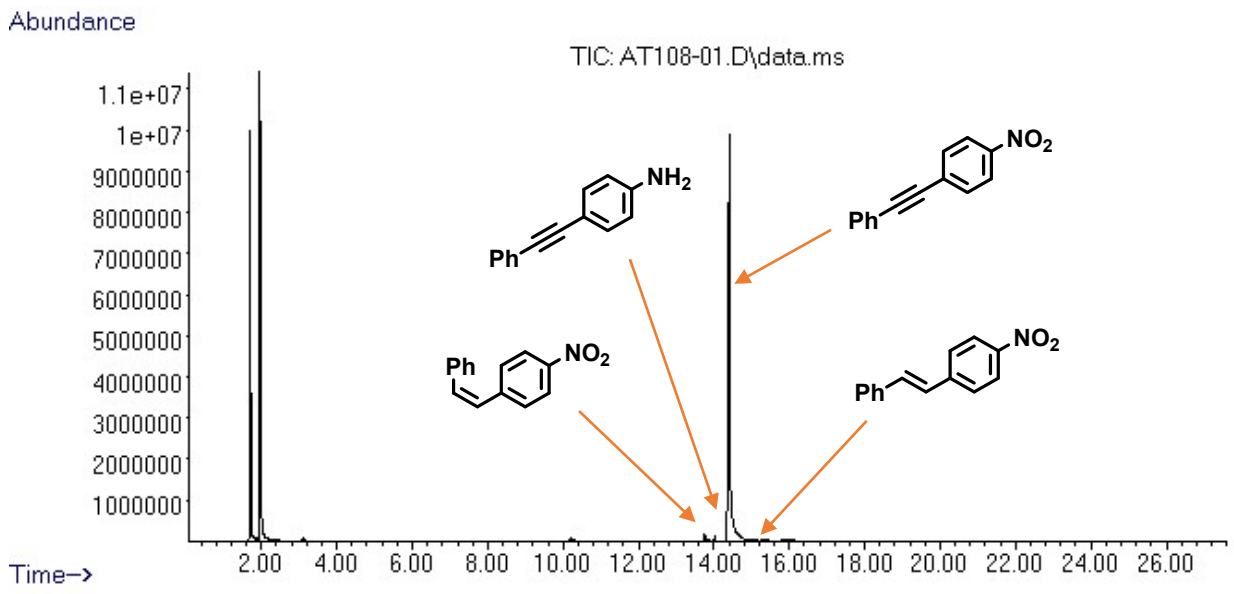

Figure S34. GC of the crude mixture of 1-nitro-4-(phenylethynyl)benzene (**4**) transfer semihydrogenation with iPrOH catalyzed by **Mn-2**

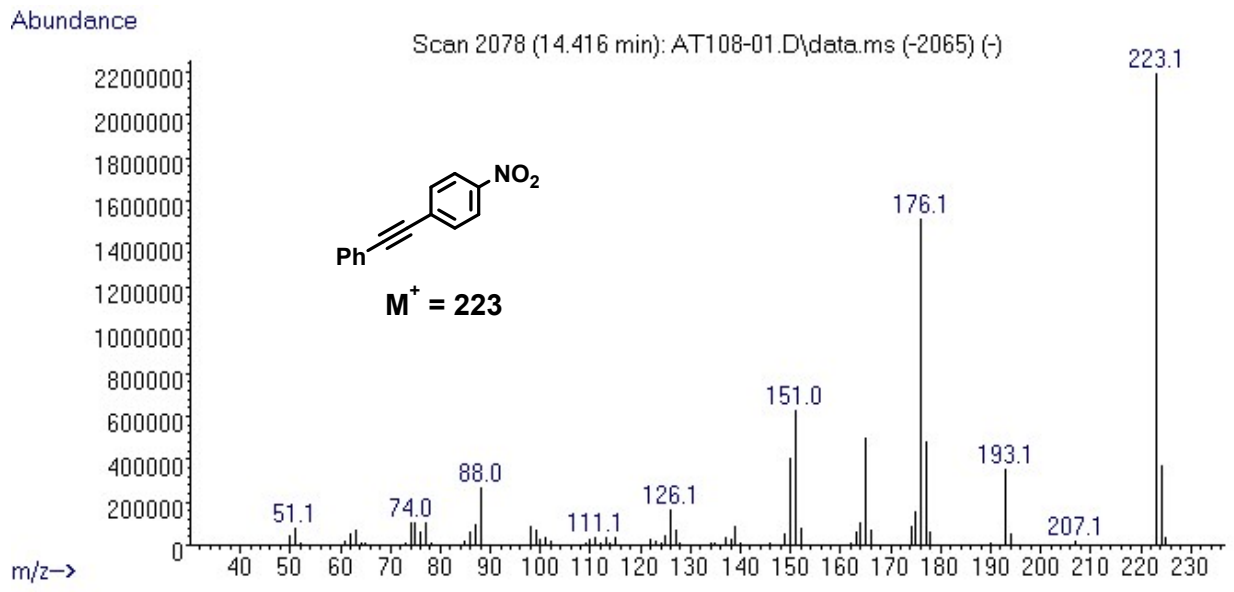

Figure S35. MS for 1-nitro-4-(phenylethynyl)benzene (**4**) detected by GC

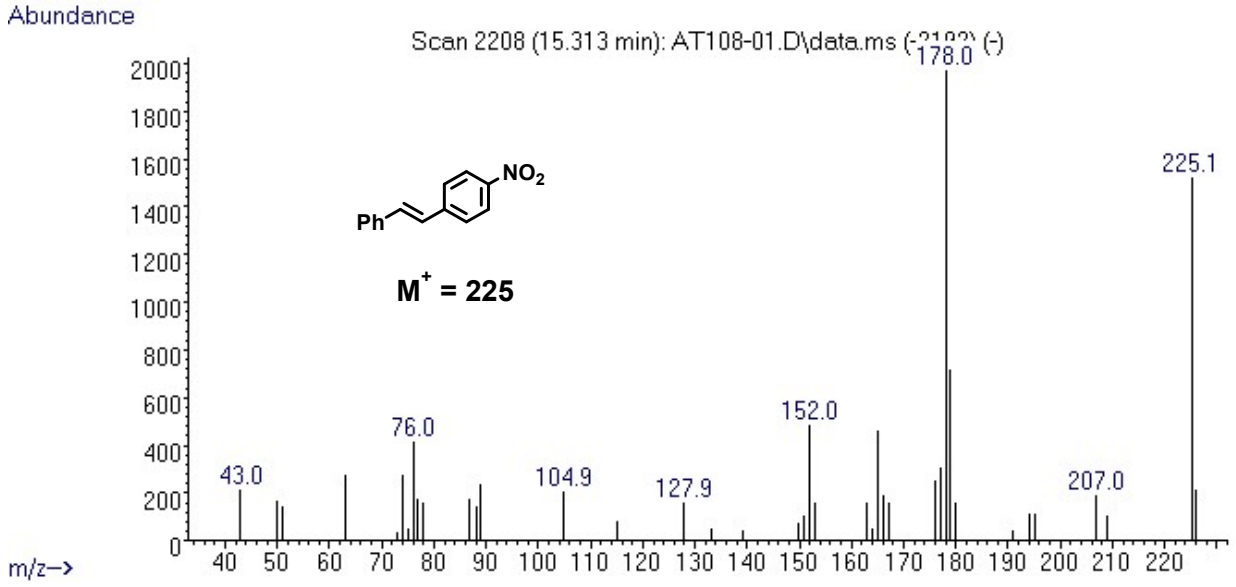

Figure S36. MS for (*E*)-1-nitro-4-styrylbenzene (**4a**) detected by GC

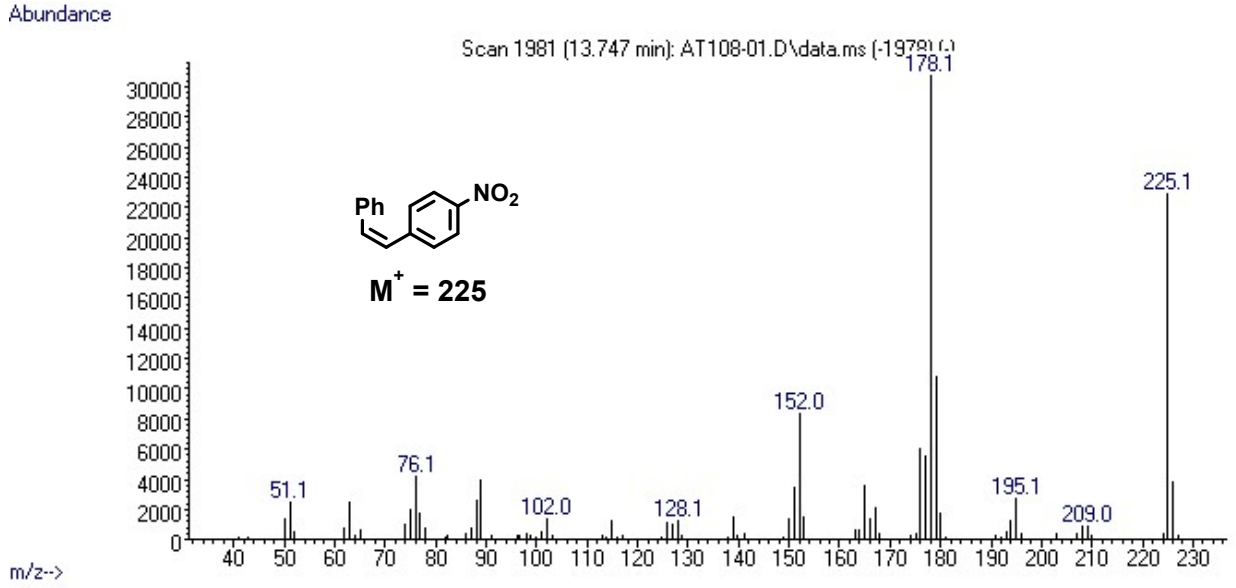

Figure S37. MS for (*Z*)-1-nitro-4-styrylbenzene (**4b**) detected by GC

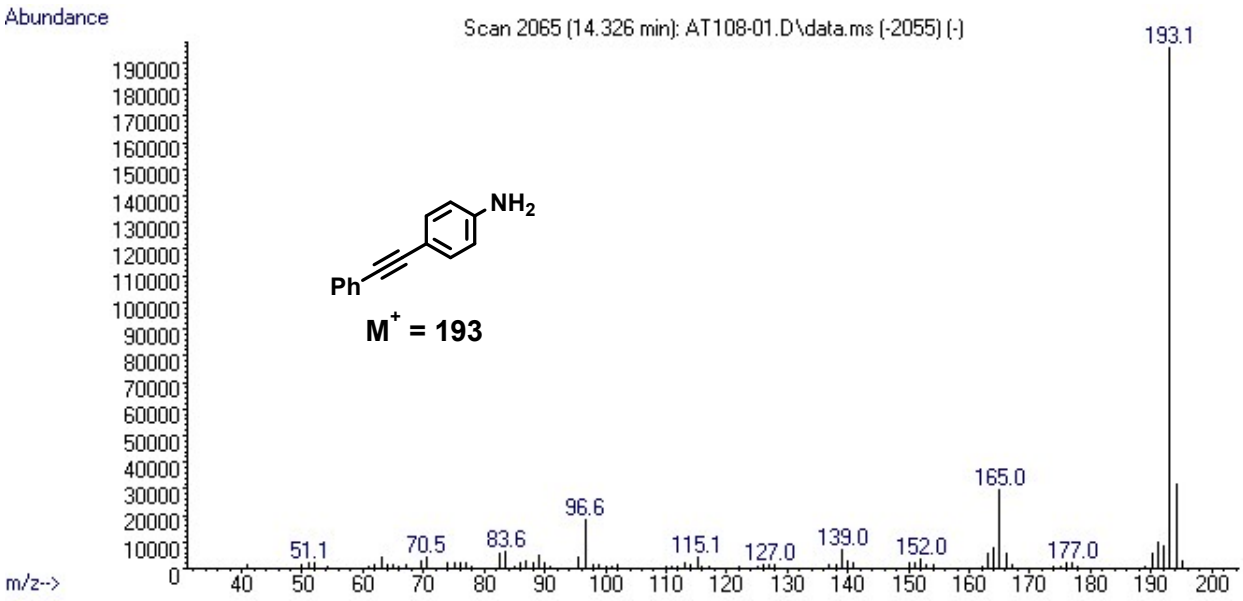

Figure S38. MS for 4-(phenylethynyl)aniline detected by GC

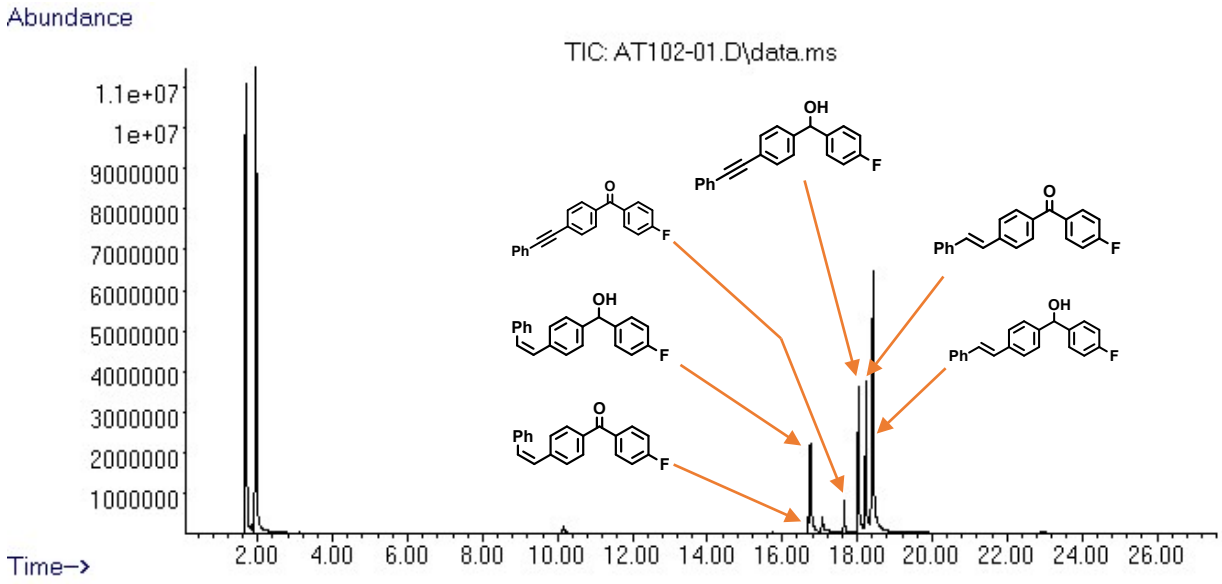

Figure S39. GC of the crude mixture of 4-fluoro-4'-(phenylethynyl)-benzophenone (**5**) transfer semihydrogenation with iPrOH catalyzed by **Mn-2**

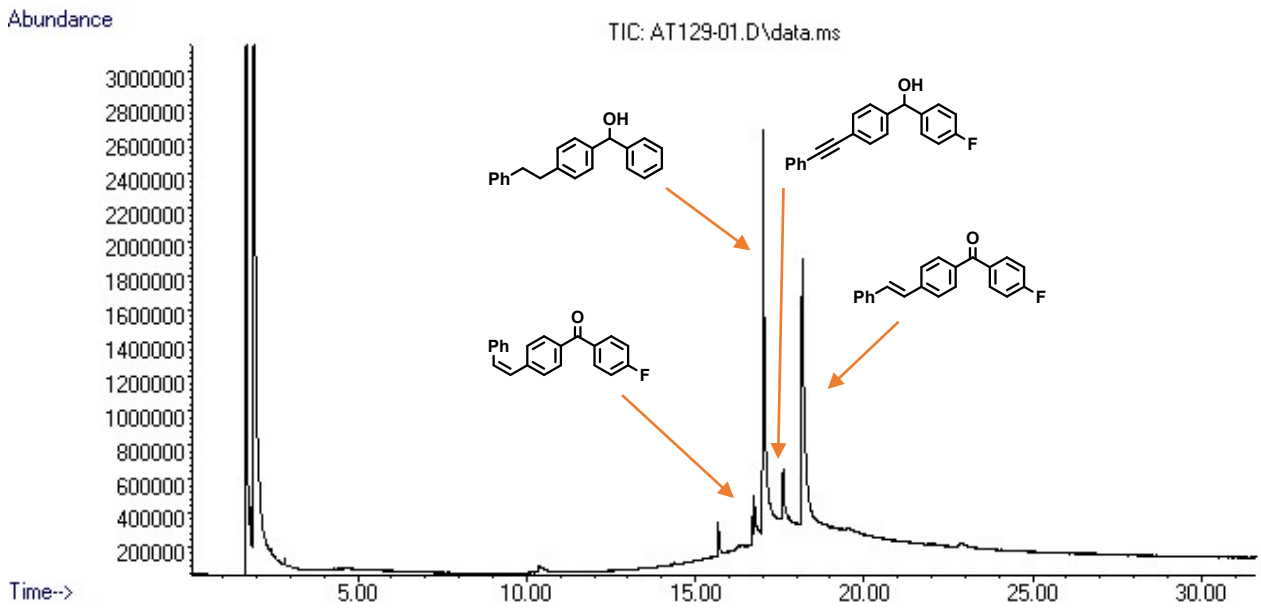

Figure S40. GC of the crude mixture of 4-fluoro-4'-(phenylethynyl)-benzophenone (**5**) transfer semihydrogenation with iPrOH catalyzed by **Mn-2** after heating at 100 °C for 16 h

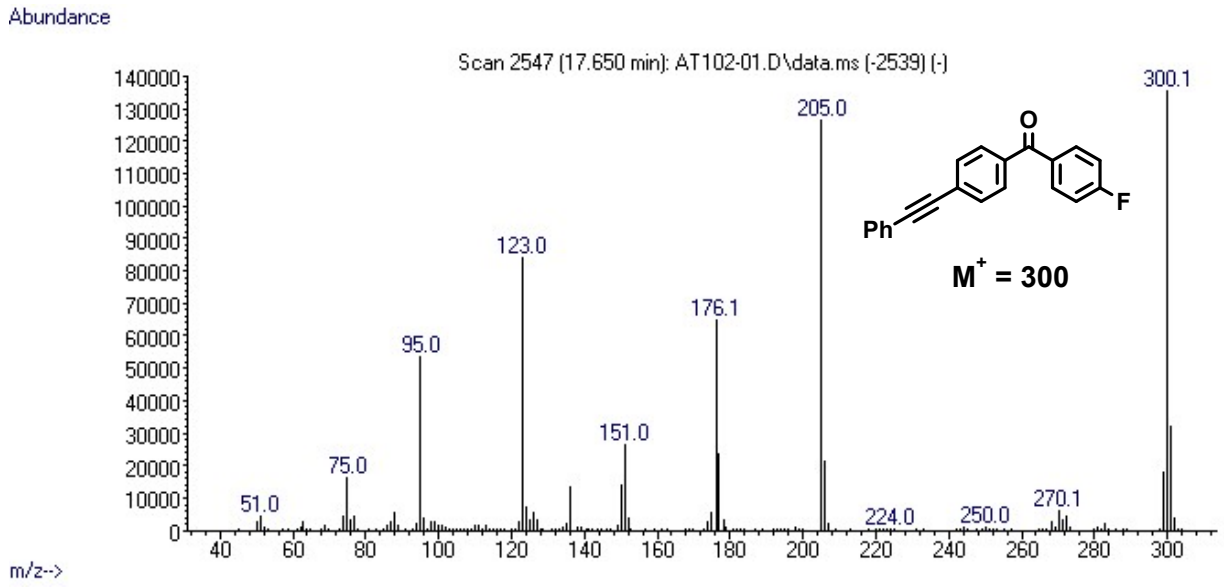

Figure S41. MS for 4-fluoro-4'-(phenylethynyl)-benzophenone (**5**) detected by GC

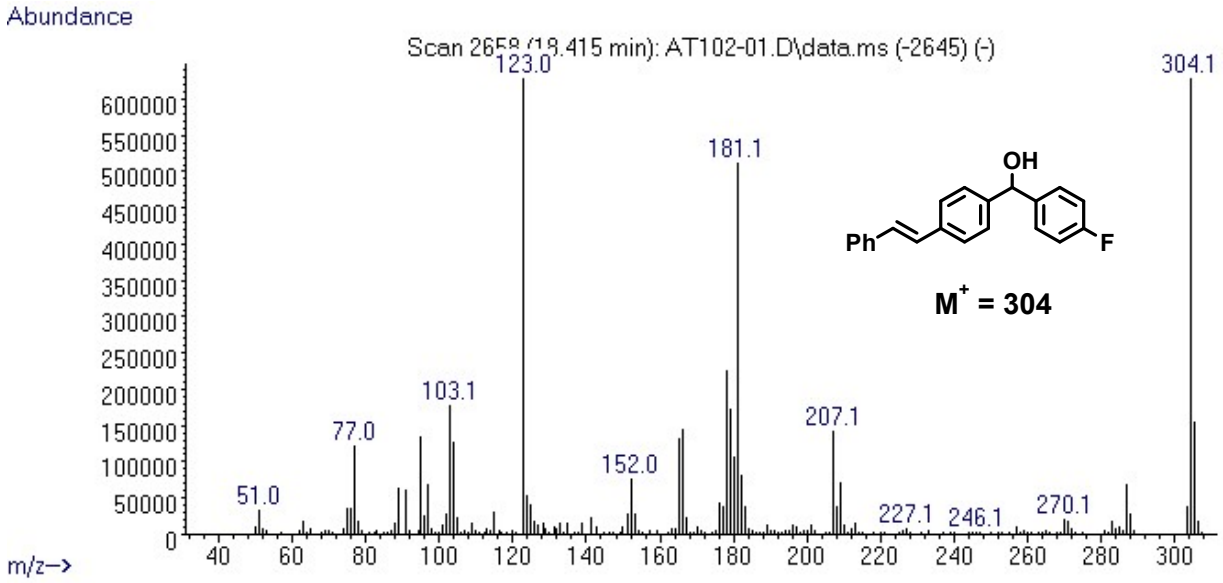

Figure S42. MS for (*E*)-(4-fluorophenyl)(4-styrylphenyl)methanol (**5a**) detected by GC

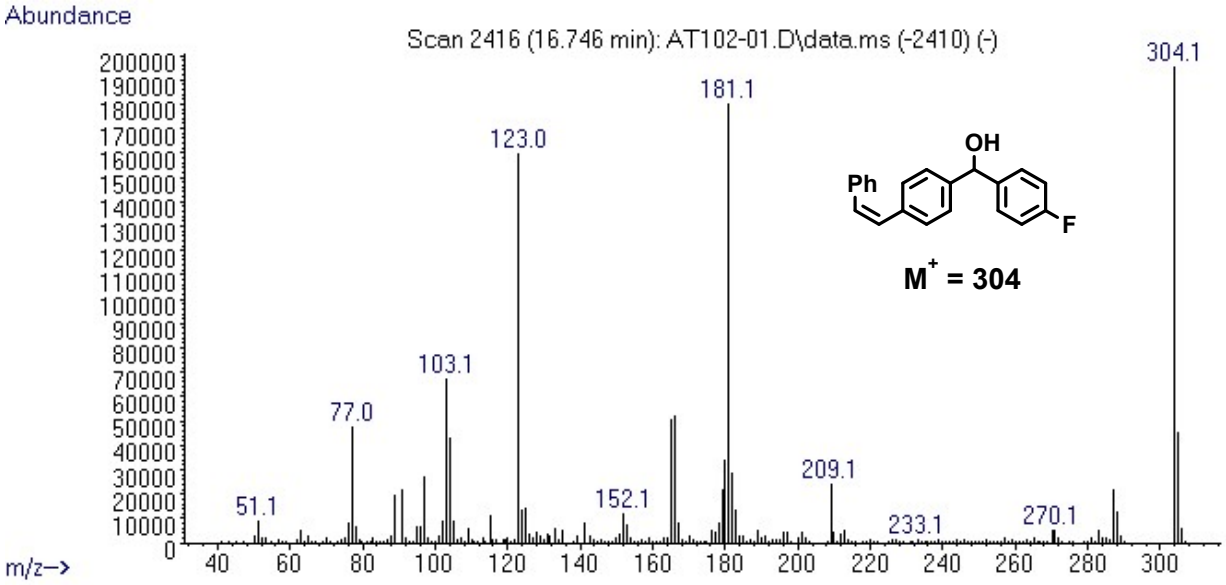

Figure S43. MS for (*Z*)-(4-fluorophenyl)(4-styrylphenyl)methanol (**5b**) detected by GC

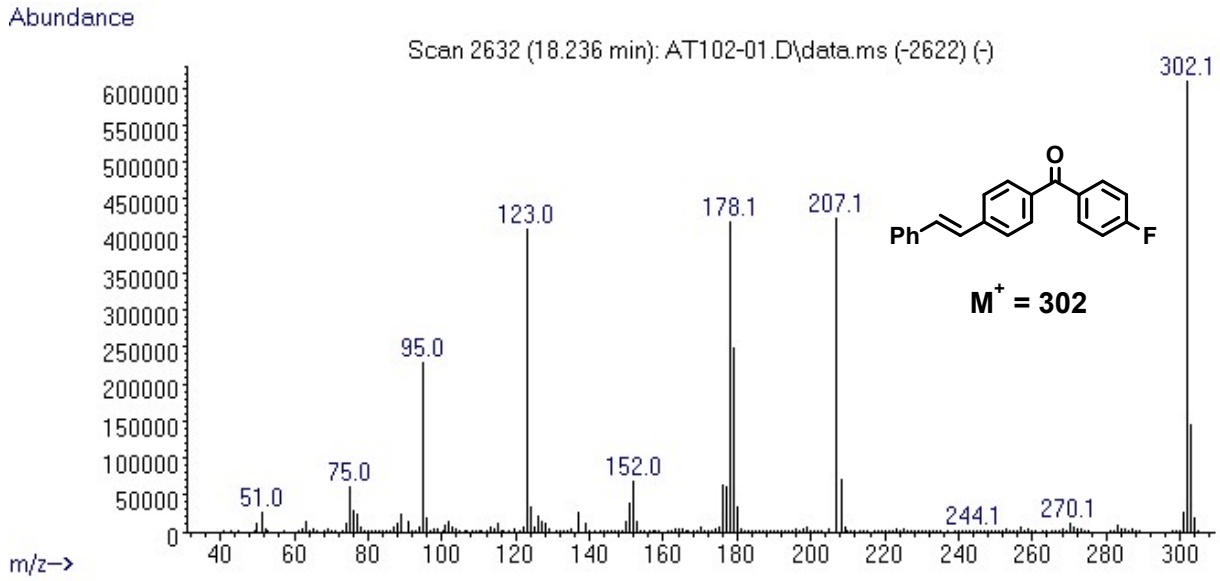

Figure S44. MS for (*E*)-(4-fluorophenyl)(4-styrylphenyl)methanone (**5a'**) detected by GC

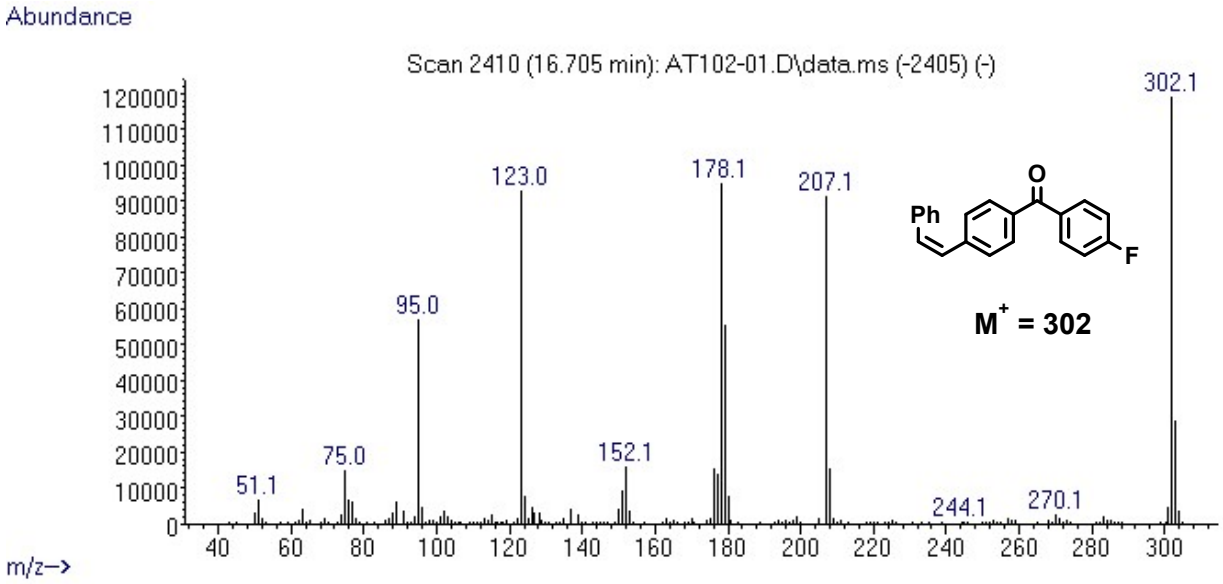

Figure S45. MS for (*Z*)-(4-fluorophenyl)(4-styrylphenyl)methanone (**5b'**) detected by GC

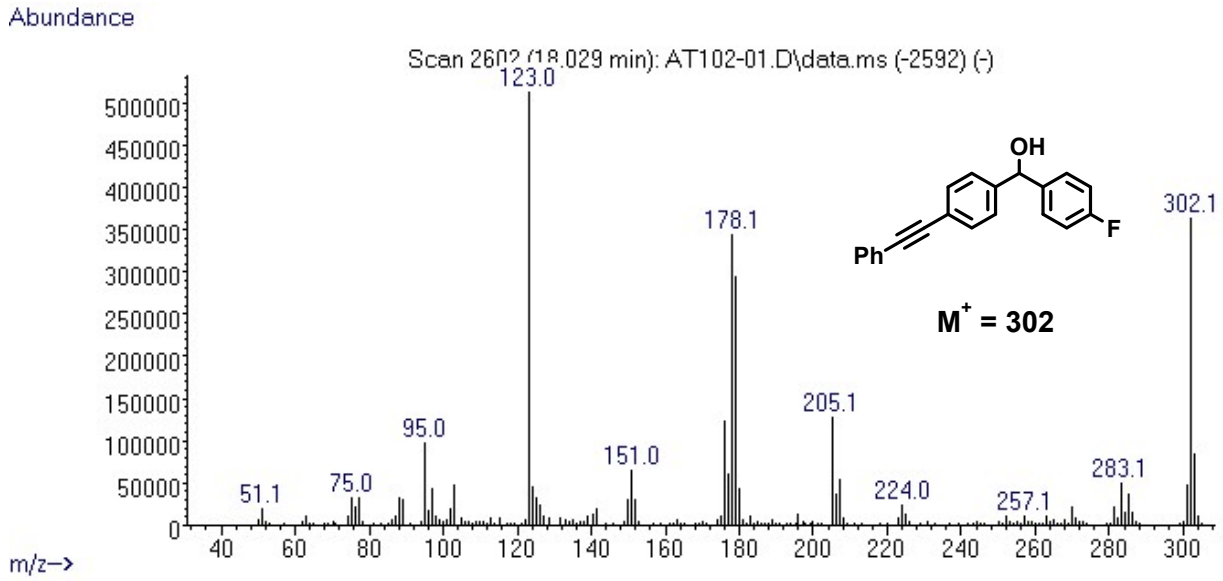

Figure S46. MS for (4-fluorophenyl)(4-(phenylethynyl)phenyl)methanol detected by GC

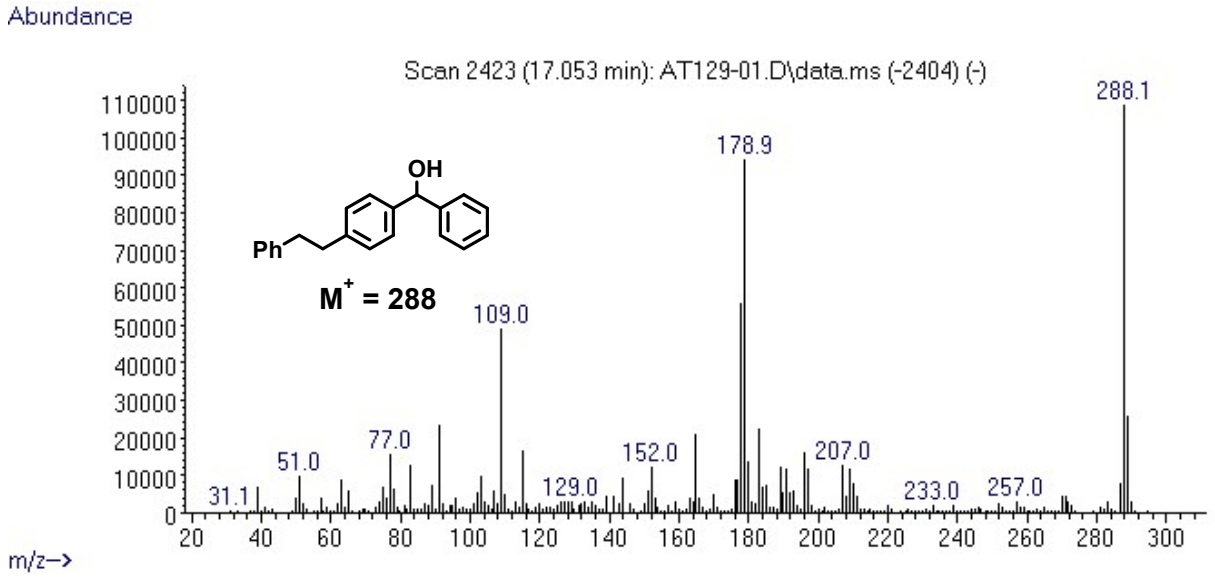

Figure S47. MS for (4-phenethylphenyl)(phenyl)methanol detected by GC

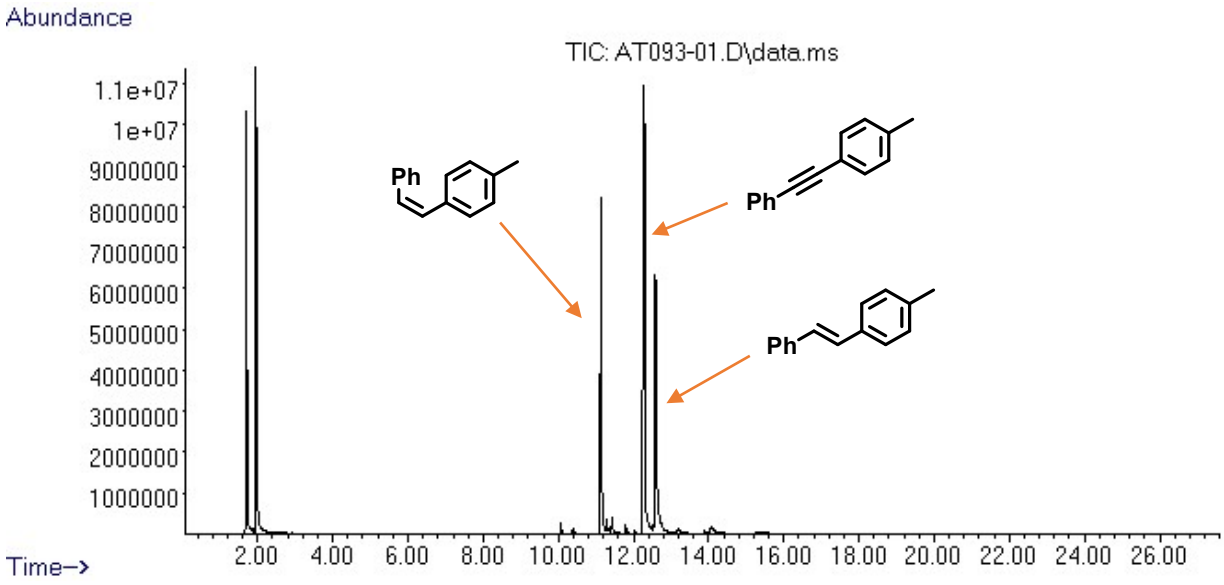

Figure S48. GC of the crude mixture of 1-methyl-4-(phenylethynyl)benzene (**6**) transfer semihydrogenation with iPrOH catalyzed by **Mn-2**

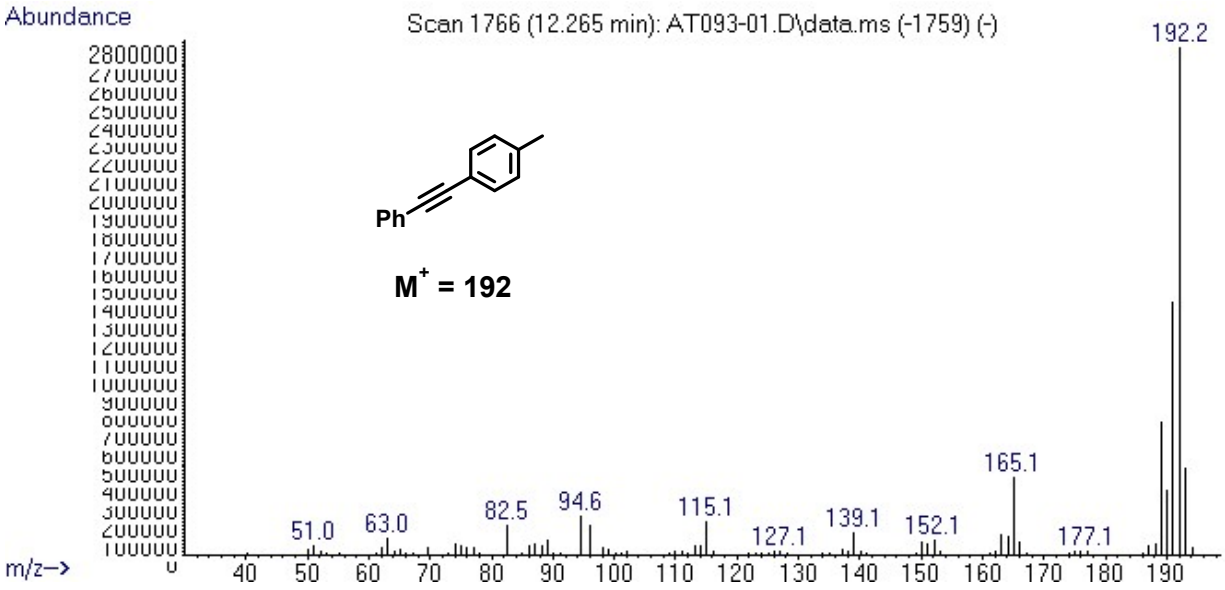

Figure S49. MS for 1-methyl-4-(phenylethynyl)benzene (**6**) detected by GC

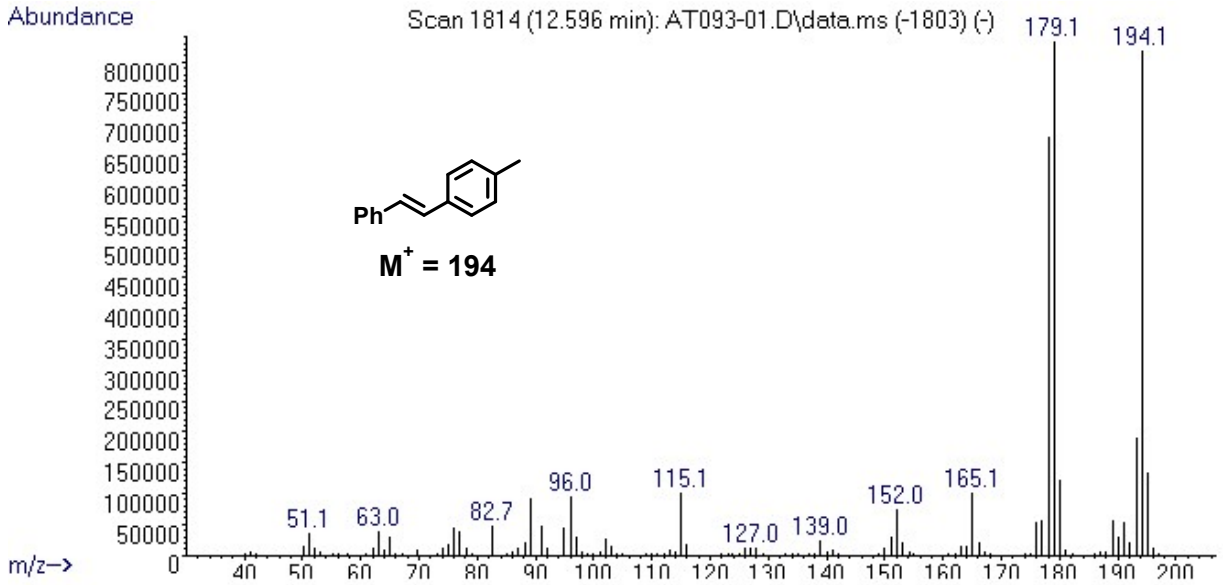

Figure S50. MS for (*E*)-1-methyl-4-styrylbenzene (**6a**) detected by GC

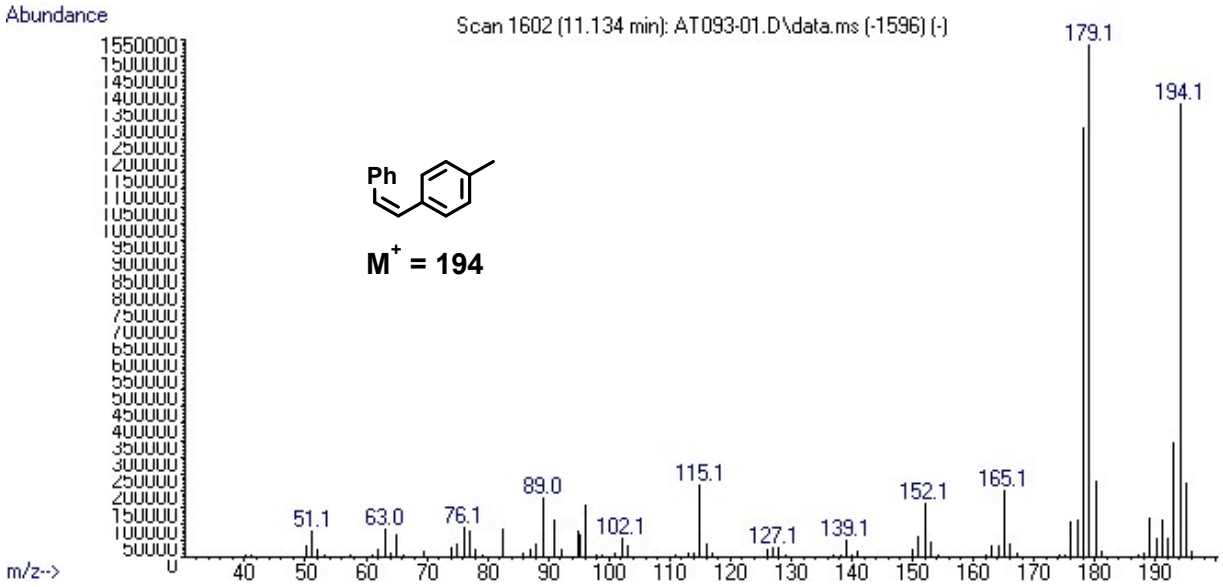

Figure S51. MS for (*Z*)-1-methyl-4-styrylbenzene (**6b**) detected by GC

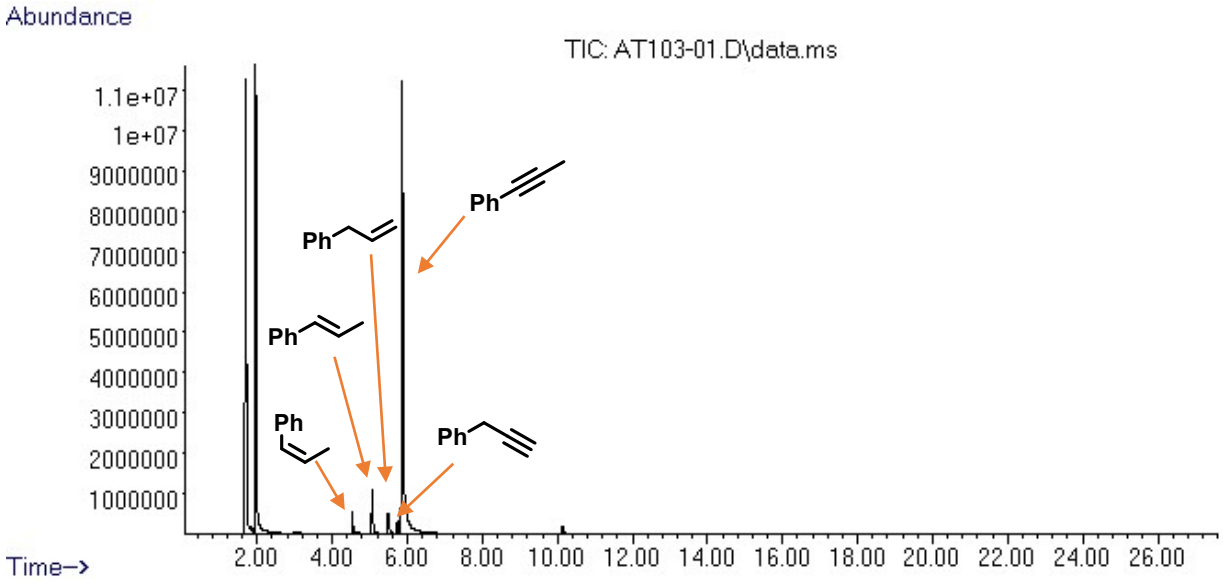

Figure S52. GC of the crude mixture of 1-phenyl-1-propyne (**7**) transfer semihydrogenation with iPrOH catalyzed by **Mn-2**

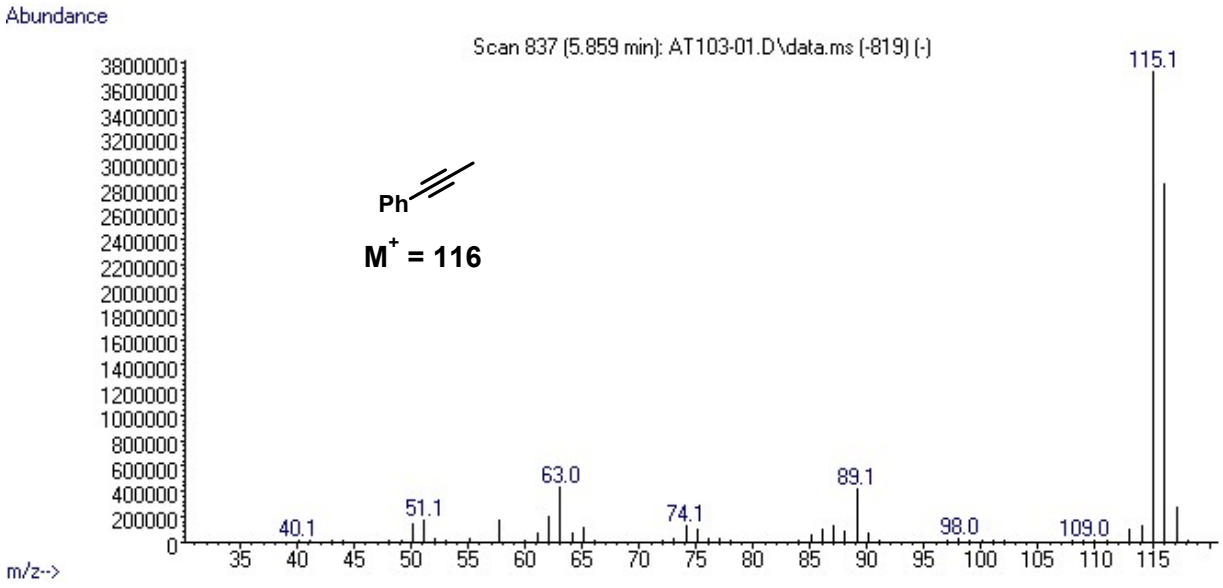

Figure S53. MS for 1-phenyl-1-propyne (**7**) detected by GC

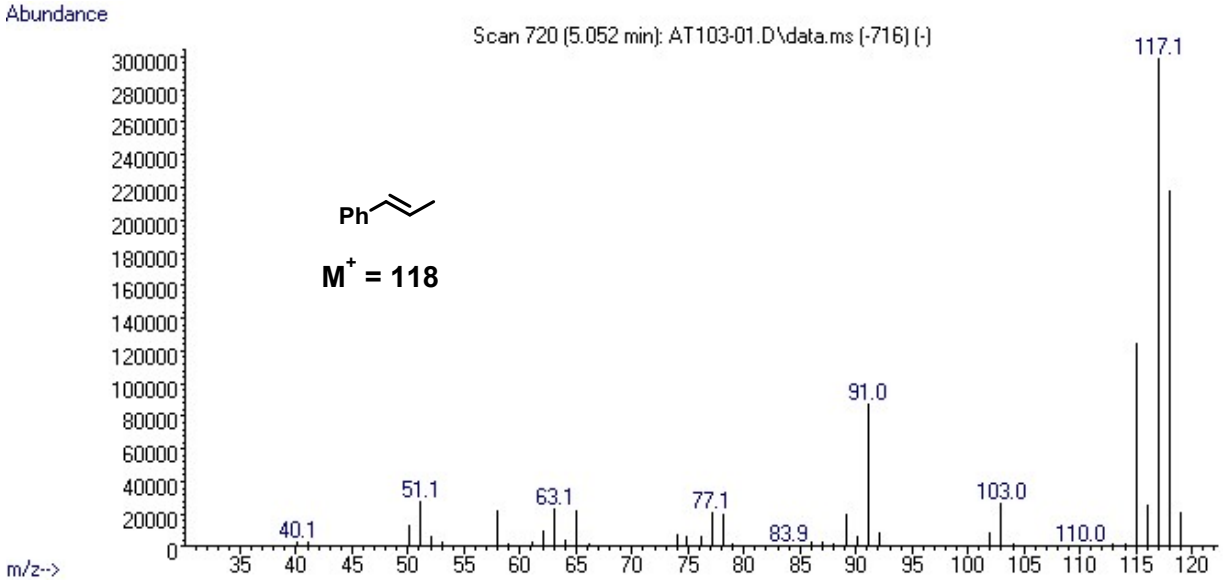

Figure S54. MS for (*E*)-prop-1-en-1-ylbenzene (**7a**) detected by GC

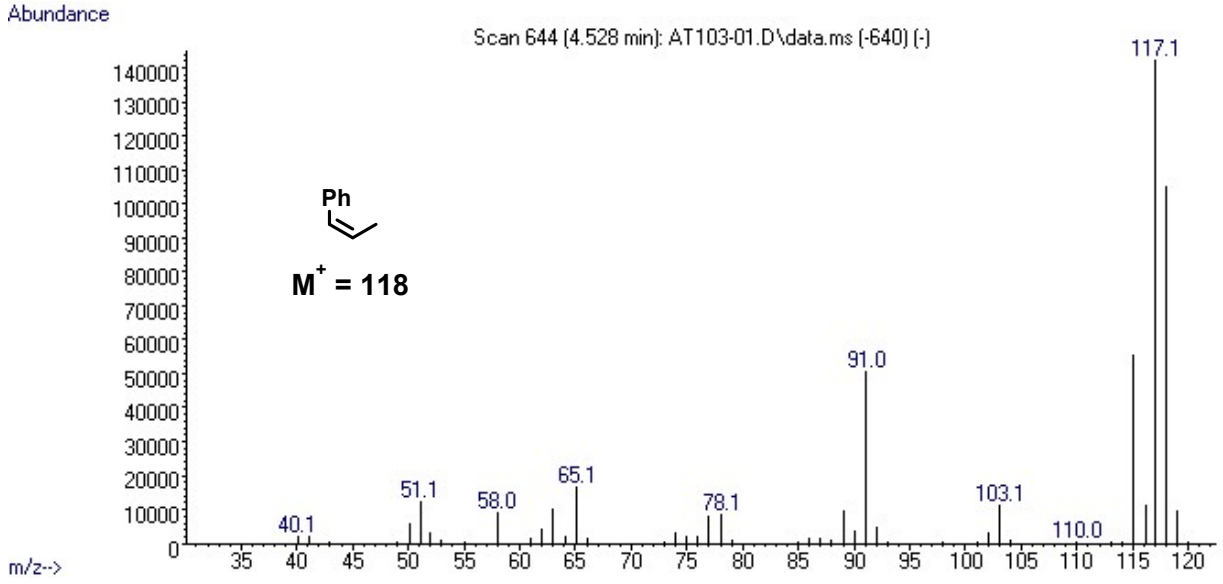

Figure S55. MS for (*Z*)-prop-1-en-1-ylbenzene (**7b**) detected by GC

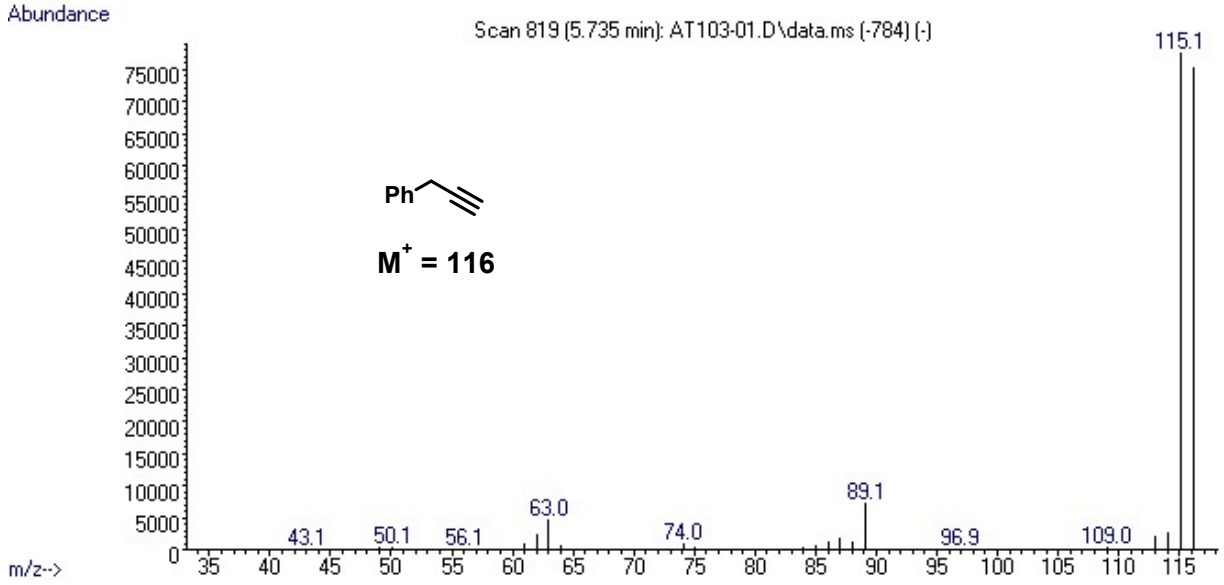

Figure S56. MS for 3-phenyl-1-propyne detected by GC

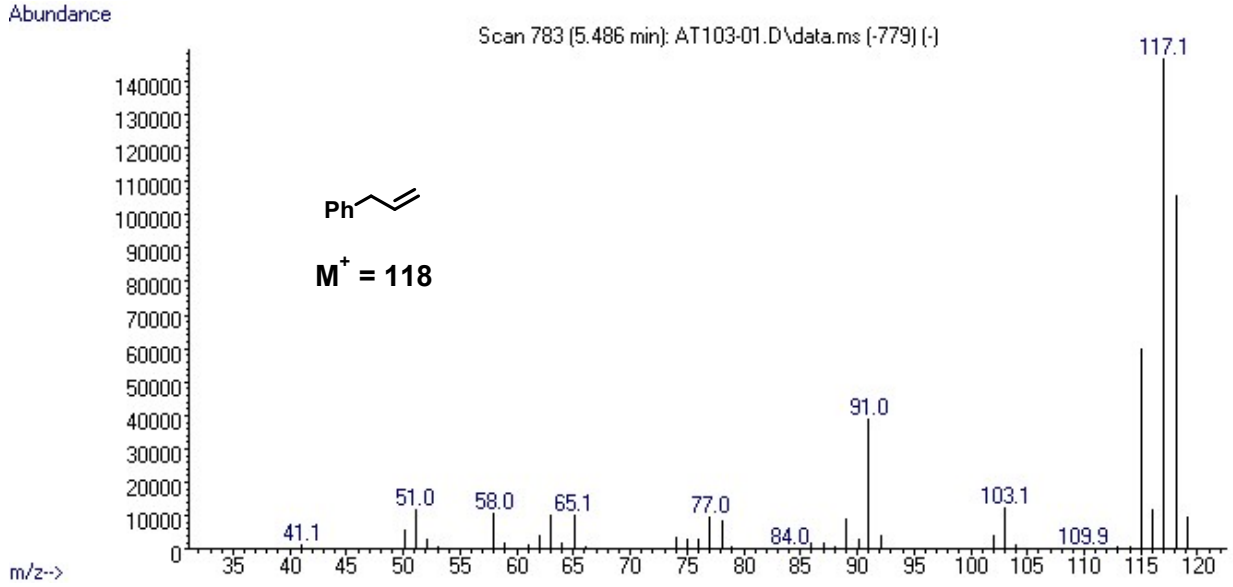

Figure S57. MS for allylbenzene detected by GC

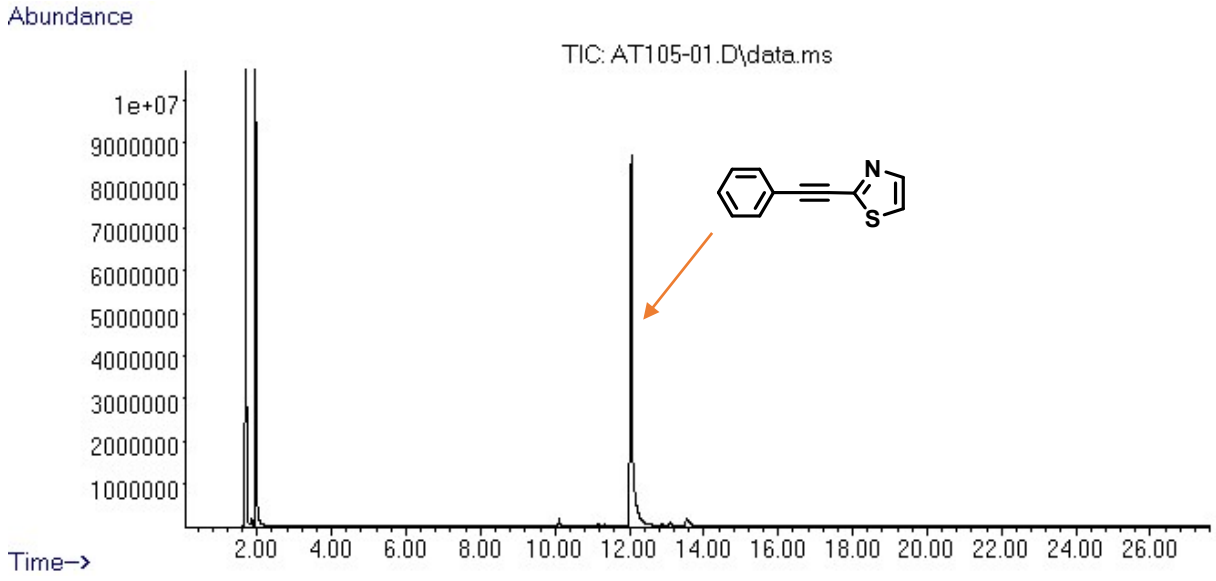

Figure S58. GC of the crude mixture of 2-(phenylethynyl)thiazole (**8**) transfer semihydrogenation with iPrOH catalyzed by **Mn-2**

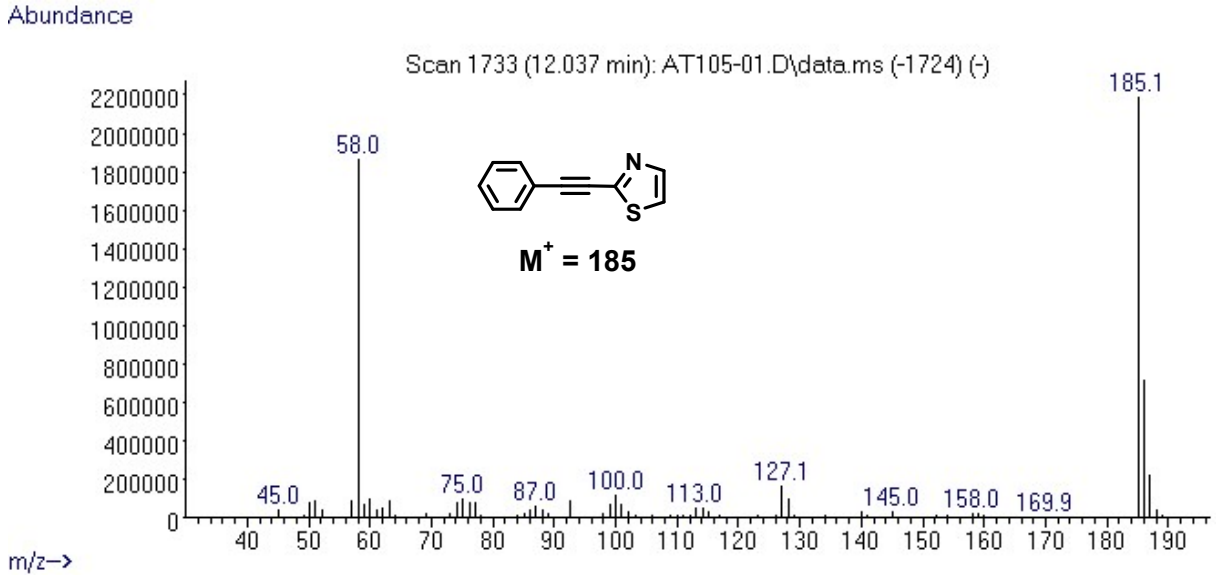

Figure S59. MS for 2-(phenylethynyl)thiazole (**8**) detected by GC

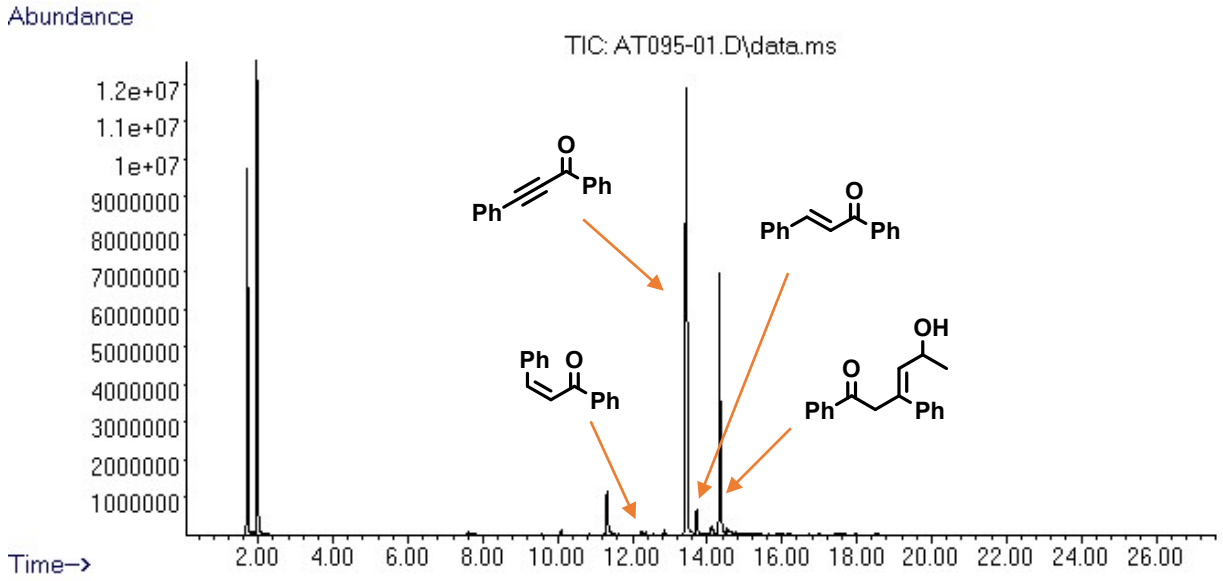

Figure S60. GC of the crude mixture of 1,3-diphenylprop-2-yn-1-one (**9**) transfer semihydrogenation with iPrOH catalyzed by **Mn-2**

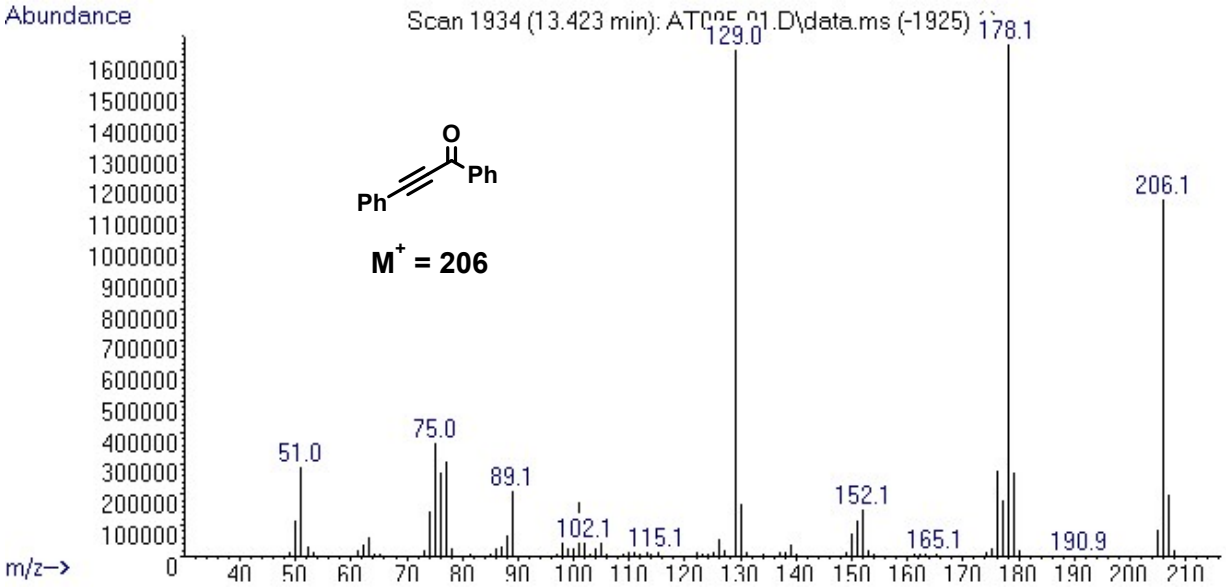

Figure S61. MS for 1,3-diphenylprop-2-yn-1-one (**9**) detected by GC

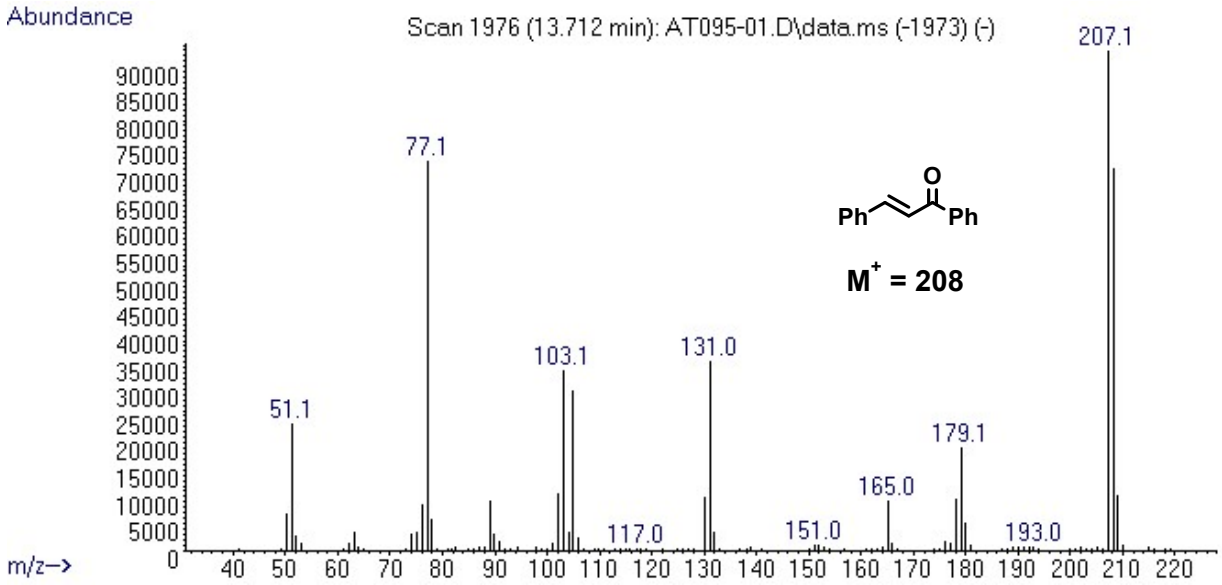

Figure S62. MS for (*E*)-chalcone (**9a**) detected by GC

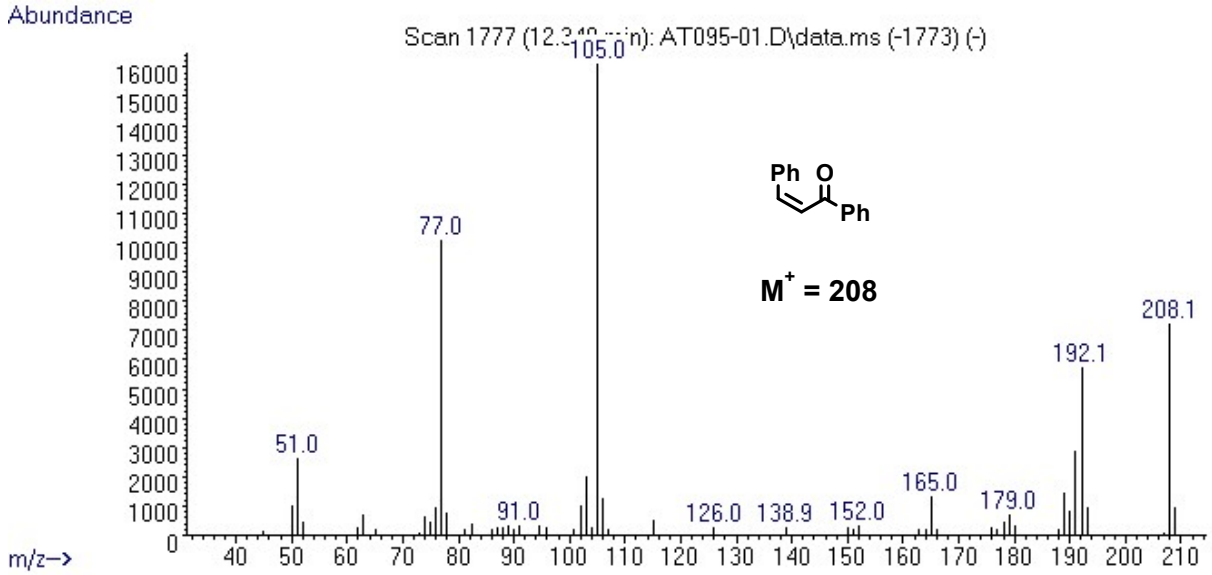

Figure S63. MS for (*Z*)-chalcone (**9b**) detected by GC

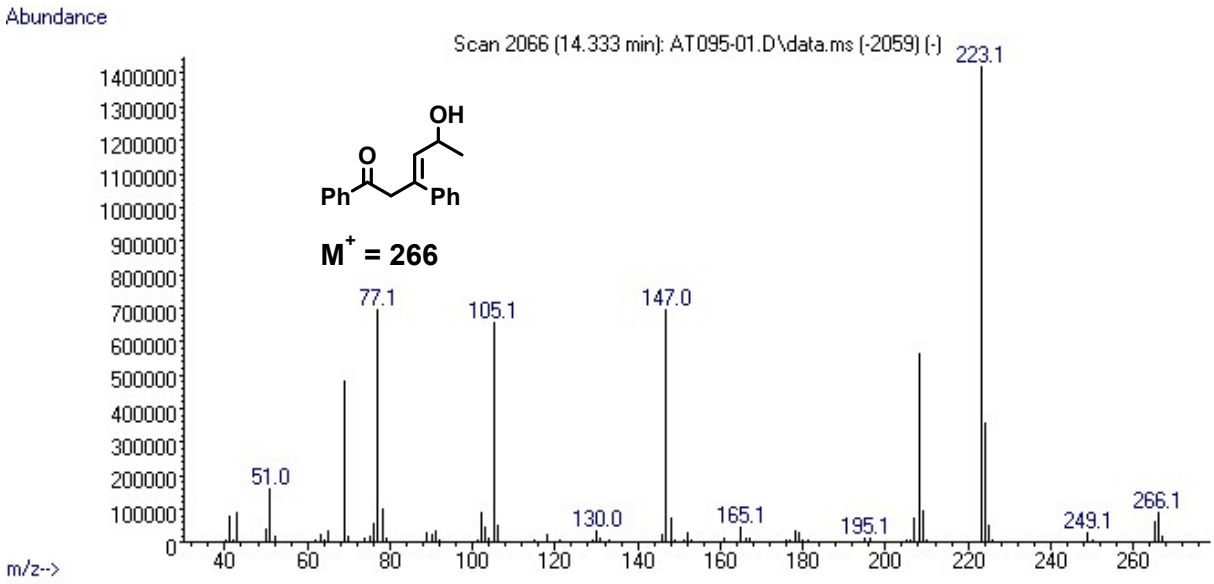

Figure S64. MS for 5-hydroxy-1,3-diphenylhex-3-en-1-one detected by GC

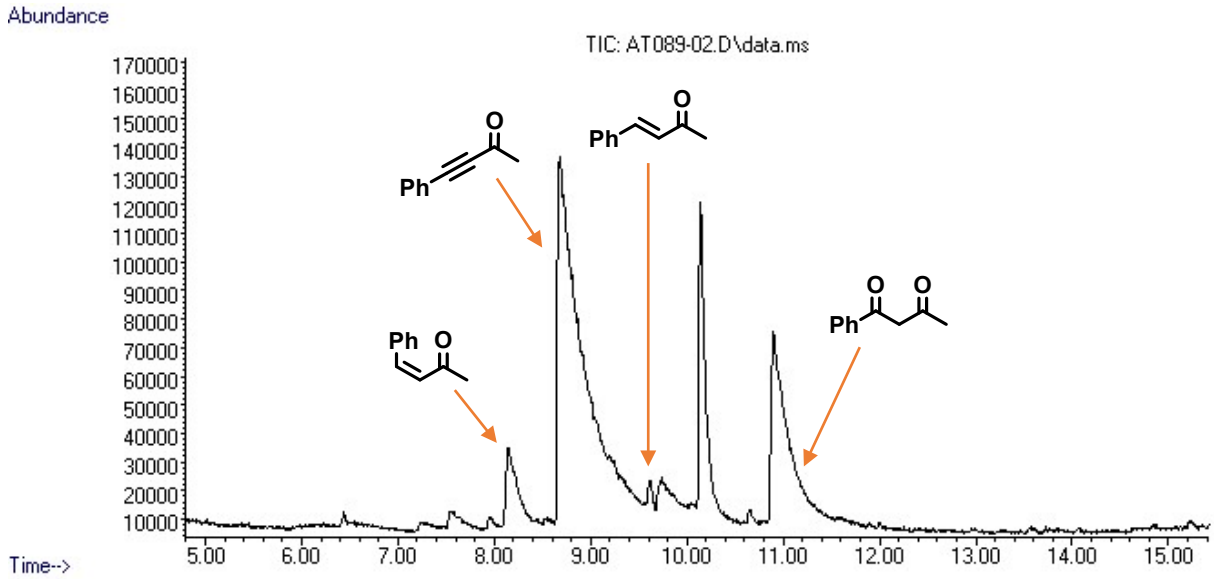

Figure S65. GC of the crude mixture of 4-phenyl-3-butyn-2-one (**10**) transfer semihydrogenation with iPrOH catalyzed by **Mn-2**

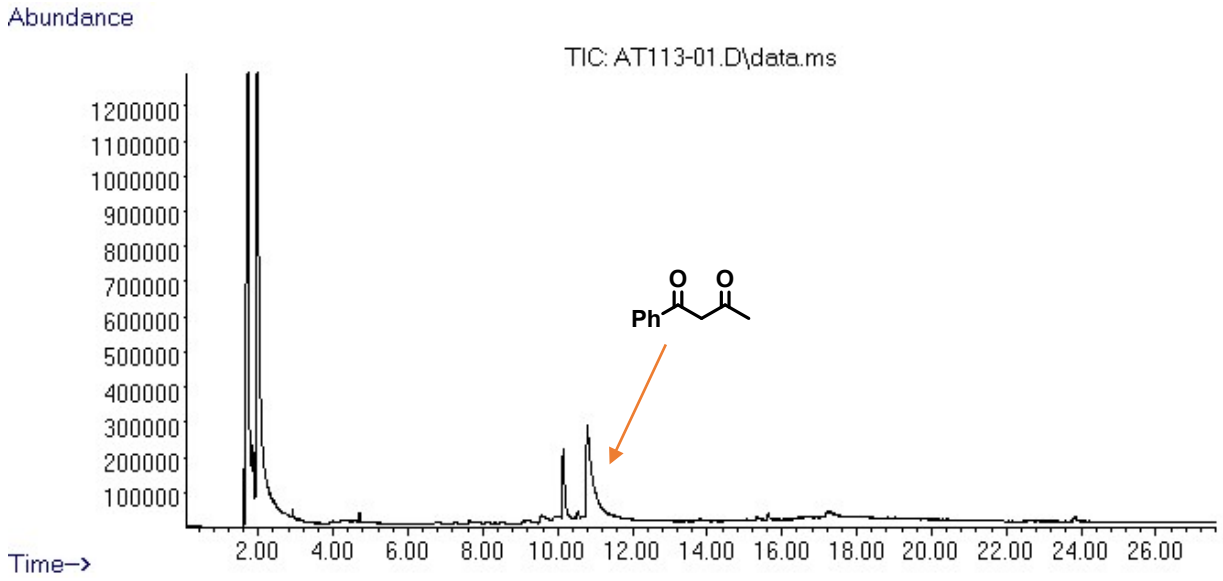

Figure S66. GC of the crude mixture of 4-phenyl-3-butyn-2-one (**10**) transfer semihydrogenation with iPrOH catalyzed by **Mn-2** after 24 h at 100 °C

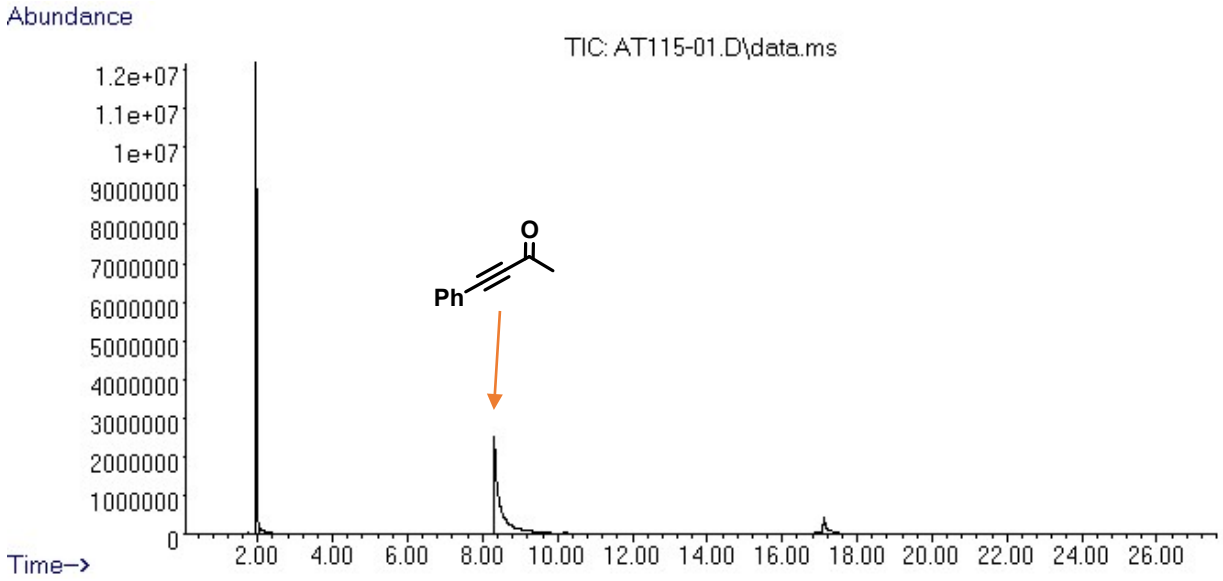

Figure S67. GC of the crude mixture of 4-phenyl-3-butyn-2-one (**10**) (0.224 mmol), MeONa (10 mol%), THF (1 mL) and H_2O (1 mL), at 100 °C for 4 h

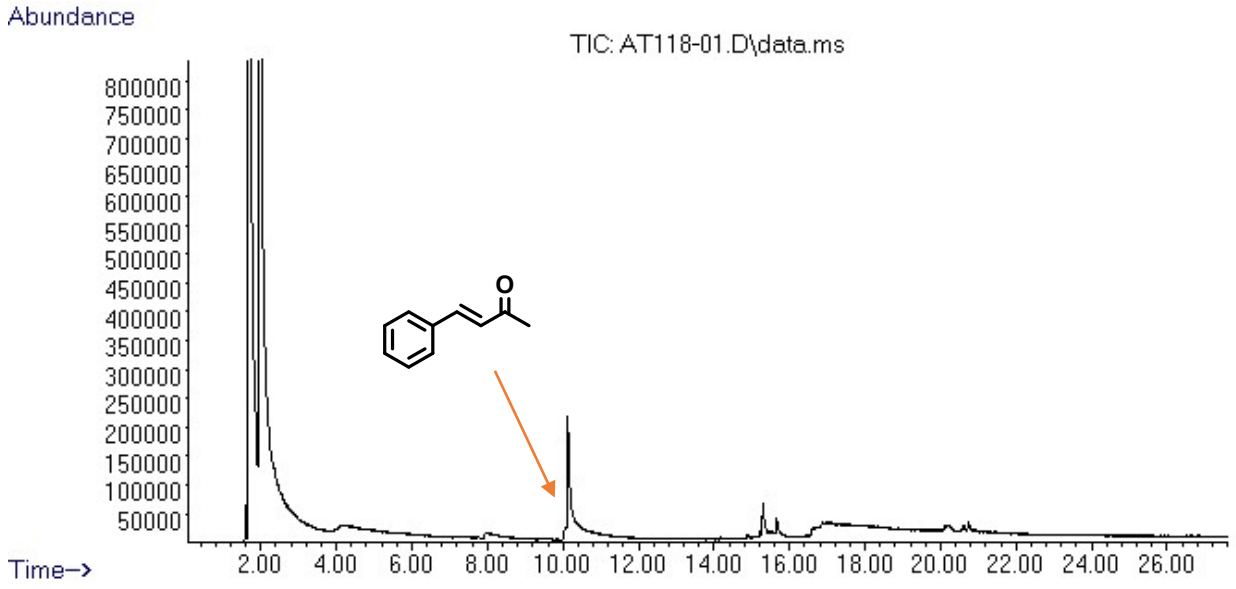

Figure S68. GC of the crude mixture of (*E*)-4-phenylbut-3-en-2-one (**10a**) (0.224 mmol), **Mn-2** (4 mol%), MeONa (10 mol%), THF (1 mL) and isopropanol (1 mL), at 100 °C for 4 h

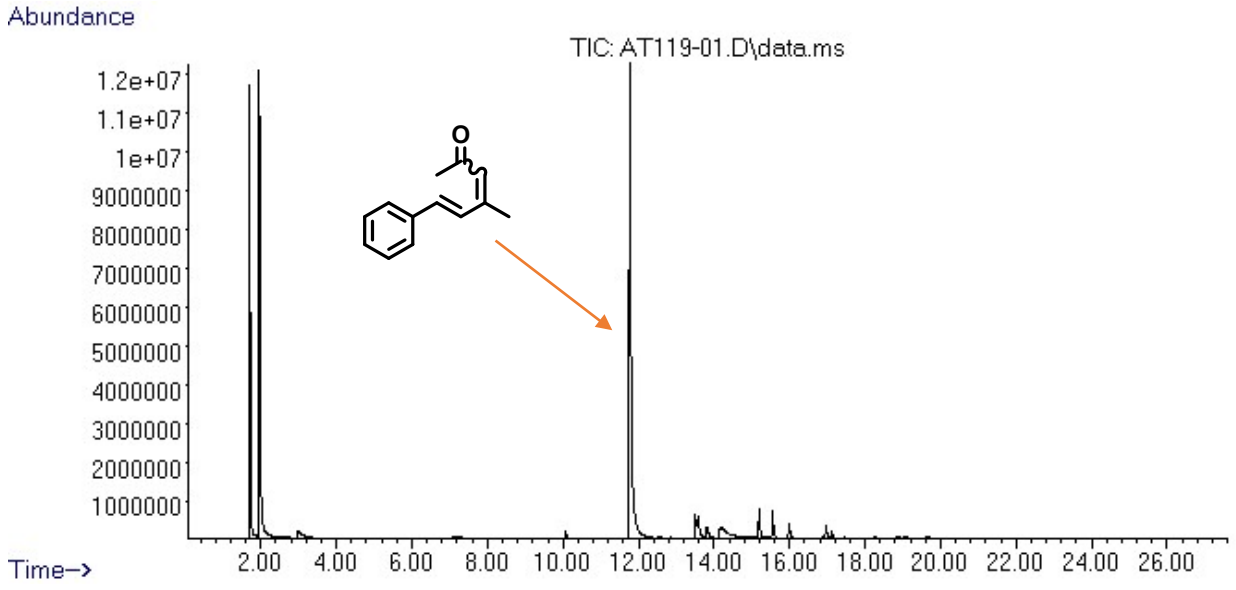

Figure S69. GC of the crude mixture of (*E*)-4-phenylbut-3-en-2-one (**10a**) (0.224 mmol), MeONa (10 mol%), THF (1 mL) and acetone (1 mL), at 100 °C for 4 h

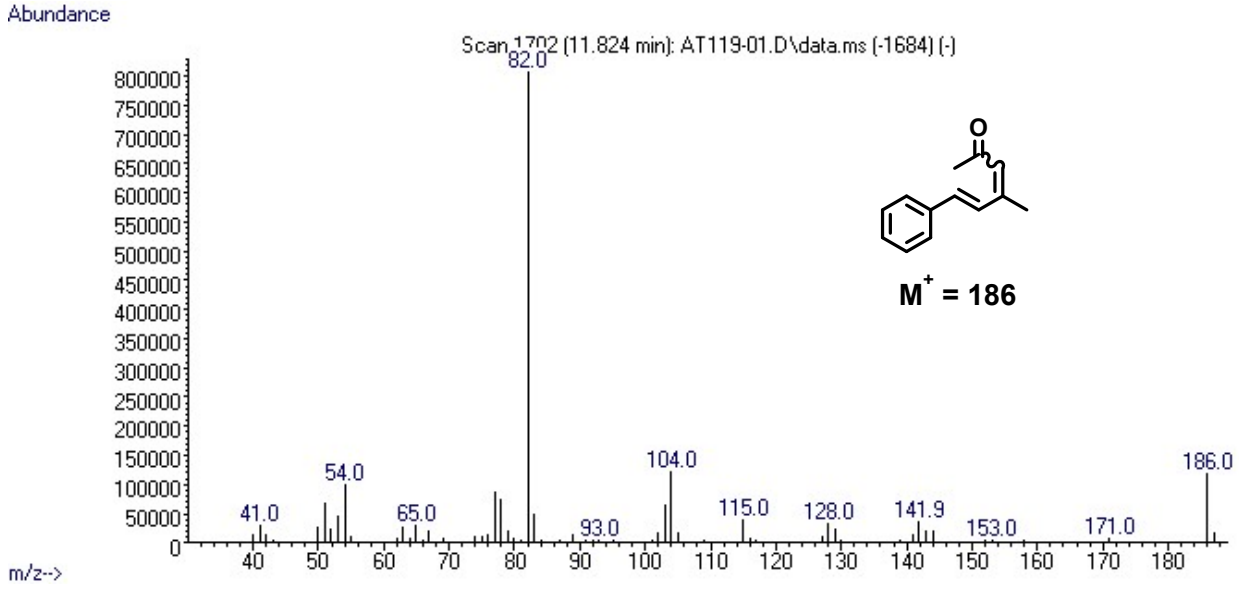

Figure S70. MS for (5*E*)-4-methyl-6-phenylhexa-3,5-dien-2-one detected by GC

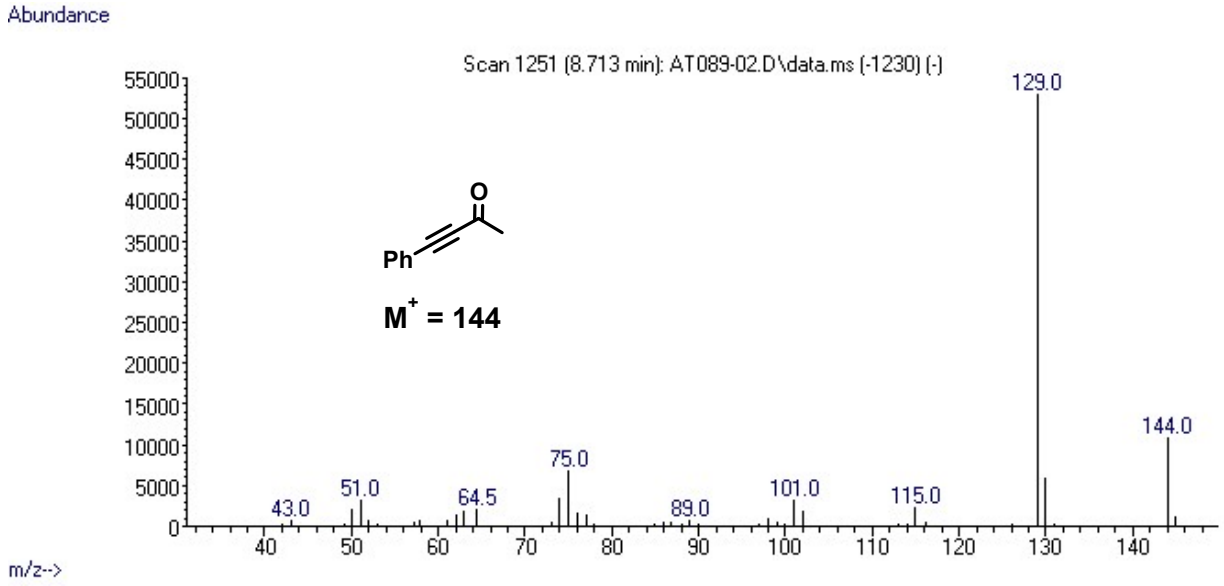

Figure S71. MS for 4-phenyl-3-butyn-2-one (**10**) detected by GC

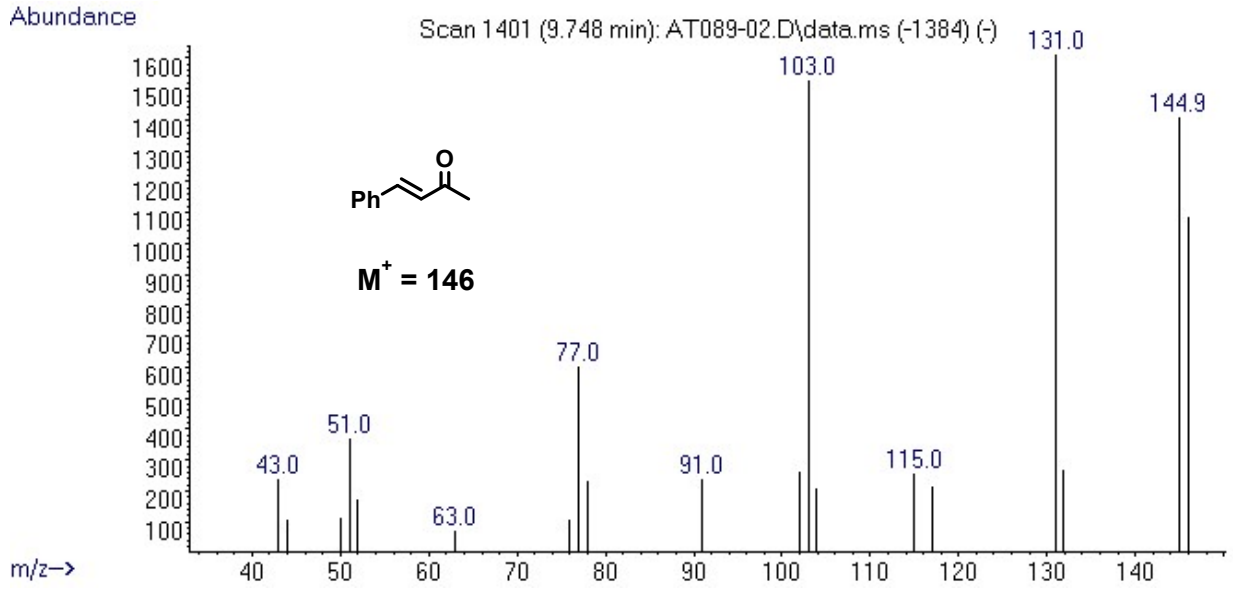

Figure S72. MS for (*E*)-4-phenylbut-3-en-2-one (**10a**) detected by GC

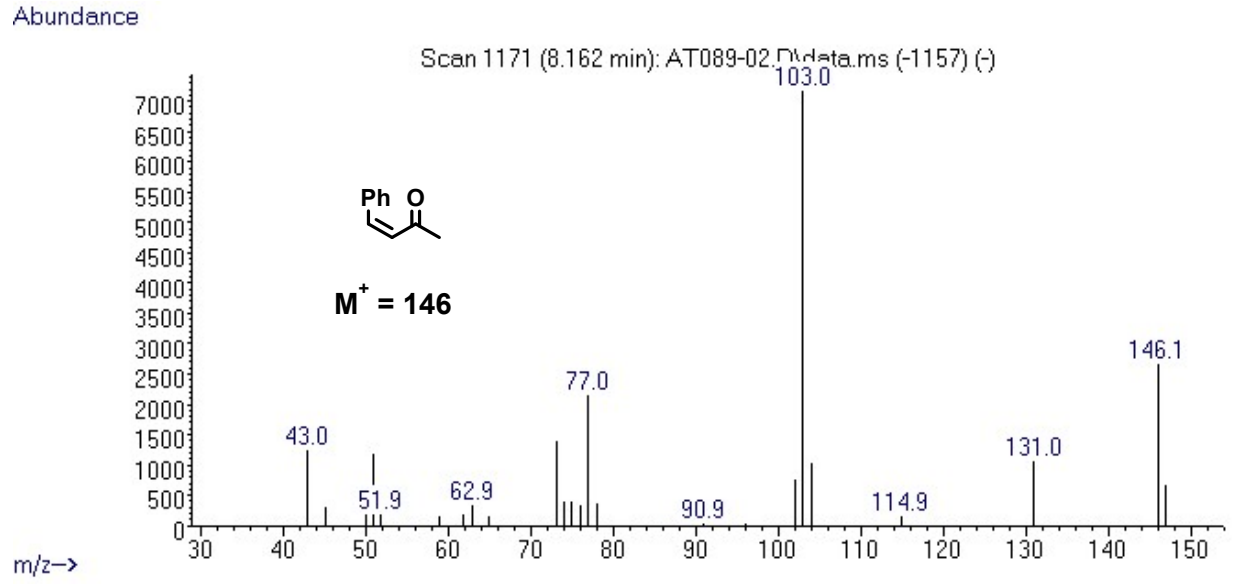

Figure S73. MS for (*Z*)-4-phenylbut-3-en-2-one (**10b**) detected by GC

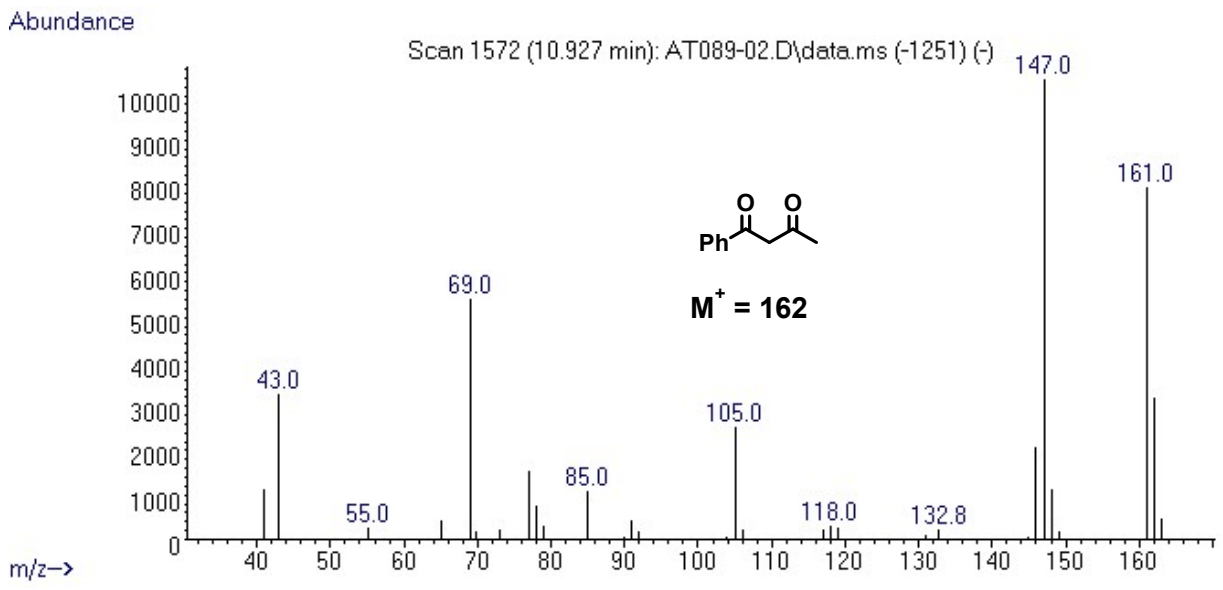

Figure S74. MS for1-phenylbutane-1,3-dione detected by GC

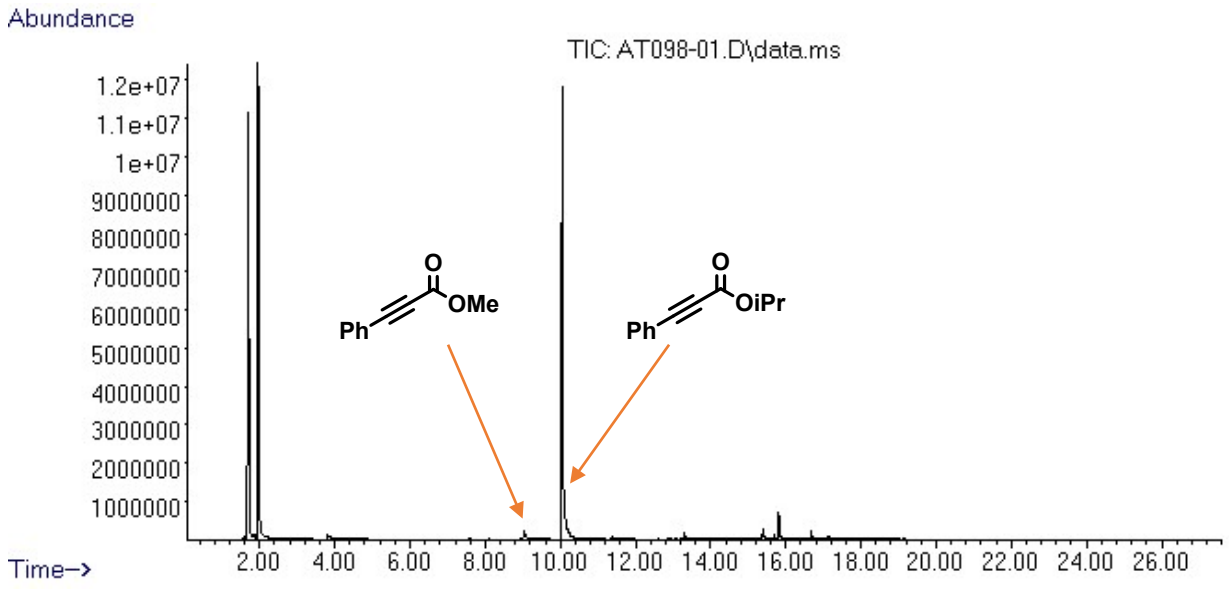

Figure S75. GC of the crude mixture of methyl phenylpropiolate (**11**) transfer semihydrogenation with iPrOH catalyzed by **Mn-2**

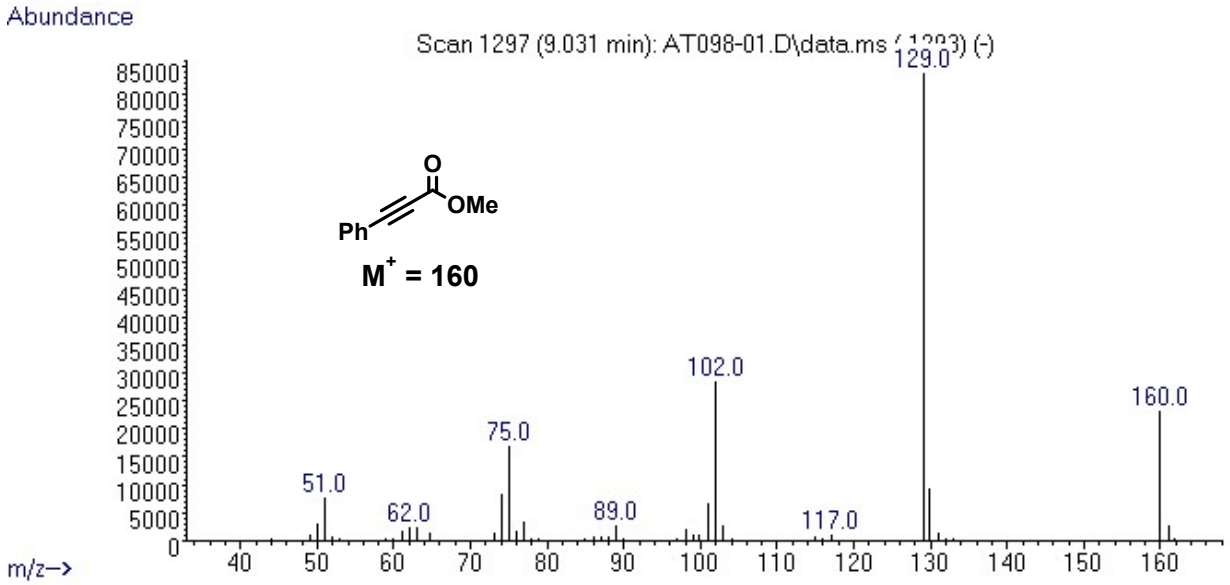

Figure S76. MS for methyl phenylpropiolate (**11**) detected by GC

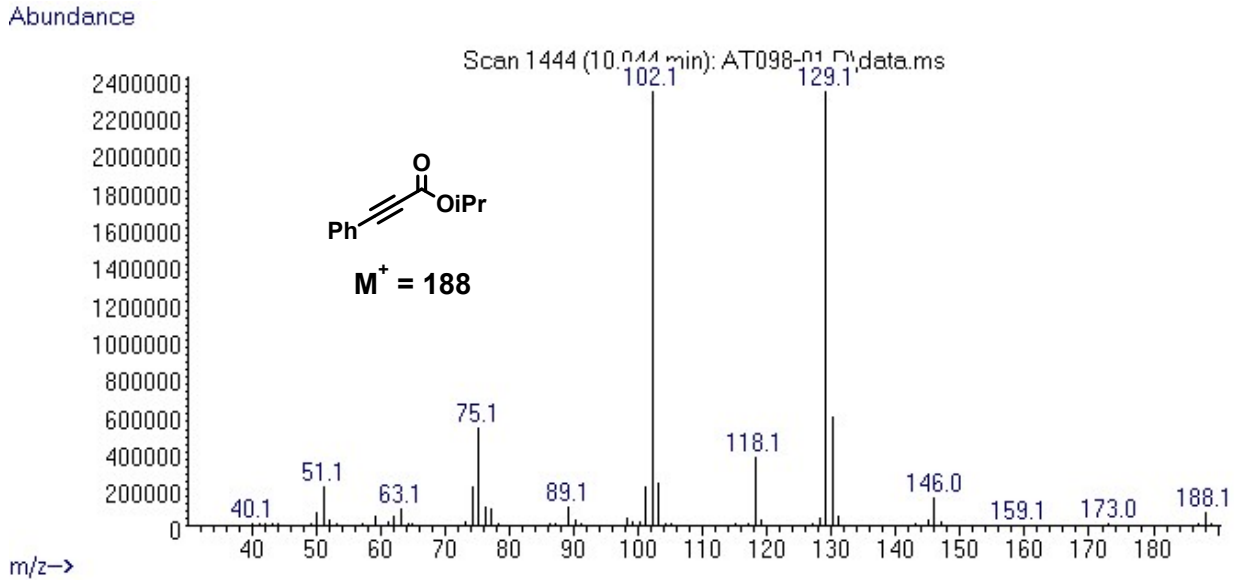

Figure S77. MS for isopropyl phenylpropiolate detected by GC

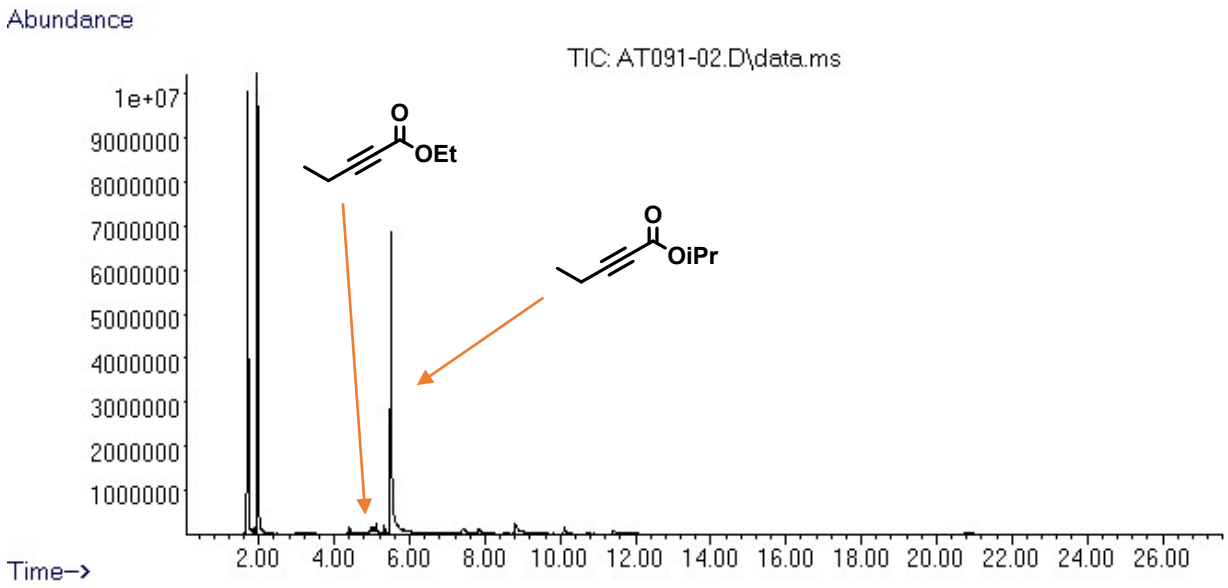

Figure S78. GC of the crude mixture of ethyl 2-pentynoate (**12**) transfer semihydrogenation with iPrOH catalyzed by **Mn-2**

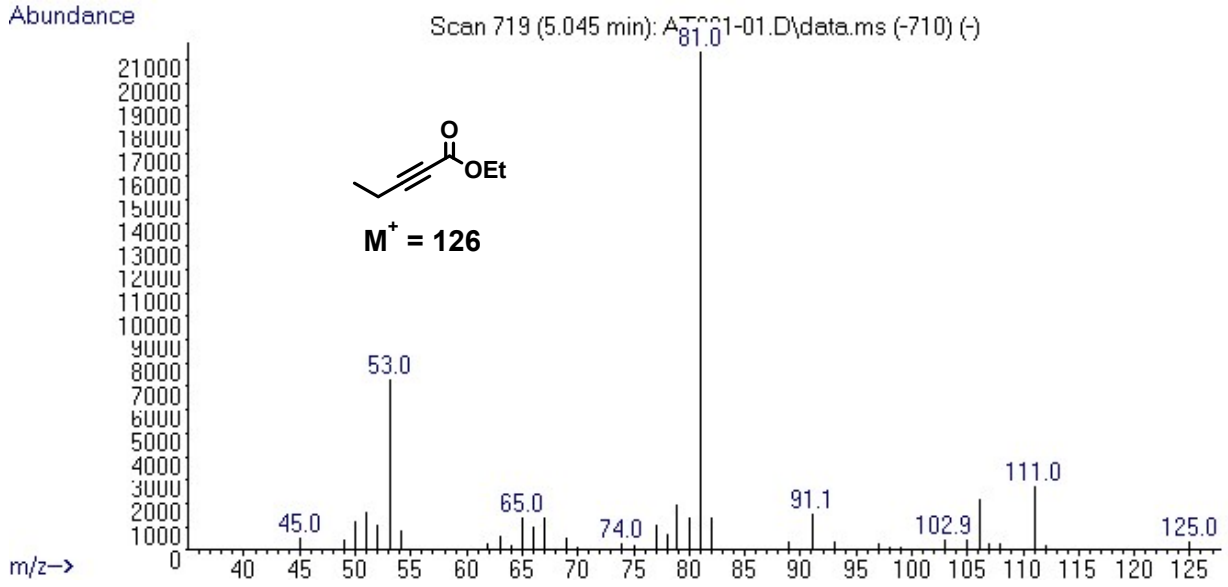

Figure S79. MS for ethyl 2-pentynoate (**12**) detected by GC

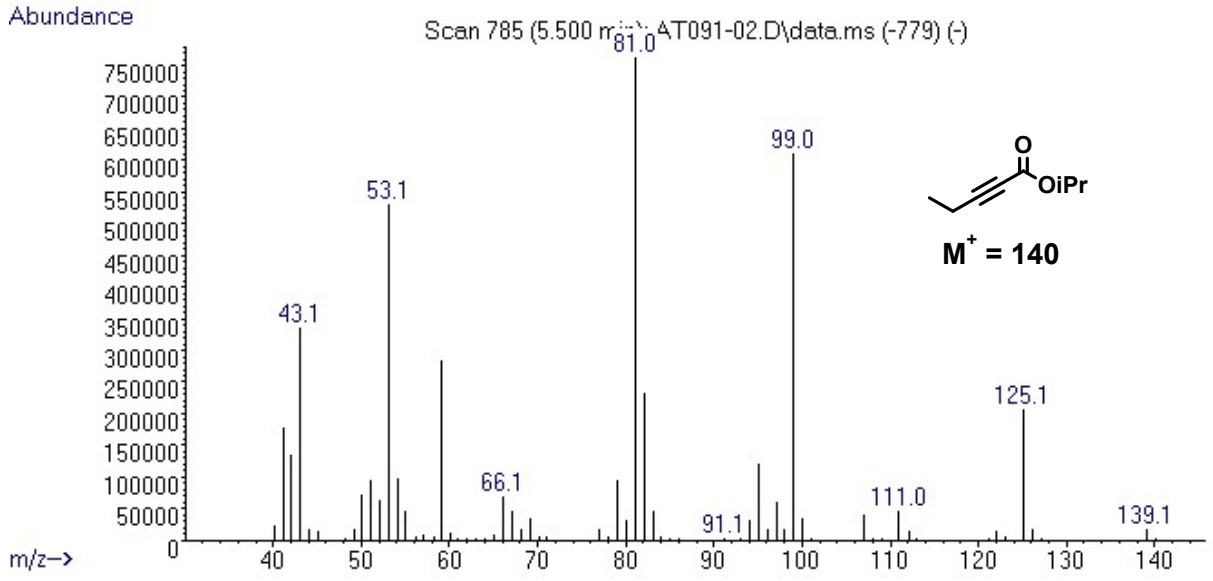

Figure S80. MS for isopropyl 2-pentynoate detected by GC

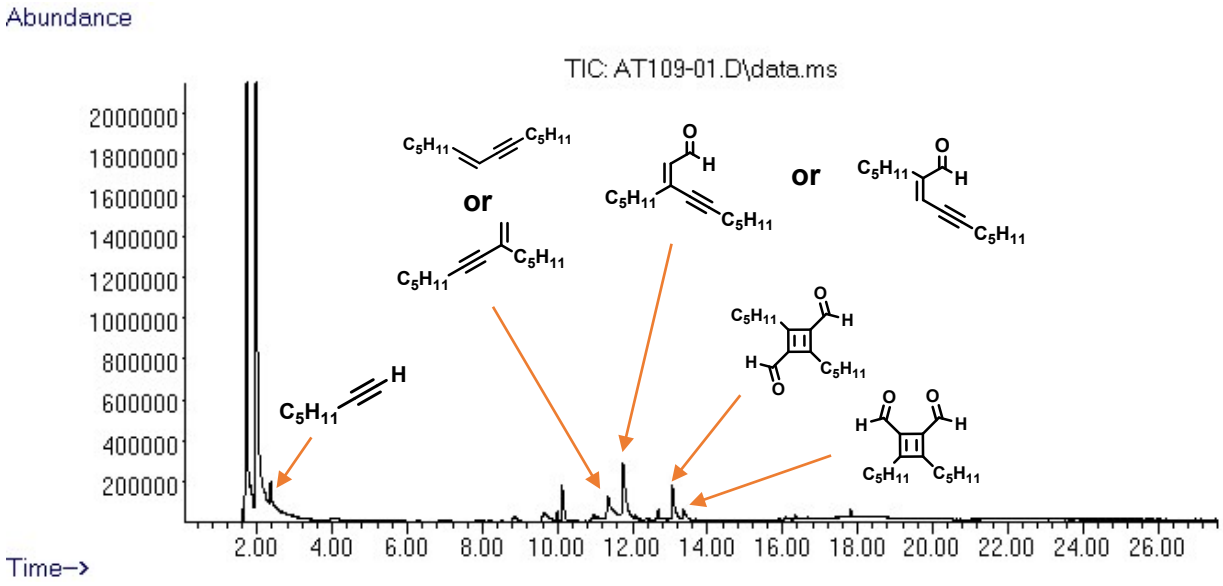

Figure S81. GC of the crude mixture of 2-octynal (**13**) transfer semihydrogenation with iPrOH catalyzed by **Mn-2**

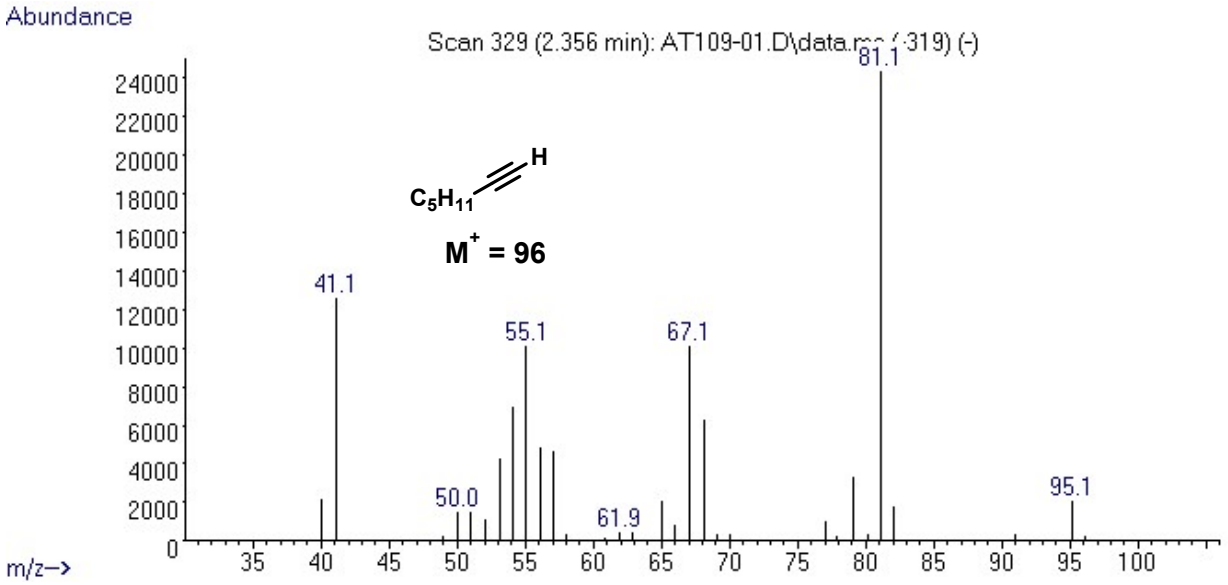

Figure S82. MS for 1-heptyne detected by GC

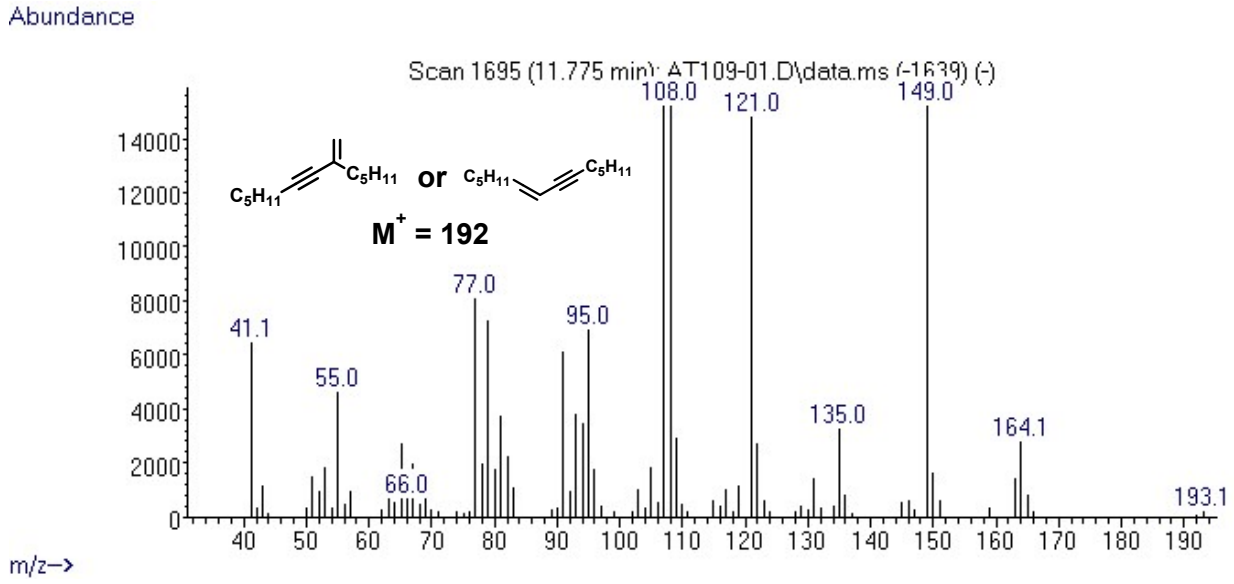

Figure S83. MS for dimerization product of 1-heptyne detected by GC

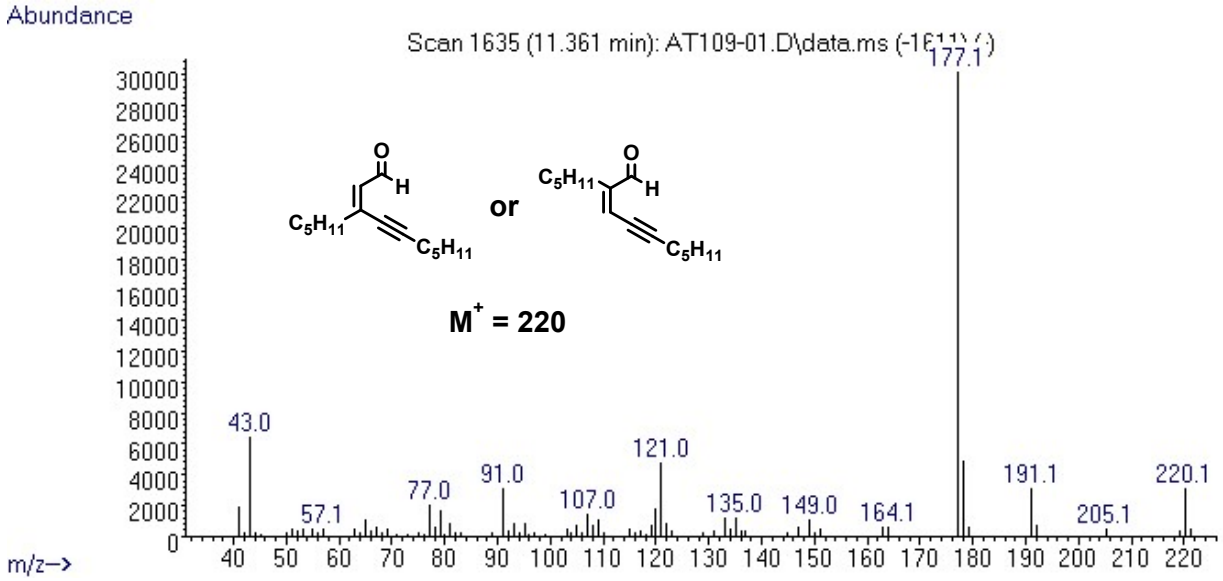

Figure S84. MS for coupling product between 1-heptyne and 2-octynal detected by GC

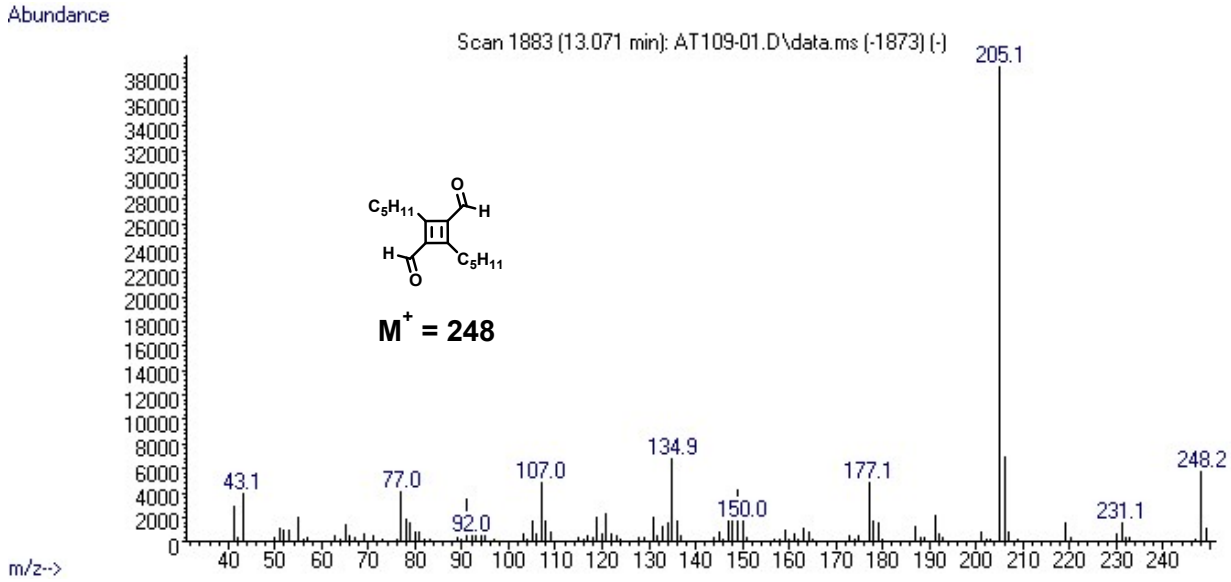

Figure S85. MS for dimerization product of 2-octynal detected by GC

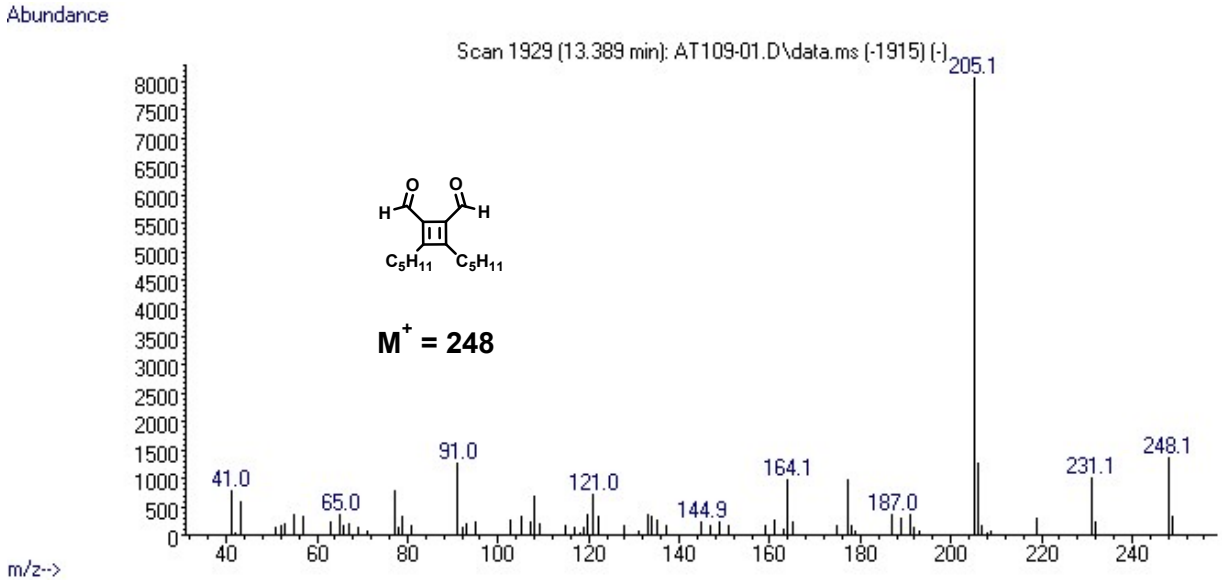

Figure S86. MS for dimerization product of 2-octynal detected by GC

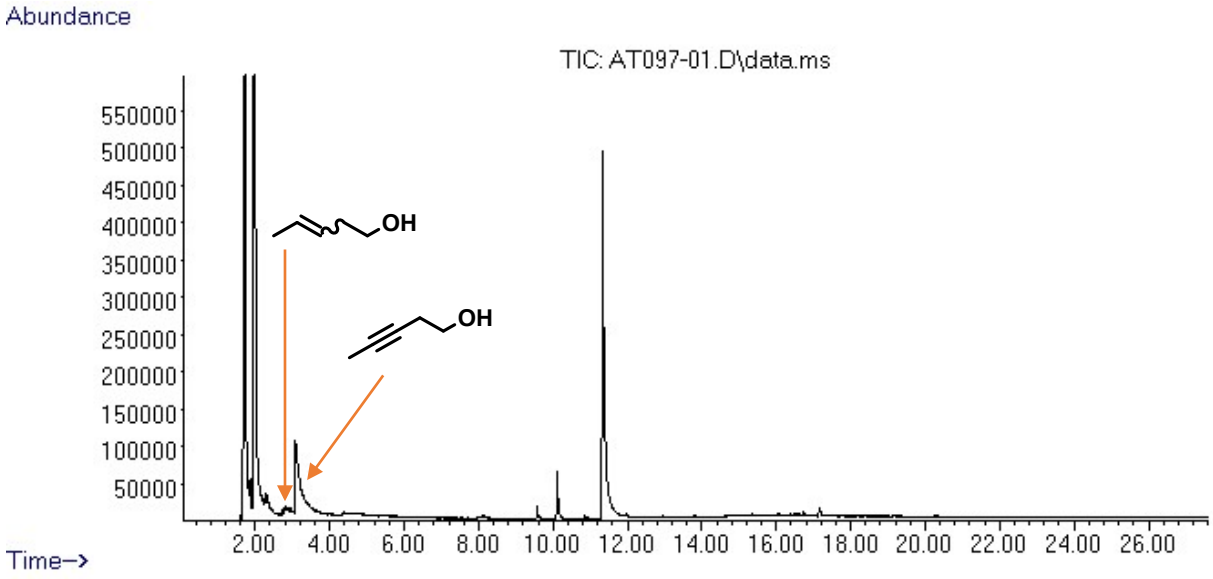

Figure S87. GC of the crude mixture of 3-pentyn-1-ol (**14**) transfer semihydrogenation with iPrOH catalyzed by **Mn-2**

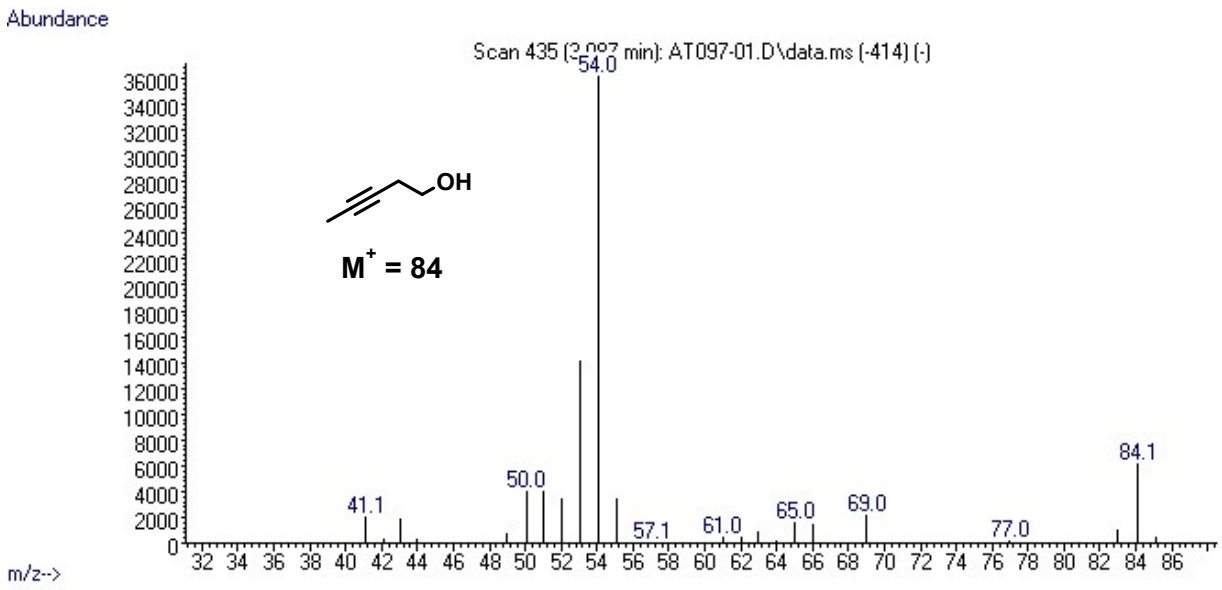

Figure S88. MS for 3-pentyn-1-ol (**14**) detected by GC

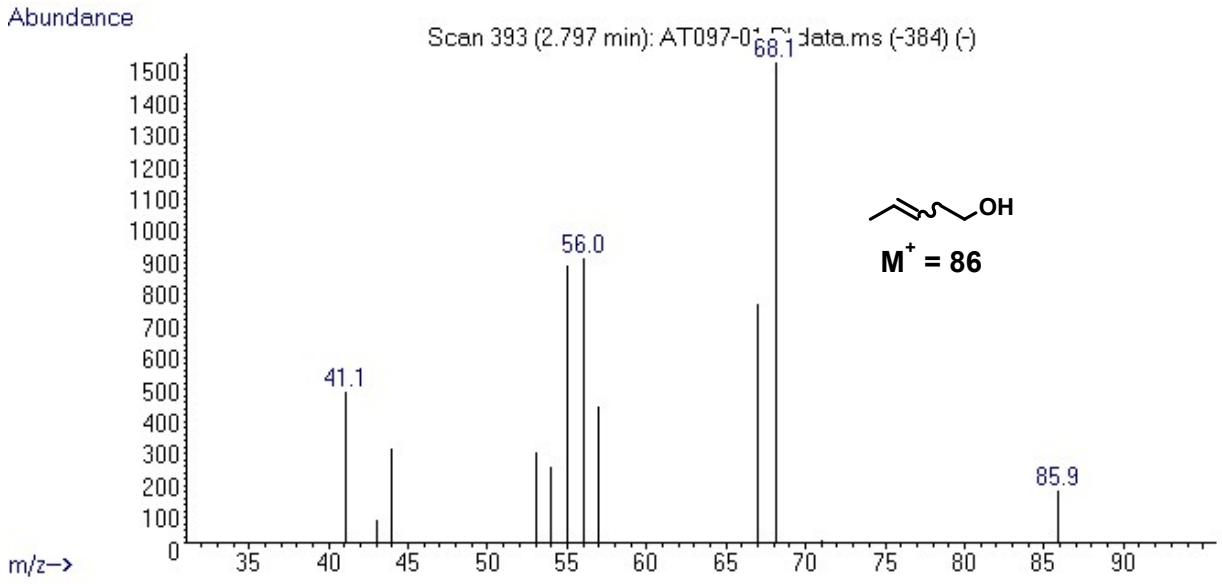

Figure S89. MS for pent-3-en-1-ol (**14a**) detected by GC

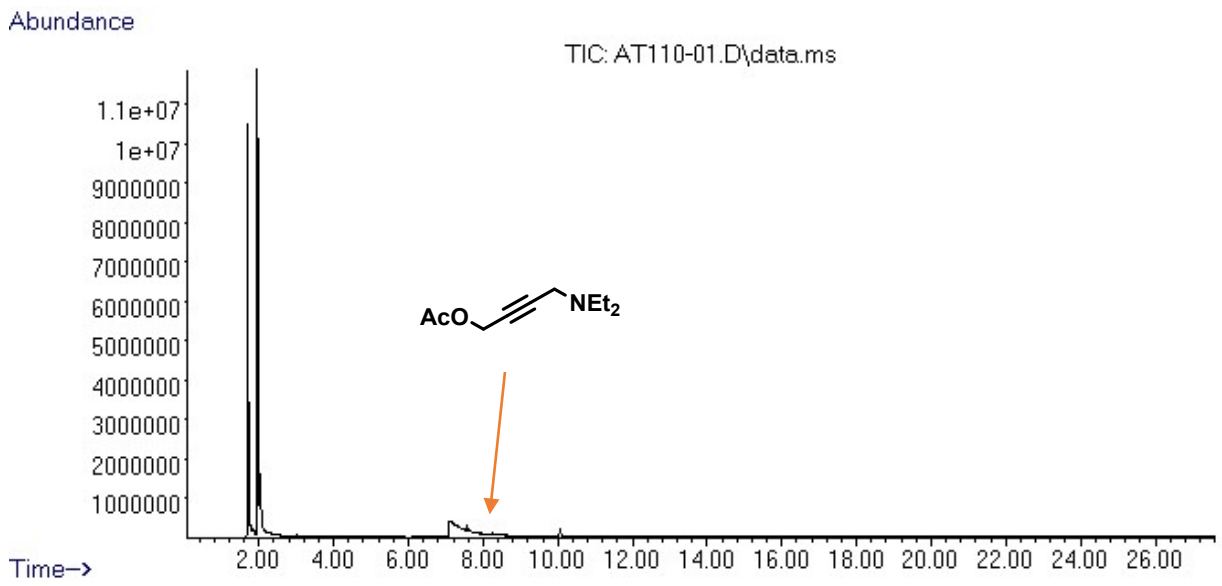

Figure S90. GC of the crude mixture of 1-acetoxy-4-diethylamino-2-butyne (**15**) transfer semihydrogenation with iPrOH catalyzed by **Mn-2**

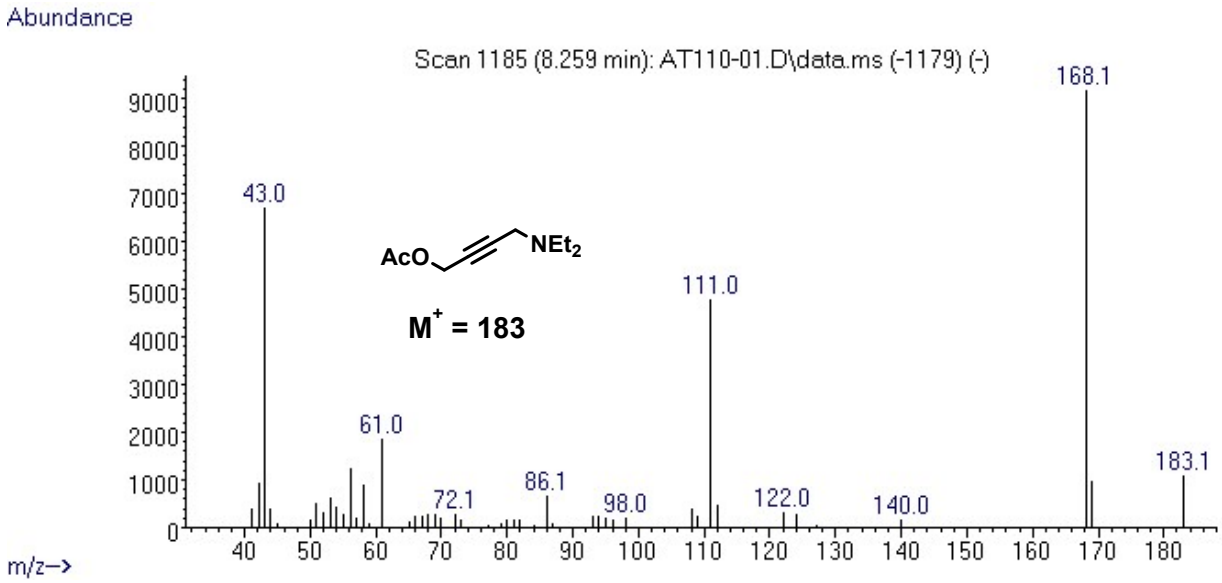

Figure S91. MS for 1-acetoxy-4-diethylamino-2-butyne (**15**) detected by GC

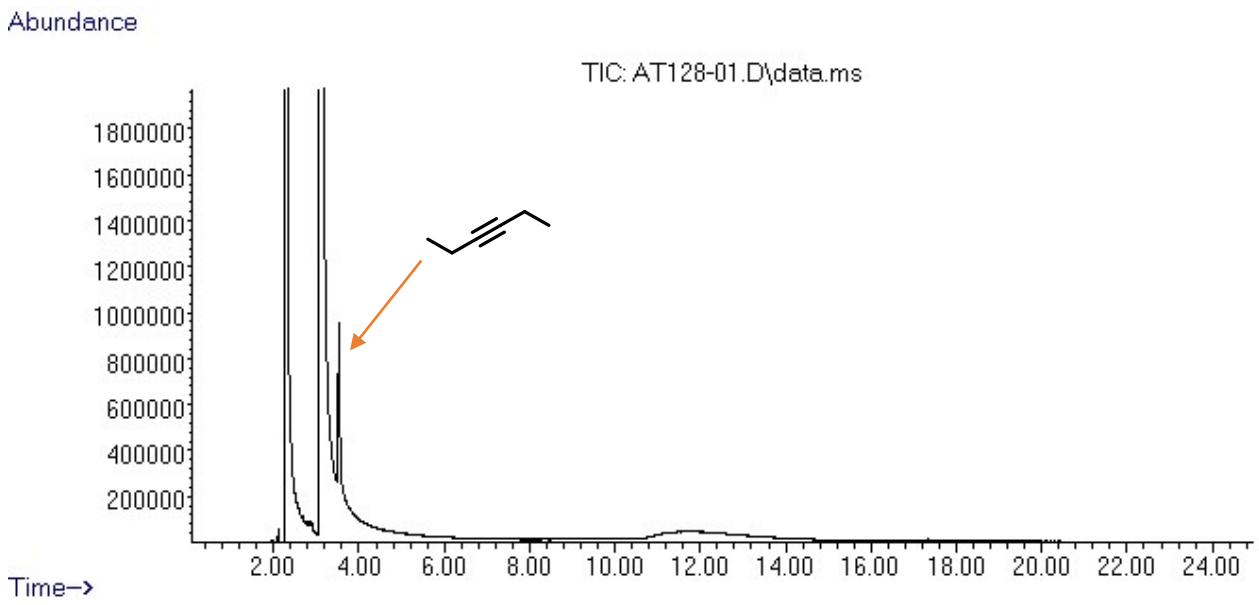

Figure S92. GC of the crude mixture of 3-hexyne (**16**) transfer semihydrogenation with iPrOH catalyzed by **Mn-2**

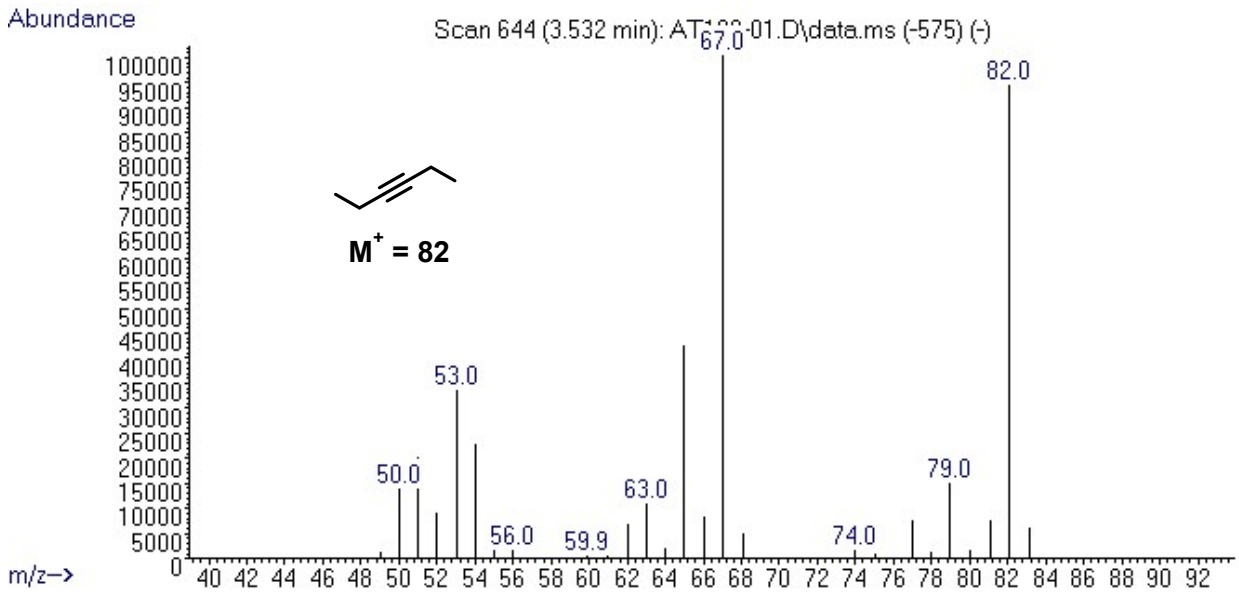

Figure S93. MS for 3-hexyne (**16**) detected by GC

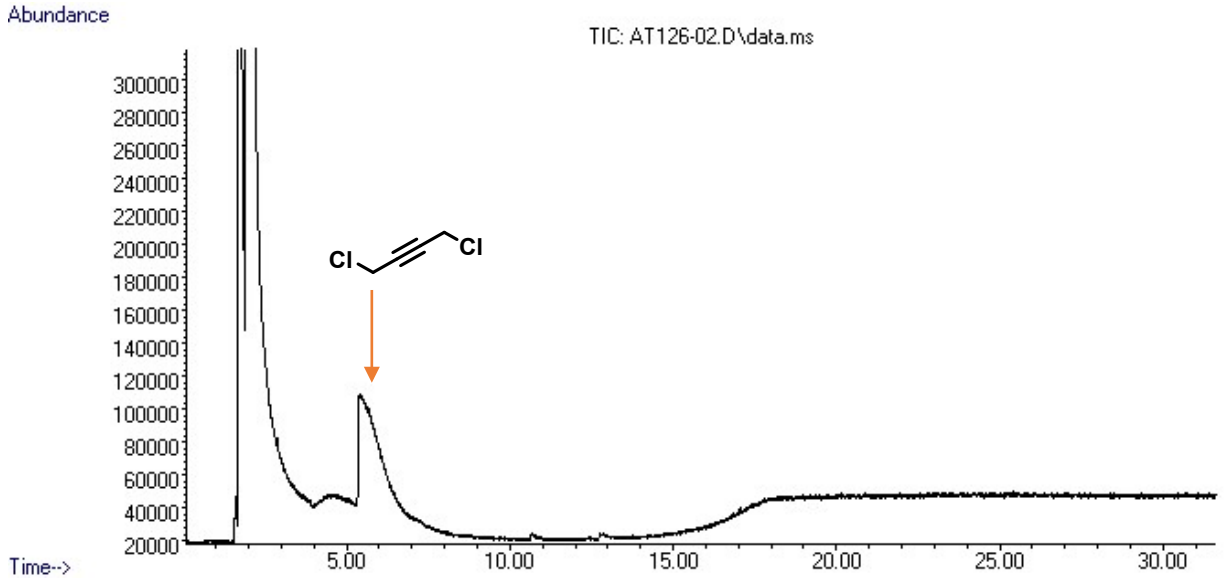

Figure S94. GC of the crude mixture of 1,4-dichloro-2-butyne (**17**) transfer semihydrogenation with iPrOH catalyzed by **Mn-2**

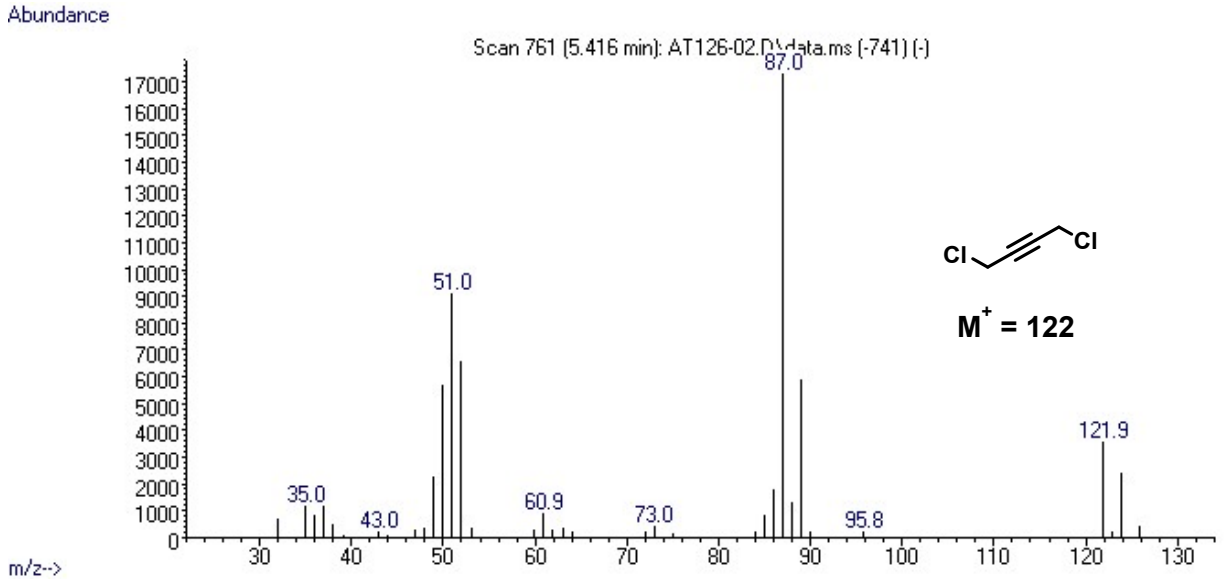

Figure S95. MS for 1,4-dichloro-2-butyne (**17**) detected by GC

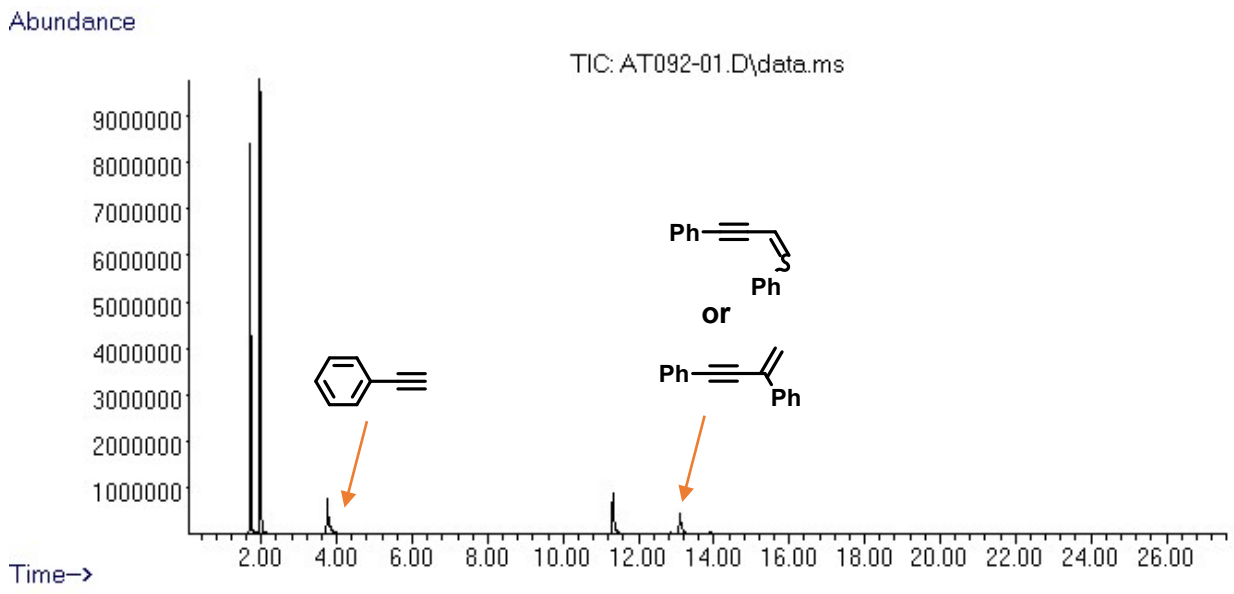

Figure S96. GC of the crude mixture of phenylacetylene (**18**) transfer semihydrogenation with iPrOH catalyzed by **Mn-2**

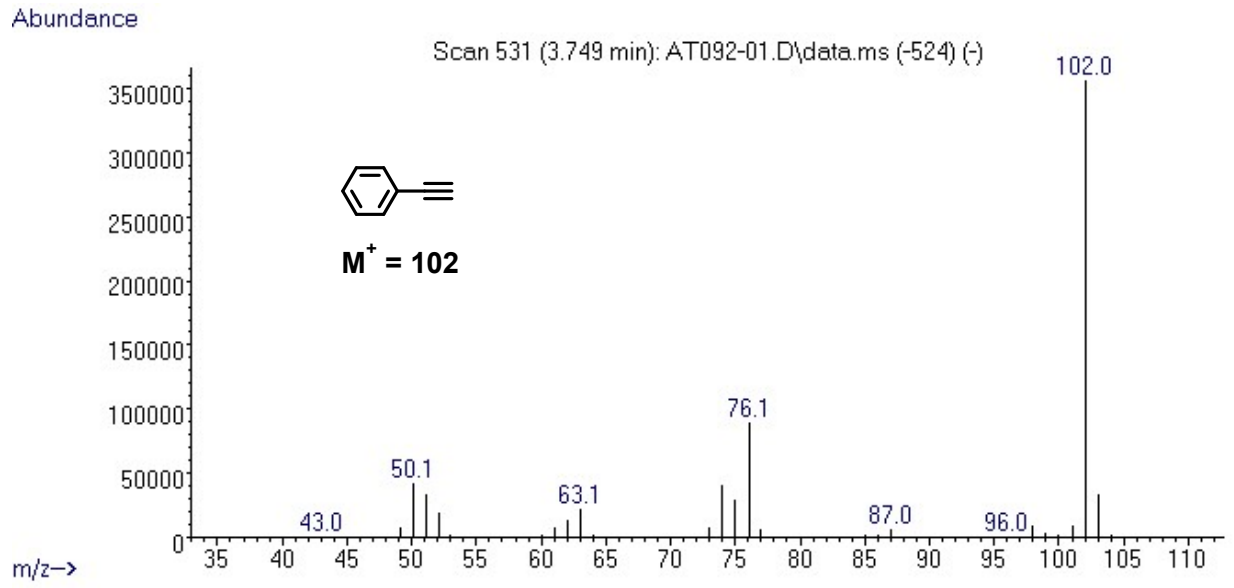

Figure S97. MS for phenylacetylene (**18**) detected by GC

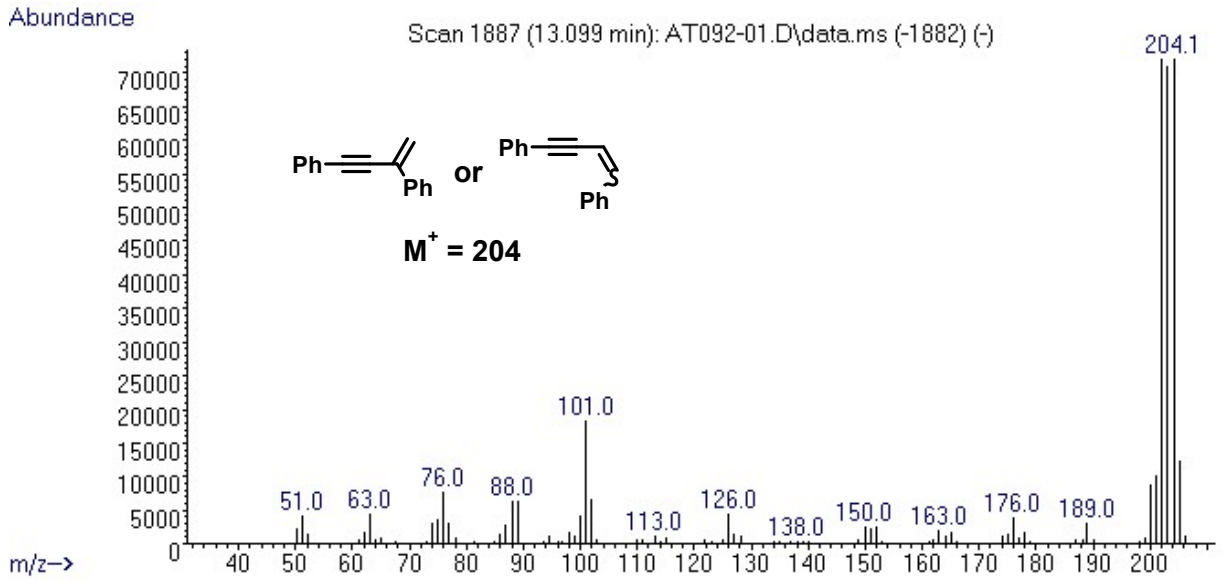

Figure S98. MS for dimerization product of phenylacetylene detected by GC

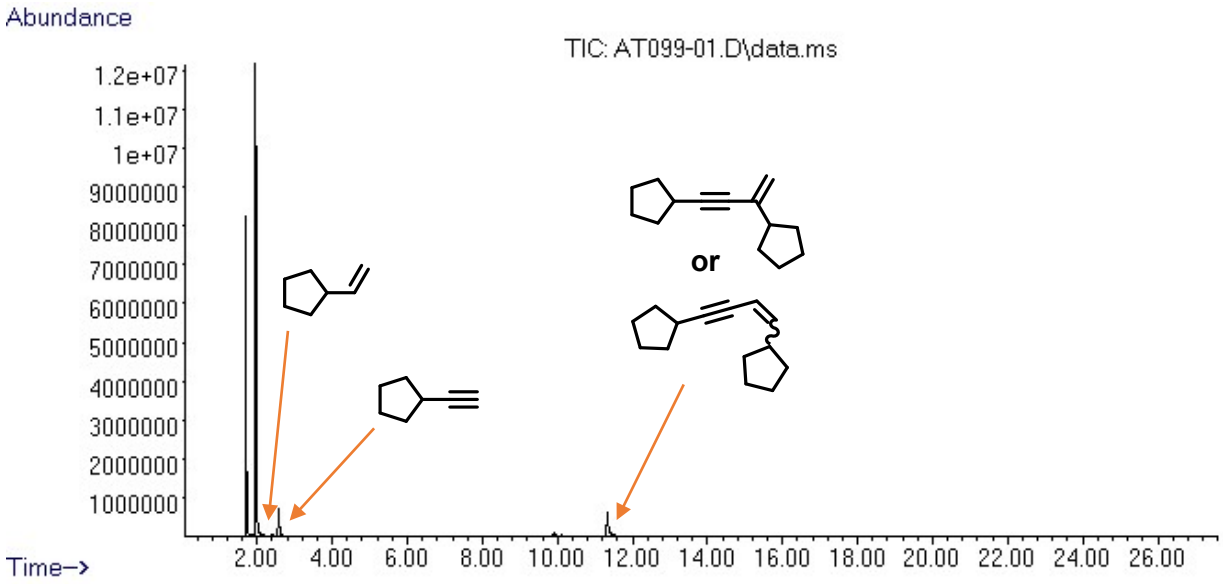

Figure S99. GC of the crude mixture of cyclopentylacetylene (**19**) transfer semihydrogenation with iPrOH catalyzed by **Mn-2**

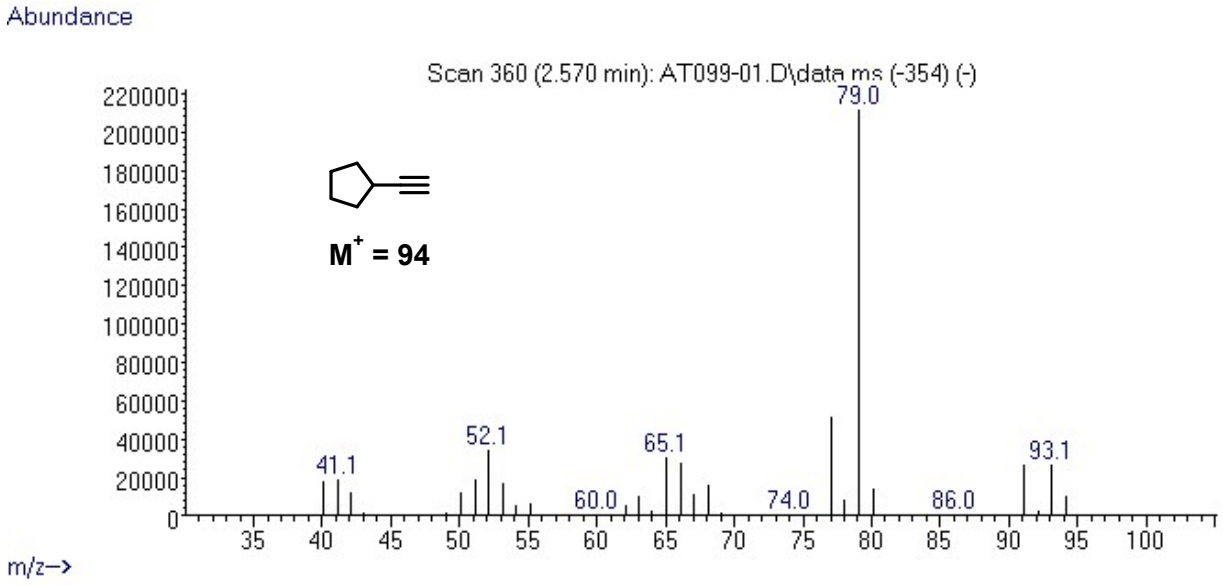

Figure S100. MS for cyclopentylacetylene (**19**) detected by GC

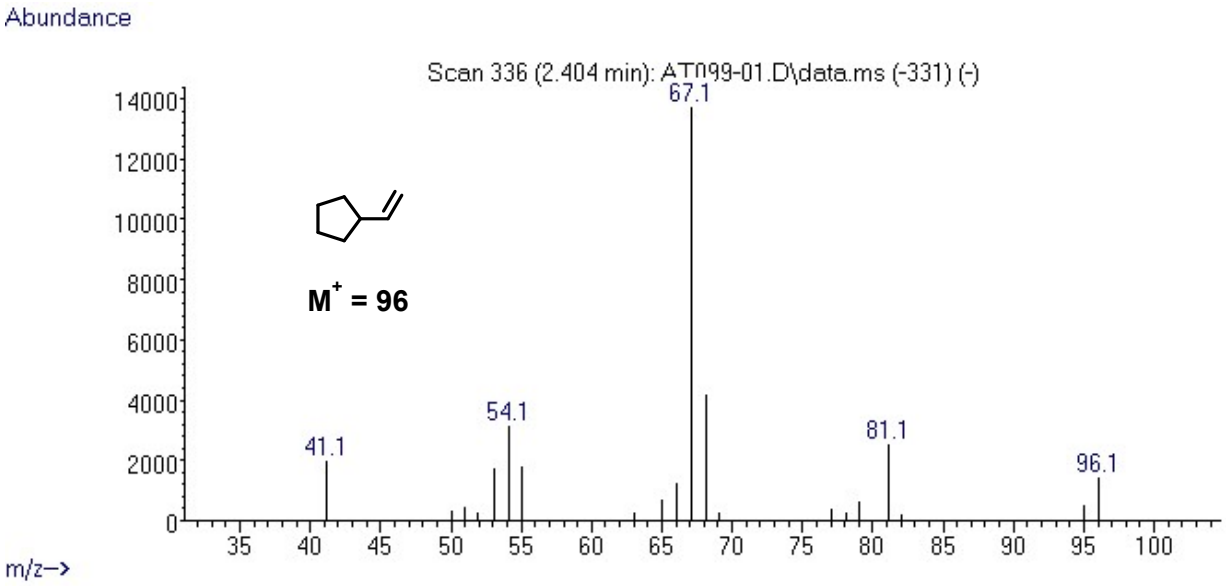

Figure S101. MS for vinylcyclopentane (**19a**) detected by GC

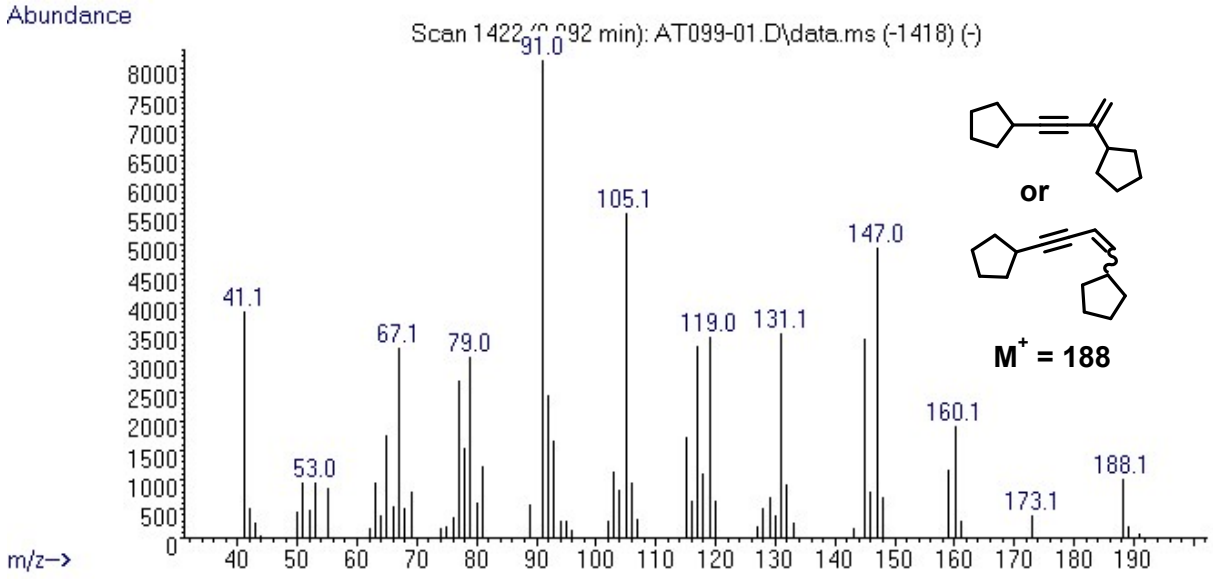

Figure S102. MS for dimerization product of cyclopentylacetylene detected by GC

IV. Mechanistic Insights

Experiments for kinetic profile

Independent experiments were carried out as described for the optimized reaction, but at different reaction times. Yields were determined by GC-MS.

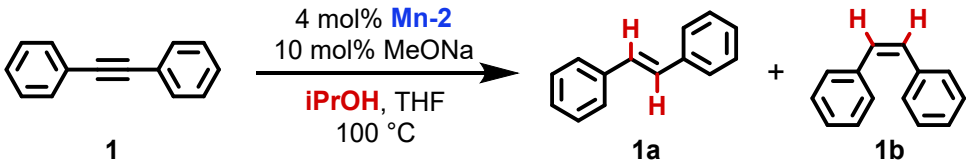

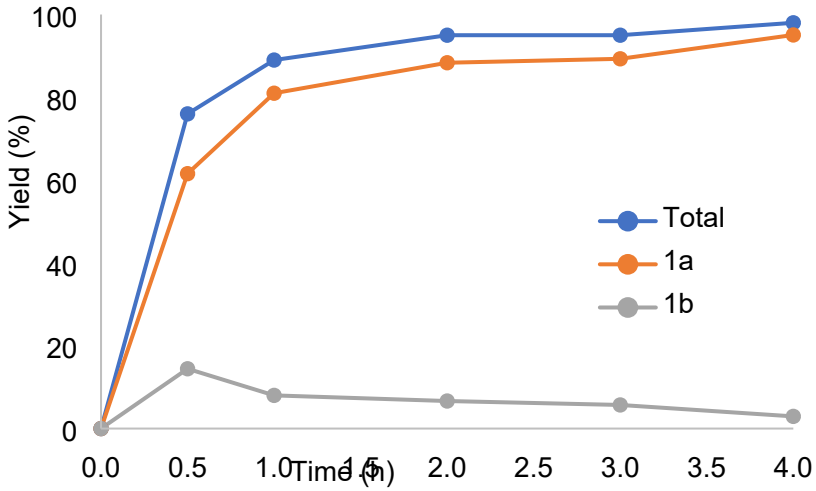

Figure S103. Kinetic profile of the semihydrogenation of **1** with iPrOH as transfer agent and **Mn-2** as pre-catalyst. Yields determined by GC-MS

Additional experiments for isomerization and internal sphere mechanism

Independent experiments were carried out as described for the optimized reaction, but with *cis*- or *trans*-stilbene as substrate, or in the presence of 1.1 eq of triphenyl phosphine. Yields were determined by GC-MS. The MS of the other molecules detected are presented in the optimization (page S13).

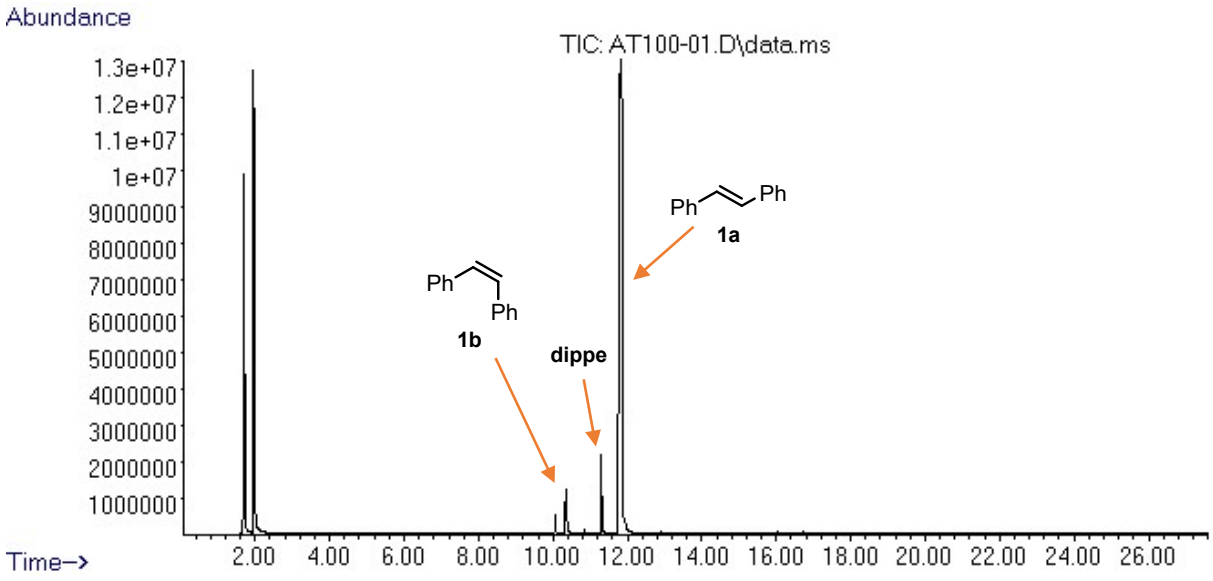

Figure S104. GC of the crude mixture of the test with *cis*-stilbene (**1b**) for the isomerization catalyzed by **Mn-2** in the presence of iPrOH

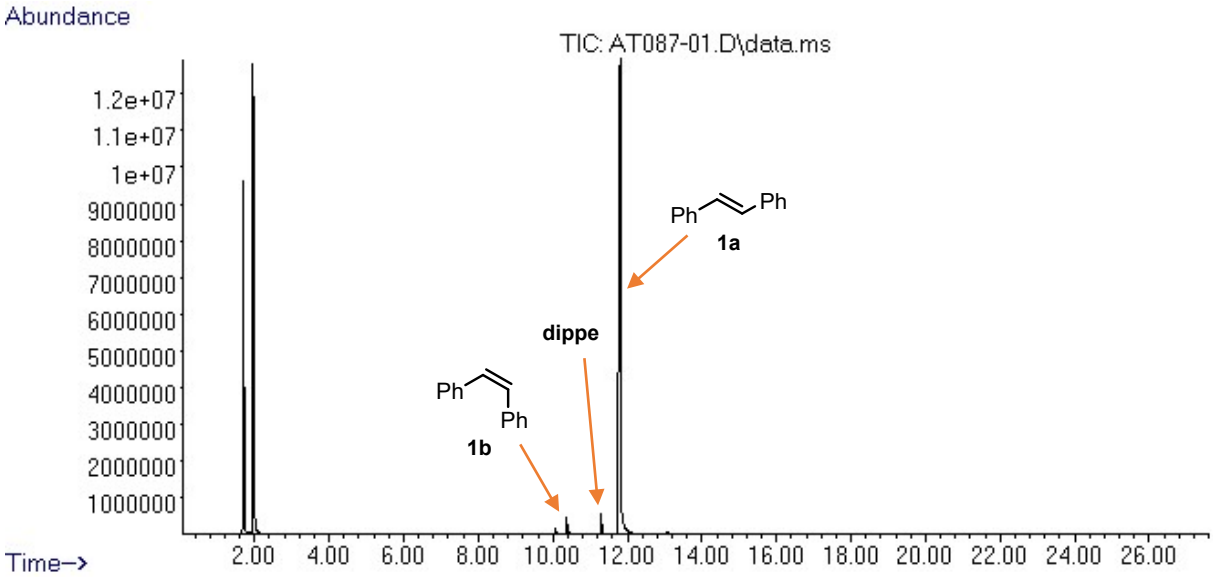

Figure S105. GC of the crude mixture of the test with *trans*-stilbene (**1a**) for the isomerization catalyzed by **Mn-2** in the presence of iPrOH

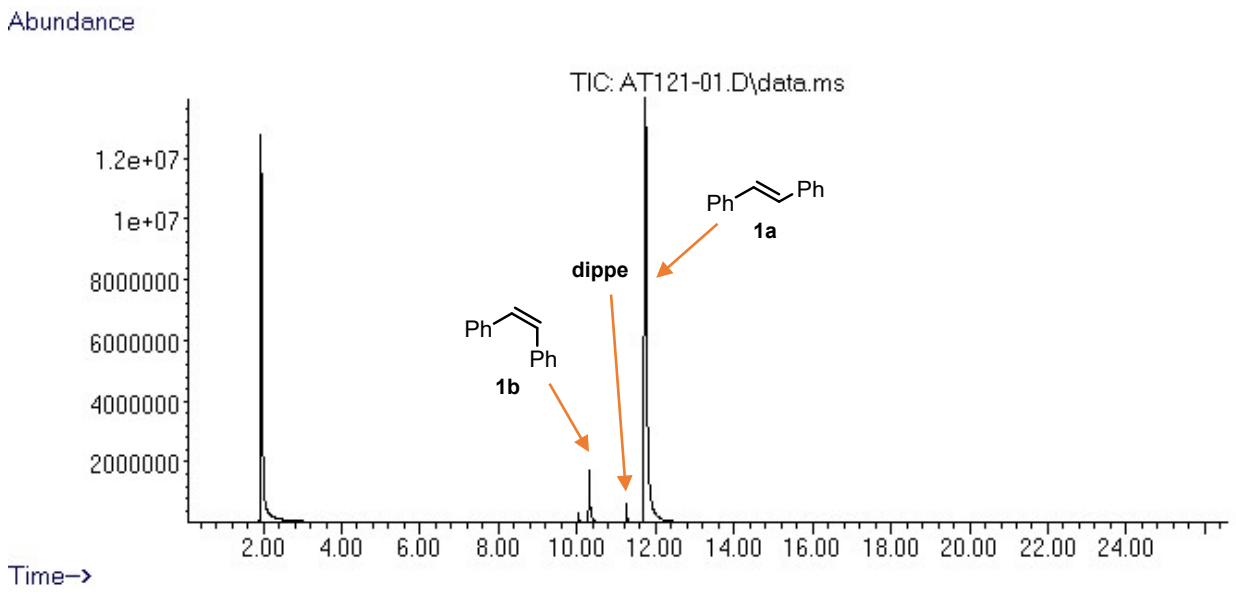

Figure S106. GC of the crude mixture of the test with *cis*-stilbene (**1a**) for the isomerization catalyzed by **Mn-2** in the absence of iPrOH

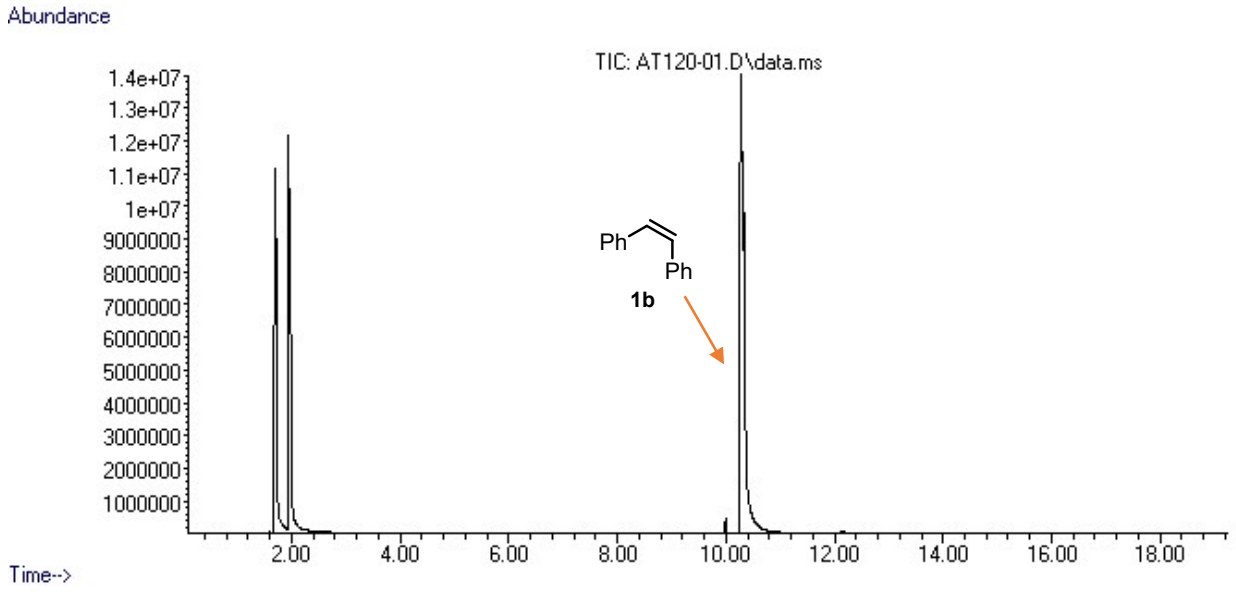

Figure S107. GC of the crude mixture of the test with *cis*-stilbene (**1a**) for the isomerization in the presence of iPrOH but in the absence of any Mn-based catalytic precursor

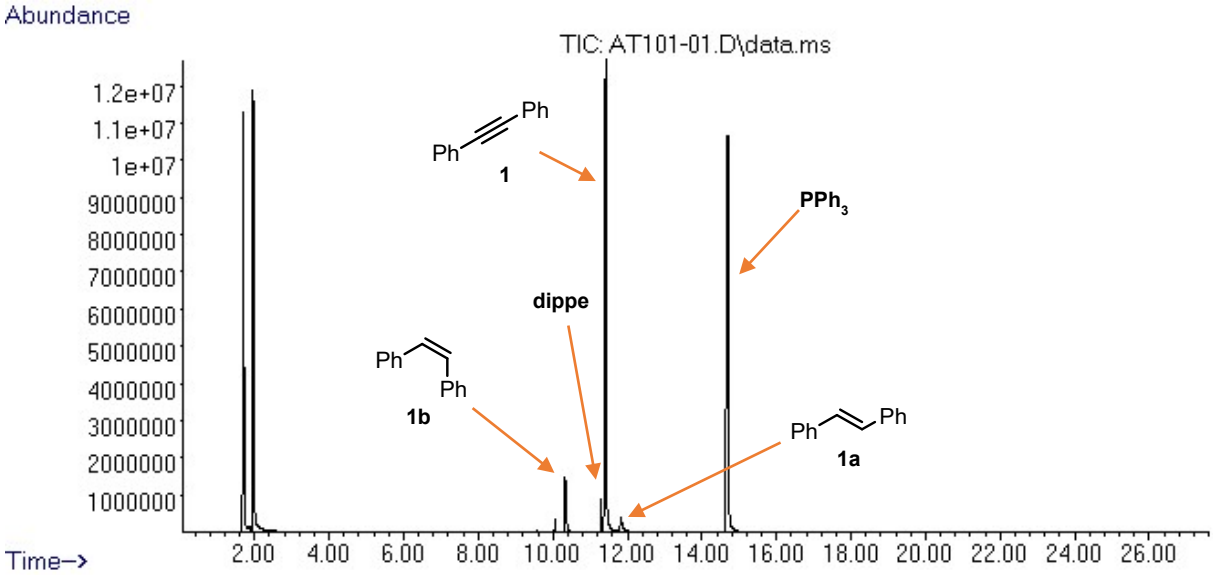

Figure S108. GC of the crude mixture of the diphenylacetylene (**1**) transfer semihydrogenation with iPrOH catalyzed by **Mn-2** in the presence of 1.1 eq of triphenylphosphine

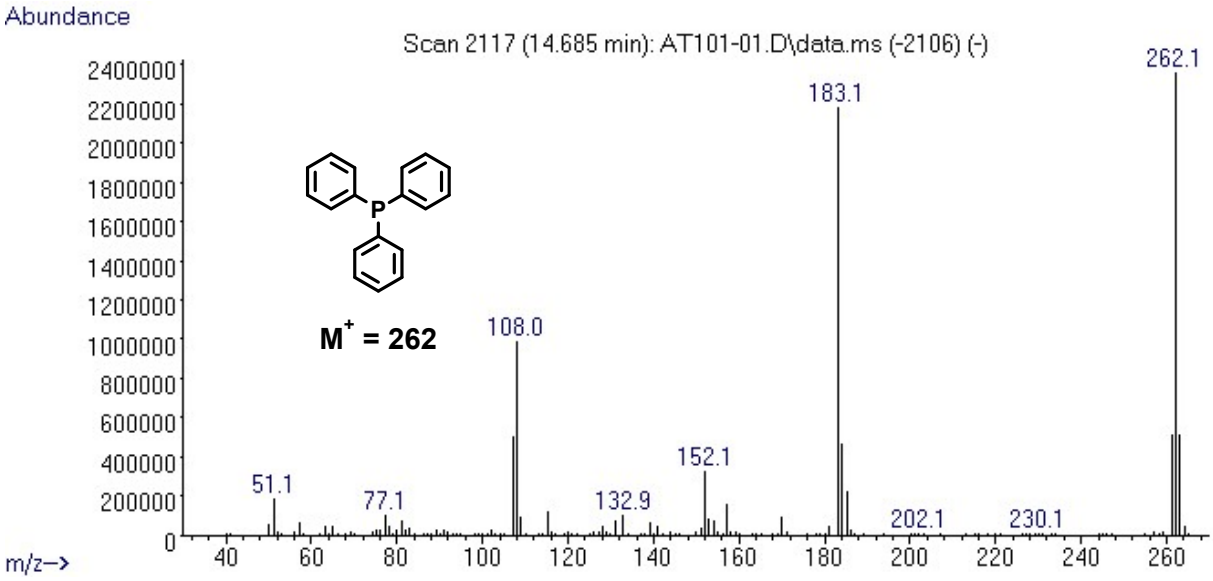

Figure S109. MS for triphenylphosphine detected by GC

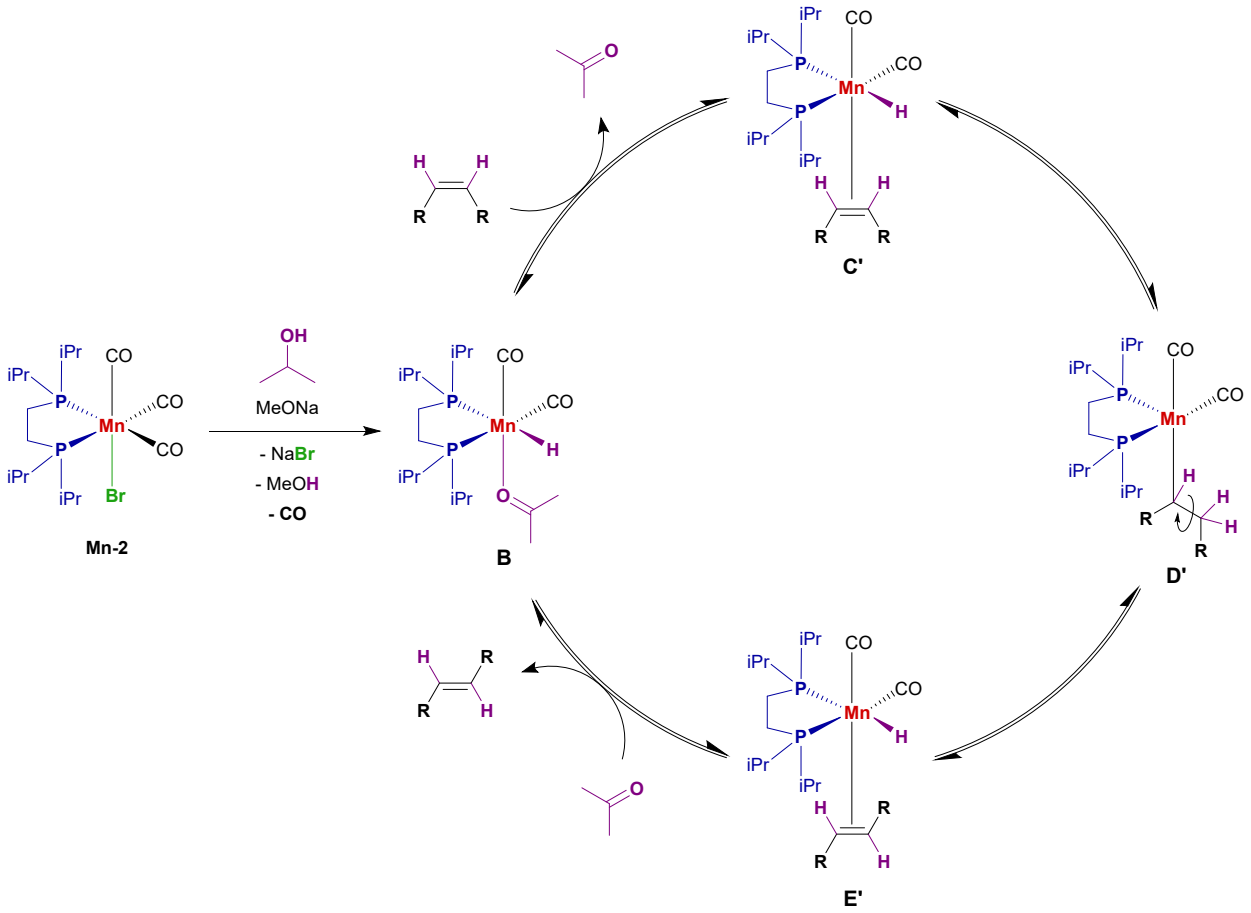

Scheme S1. Mechanistic proposal for the Mn-catalyzed reversible isomerization of *Z*- and *E*-alkenes with **Mn-2** as catalytic precursor and iPrOH as hydrogen source

NMR following up of the transfer semihydrogenation of 1 with iPrOH using Mn-2 as catalytic precursor

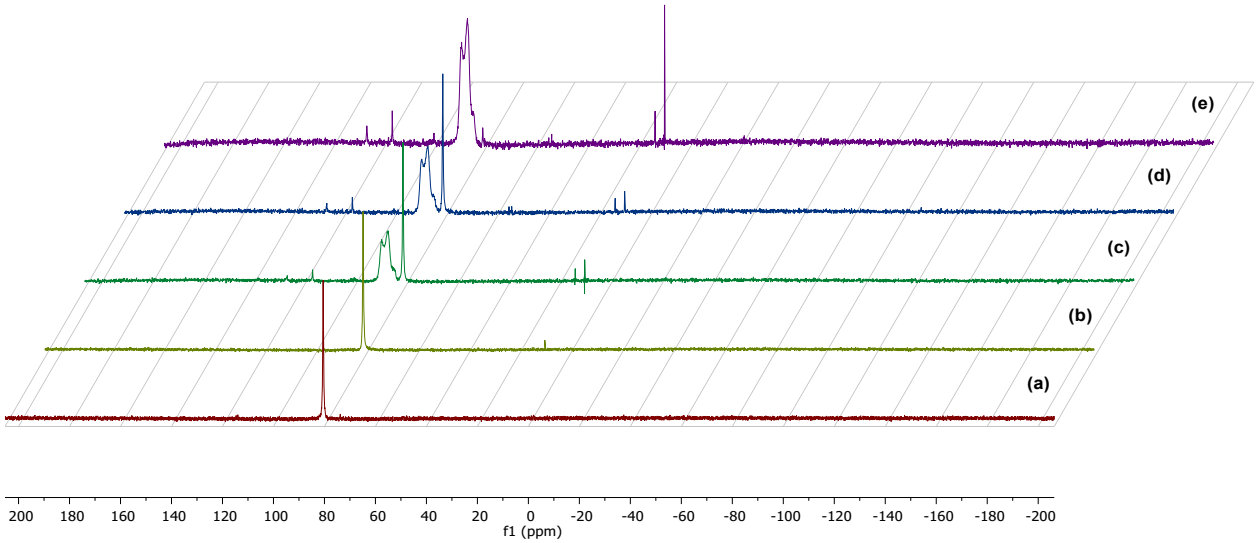

Figure S110. $^{31}P\{^{1}H\}$ NMR (243 MHz, THF-d_8) monitoring of transfer semihydrogenation of **1** with iPrOH catalyzed by **Mn-2**. **(a) Mn-2** and iPrOH; **(b) Mn-2**, iPrOH and MeONa; **(c) b** after heating at 70 °C for 30 min; **(d) c** after addition of **1**; **(e) d** after heating at 70 °C for 30 min. The final molar ratio of **Mn-2**, iPrOH, MeONa and **1** was 1:4:2:1

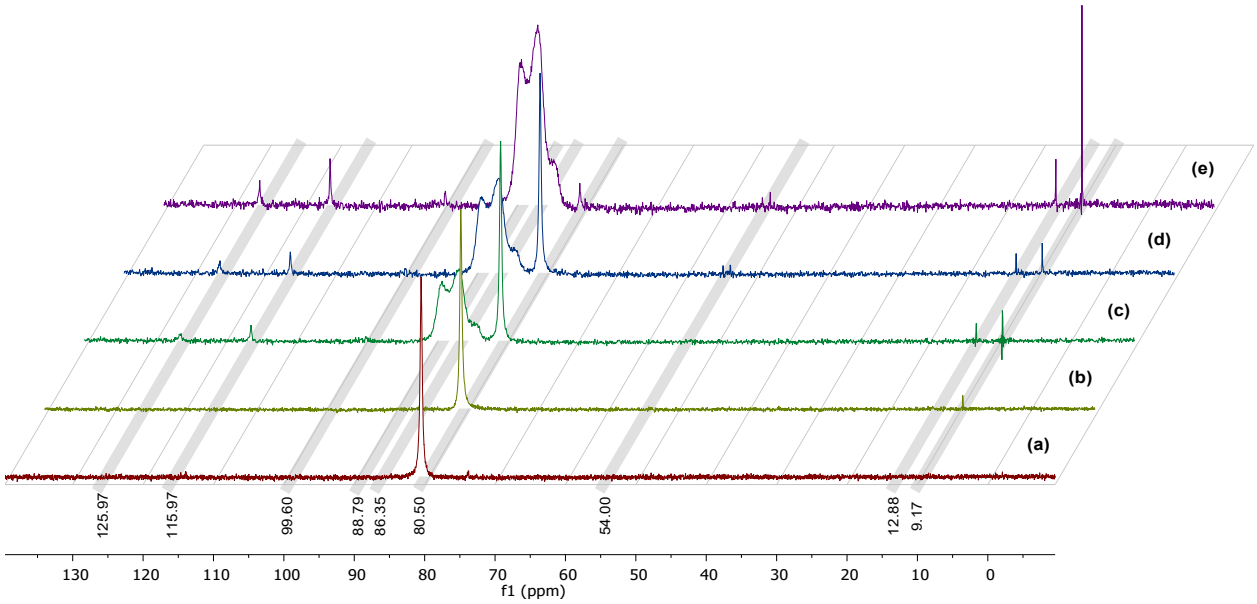

Figure S111. Enlargement of $^{31}P\{^{1}H\}$ NMR (243 MHz, THF-d_8) monitoring of transfer semihydrogenation of **1** with iPrOH catalyzed by **Mn-2**. **(a) Mn-2** and iPrOH; **(b) Mn-2**, iPrOH and MeONa; **(c) b** after heating at 70 °C for 30 min; **(d) c** after addition of **1**; **(e) d** after heating at 70 °C for 30 min. The final molar ratio of **Mn-2**, iPrOH, MeONa and **1** was 1:4:2:1

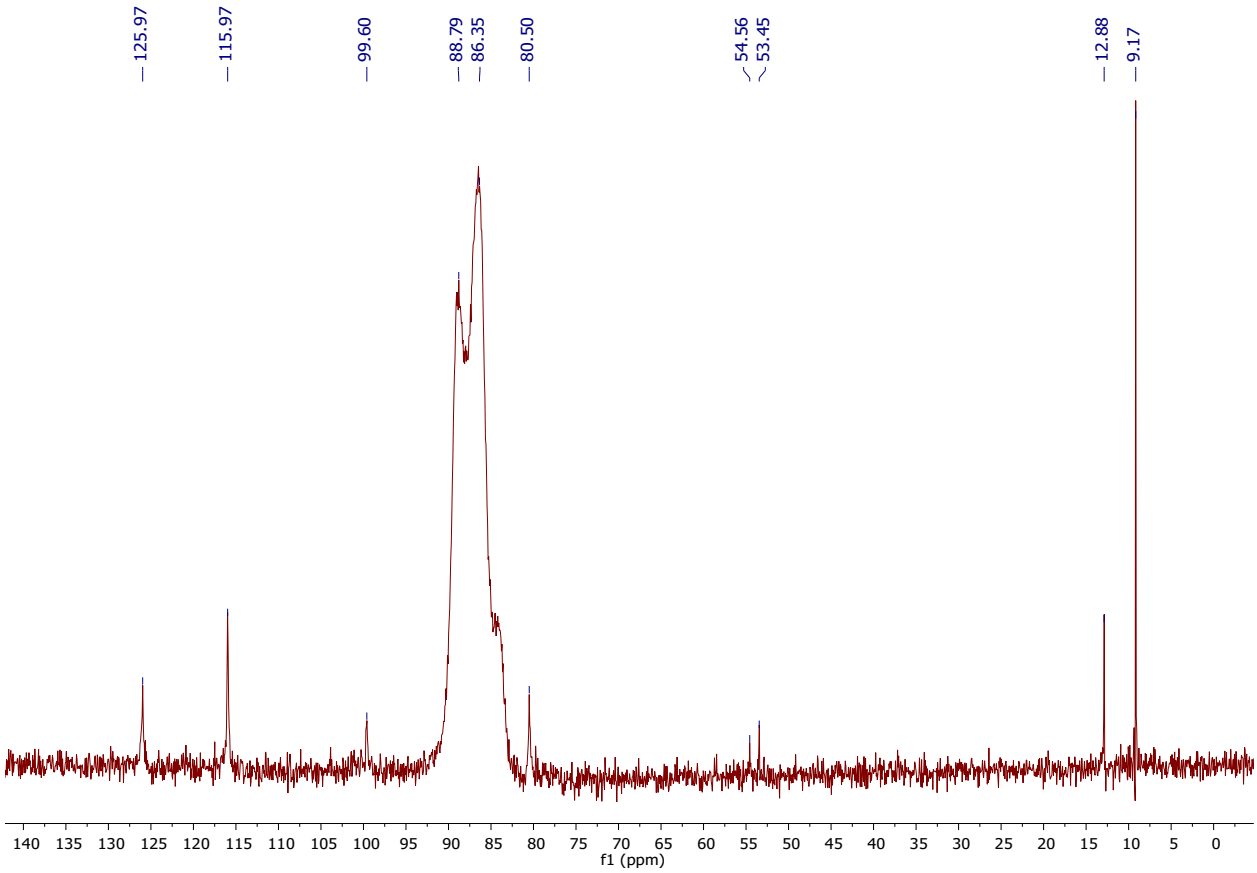

Figure S112. Enlargement of $^{31}P\{^{1}H\}$ NMR (243 MHz, THF-d_8) spectrum of reaction mixture **e**. The molar ratio of **Mn-2**, iPrOH, MeONa and **1** was 1:4:2:1

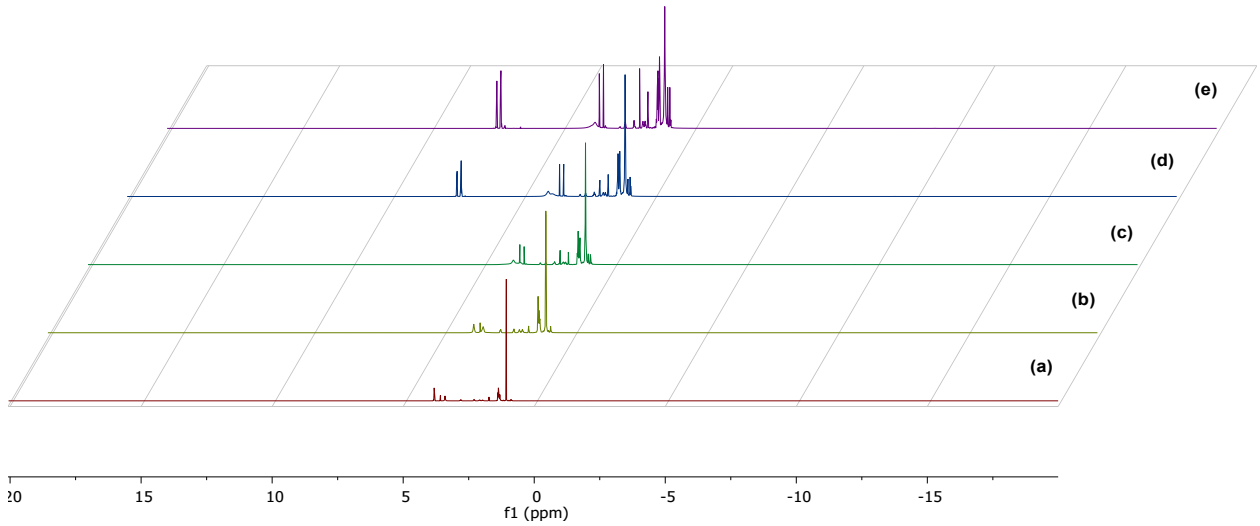

Figure S113. ^{1}H NMR (600 MHz, THF-d_8) monitoring of transfer semihydrogenation of **1** with iPrOH catalyzed by **Mn-2**. **(a) Mn-2** and iPrOH; **(b) Mn-2**, iPrOH and MeONa; **(c) b** after heating at 70 °C for 30 min; **(d) c** after addition of **1**; **(e) d** after heating at 70 °C for 30 min. The final molar ratio of **Mn-2**, iPrOH, MeONa and **1** was 1:4:2:1

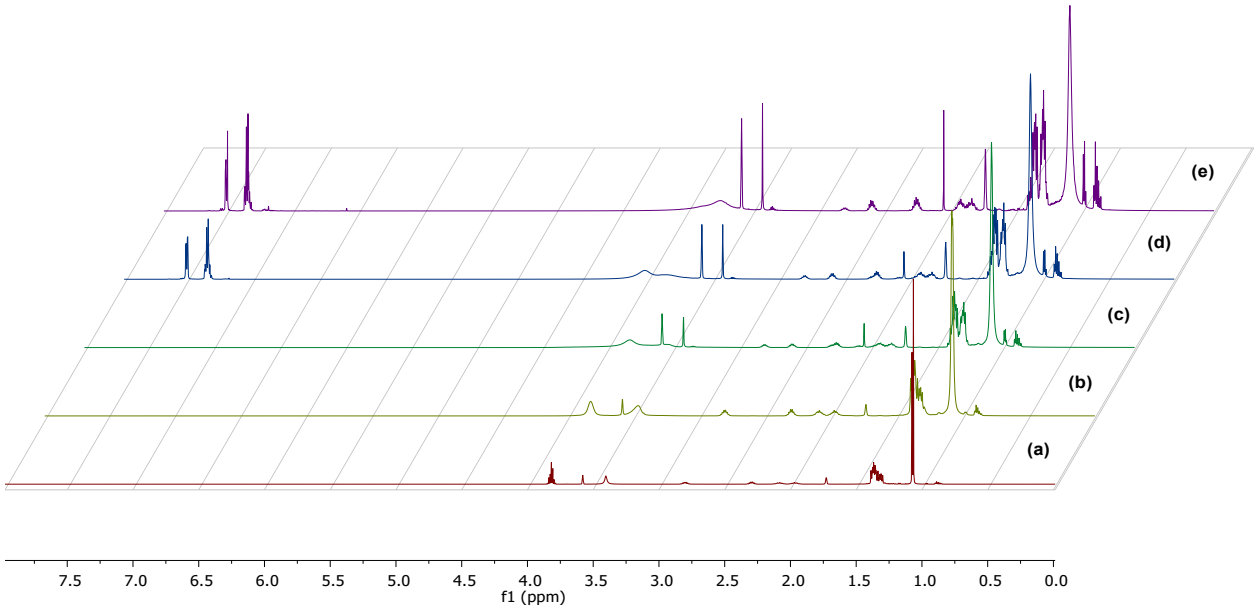

Figure S114. Enlargement of non-hydride region of the ^{1}H NMR (600 MHz, THF-d_8) monitoring of transfer semihydrogenation of **1** with iPrOH catalyzed by **Mn-2**. **(a) Mn-2** and iPrOH; **(b) Mn-2**, iPrOH and MeONa; **(c) b** after heating at 70 °C for 30 min; **(d) c** after addition of **1**; **(e) d** after heating at 70 °C for 30 min. The final molar ratio of **Mn-2**, iPrOH, MeONa and **1** was 1:4:2:1

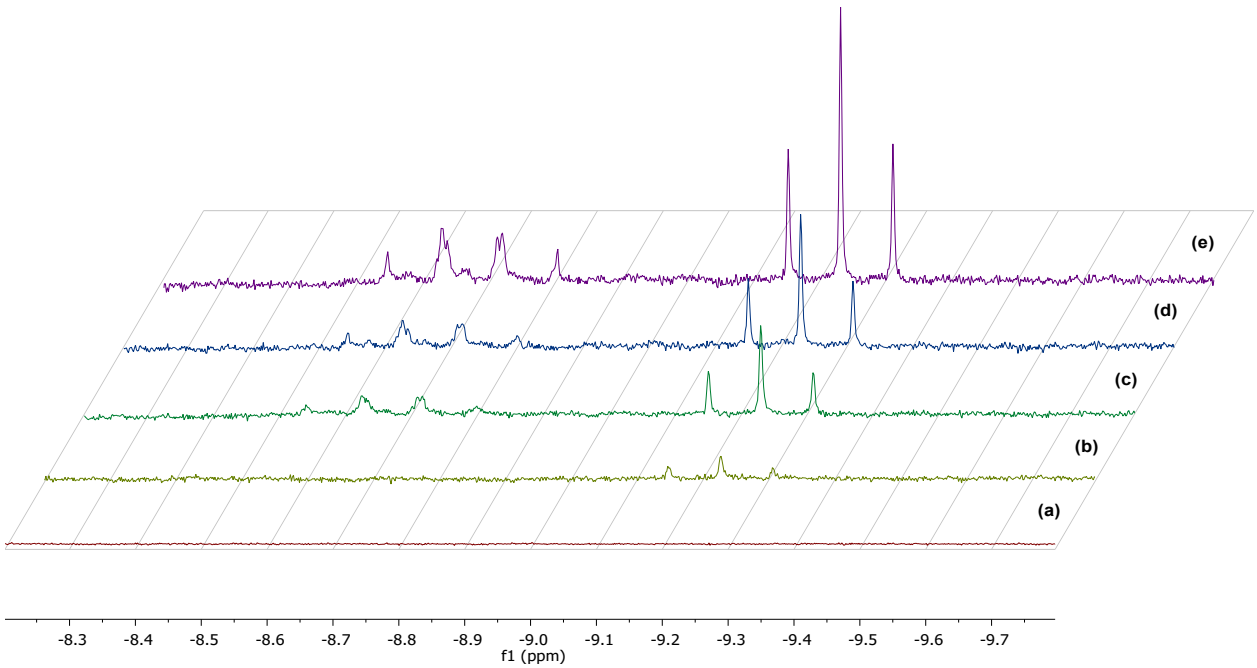

Figure S115. Enlargement of hydride region of the ^{1}H NMR (600 MHz, THF-d_8) monitoring of transfer semihydrogenation of **1** with iPrOH catalyzed by **Mn-2**. **(a) Mn-2** and iPrOH; **(b) Mn-2**, iPrOH and MeONa; **(c) b** after heating at 70 °C for 30 min; **(d) c** after addition of **1**; **(e) d** after heating at 70 °C for 30 min. The final molar ratio of **Mn-2**, iPrOH, MeONa and **1** was 1:4:2:1

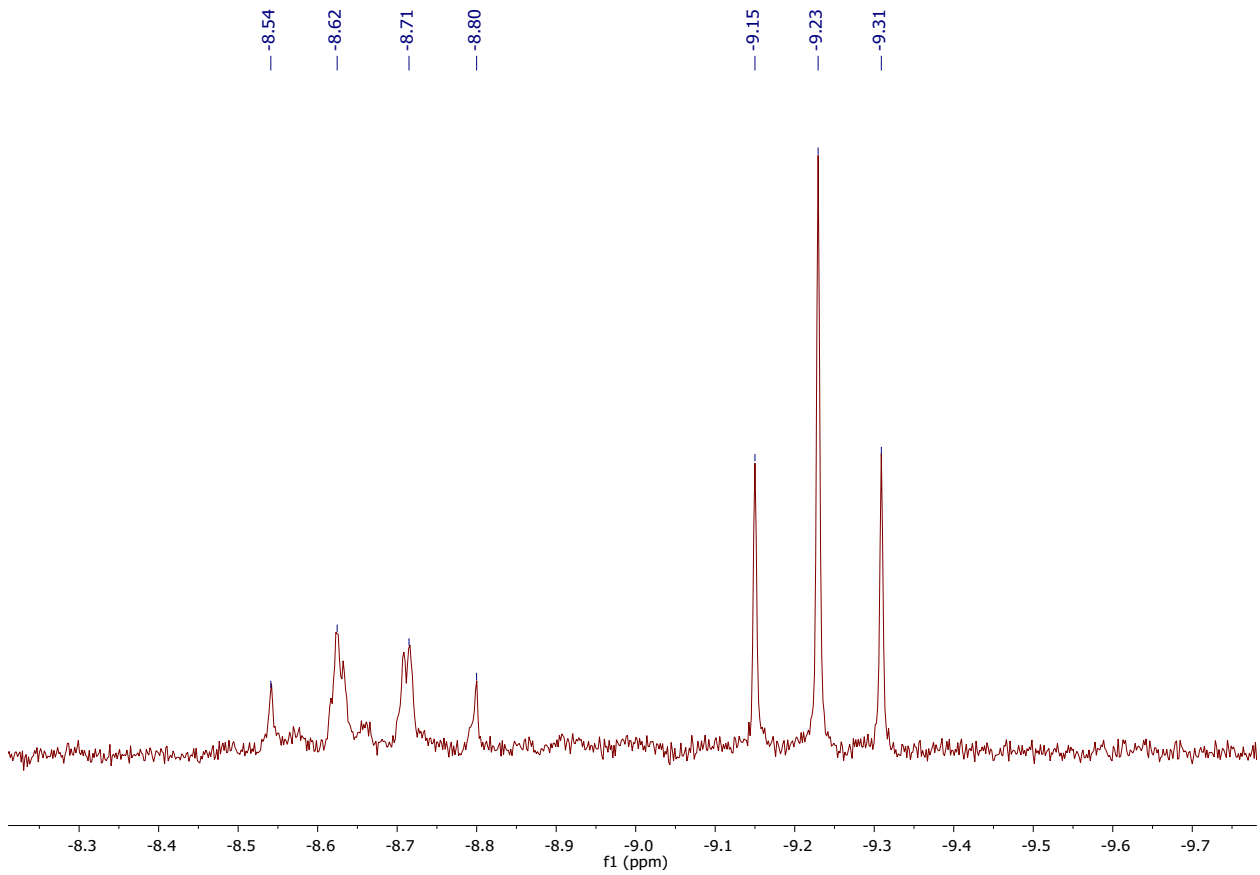

Figure S116. Enlargement of hydride region of the ^{1}H NMR (600 MHz, THF-d_8) spectrum of reaction mixture **e**. The molar ratio of **Mn-2**, iPrOH, MeONa and **1** was 1:4:2:1

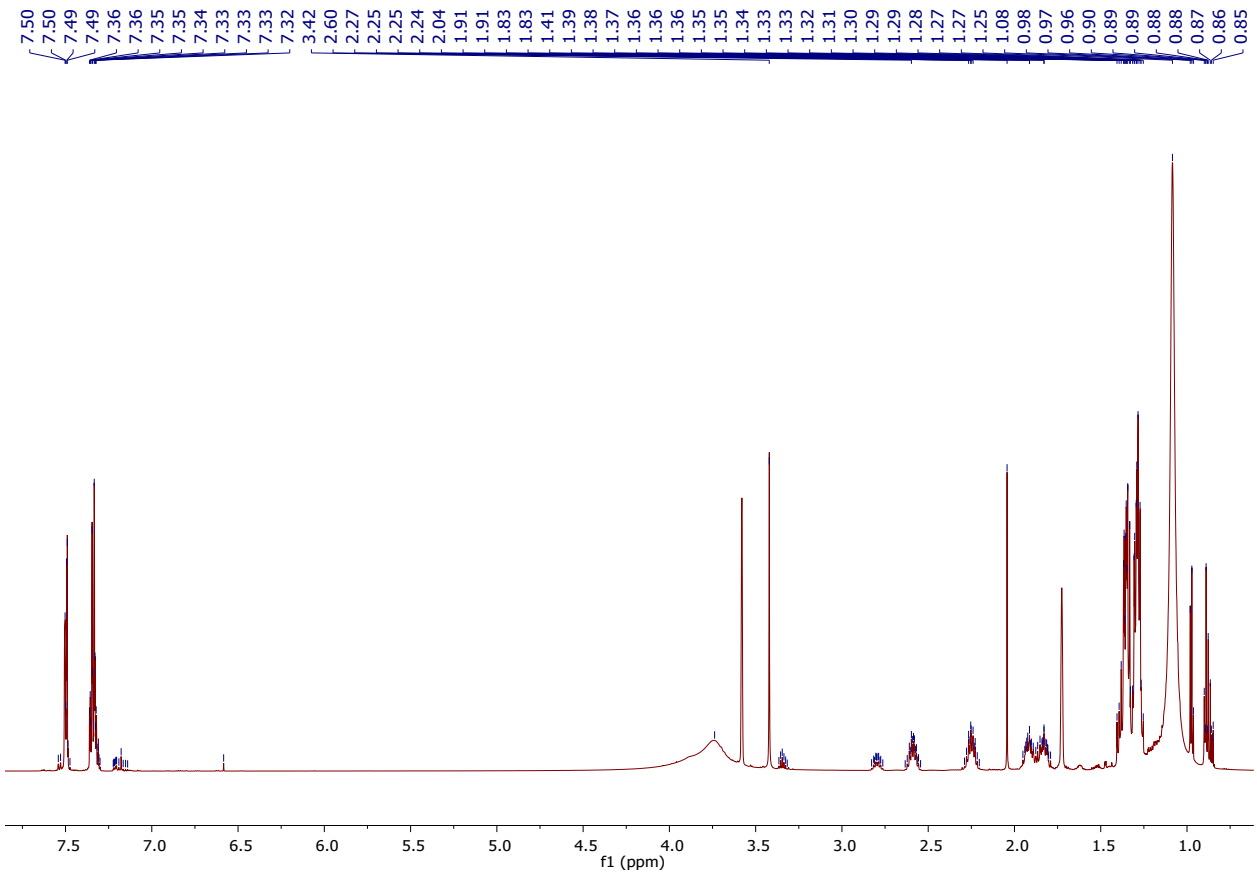

Figure 117. Enlargement of non-hydride region of the ^{1}H NMR (600 MHz, THF-d_8) spectrum of reaction mixture **e**. The molar ratio of **Mn-2**, iPrOH, MeONa and **1** was 1:4:2:1